General Disclaimer

One or more of the Following Statements may affect this Document

- This document has been reproduced from the best copy furnished by the organizational source. It is being released in the interest of making available as much information as possible.

- This document may contain data, which exceeds the sheet parameters. It was furnished in this condition by the organizational source and is the best copy available.

- This document may contain tone-on-tone or color graphs, charts and/or pictures, which have been reproduced in black and white.

- This document is paginated as submitted by the original source.

- Portions of this document are not fully legible due to the historical nature of some of the material. However, it is the best reproduction available from the original submission.

JPL PUBLICATION 82-49

Starprobe

Scientific Rationale

A Report of the Ad Hoc Working Groups

June 15, 1982

NASA
National Aeronautics and
Space Administration

Jet Propulsion Laboratory
California Institute of Technology
Pasadena, California

JPL PUBLICATION 82-49

Starprobe

Scientific Rationale

A Report of the Ad Hoc Working Groups

J.H. Underwood
J.E. Randolph
Editors

June 15, 1982

NASA
National Aeronautics and
Space Administration

Jet Propulsion Laboratory
California Institute of Technology
Pasadena, California

This publication was prepared by the Jet Propulsion Laboratory, California Institute of Technology, under a contract with the National Aeronautics and Space Administration.

CONTENTS

Tables

Figures

FOREWORD

The concept of a space mission that might send a spacecraft to within a few solar radii of the Sun's surface was first discussed in depth at a symposium held at the California Institute of Technology in May 1978. The popularity of this symposium and its subsequent proceedings, A Close-Up of the Sun (JPL Publication 78-70, 1978), clearly demonstrates a strong interest by a broad cross-section of scientists in a Sun-grazing mission. First, space plasma scientists want to directly sample in situ that portion of the Sun's outermost atmosphere where the corona is heated and the solar wind is formed and accelerated. Second, solar physicists appreciate the unique, ultra-high-resolution optical imaging that can be done of the Sun's surface and the inner corona. Finally, physicists interested in experimentally testing the theories of relativity, gravity, and the internal structure of the Sun see an opportunity to conduct experiments of uniqueness and/or precision essentially impossible in any other way.

During the two years following this symposium, a solar flyby mission was discussed in detail by the Space Science Board's Committee on Space Astronomy and Astrophysics which endorsed the potential science that could be accomplished and called for further study and review (A Strategy for Space Astronomy and Astrophysics for the 1980's, NAS, 1979). Closely following this endorsement, the SSB's Committee on Solar and Space Physics gave it a firm recommendation in its report (Solar-System Space Physics in the 1980's: A Research Strategy, NAS, 1980). In the same timeframe as these reports were being prepared, the National Aeronautics and Space Administration was funding the intensive study of mission concept schemes and the requisite technology areas through the Jet Propulsion Laboratory.

By the spring of 1980 it became clear that further review of both the science content and the mission implementation schemes was in order. A Science/Mission Review was thus held at NASA Headquarters May 15-16, 1980, attended by the JPL Project Study Office personnel and 13 scientists representing the three major discipline areas noted above. The conclusion of this meeting was to form ad hoc science study teams to conduct formal, in-depth reviews of the three major areas of science investigation and to provide further direction of the Project Office for technology studies. The results of these study efforts were then presented at a second Science/Mission Review held March 31, 1981, again at Headquarters. This present document contains the final reports from that meeting, and thus represents the most current work on the possible science content and mission implementation schemes of a solar flyby mission, now called officially "STARPROBE."

Extensive technology studies are currently being jointly funded by the Office of Space Science and the Office of Aeronautics and Space Technology. At their completion, a technology readiness review will be held to judge the possibilities of and limitations on a solar flyby mission. Unfortunately, however, the prognosis for an early new start authorization for a program of this magnitude has deteriorated with the decreasing resources available for space science missions in general.

The potential science return from this type of mission is truly prodigious. The region very close to the Sun is one of the last unexplored regions of the solar system and must be investigated if we are ever to understand some of the most fundamental properties of stars, the Sun, and the heliosphere, in addition to performing unique experiments in the areas of relativistic and gravitational physics. The importance of these science objectives is invariant to the timeframe of the mission.

Many people have been involved in the formulation of this document. In particular, Frederick L. Scarf, Robert D. Reasenberg and Arthur B. C. Walker, Jr., contributed unselfishly of their time to chair the three ad hoc science study teams and see that the final reports were written. James E. Randolph, Manager of the JPL STARPROBE Project Study Office, and Bruce E. Goldstein and James H. Underwood, the JPL STARPROBE Study Scientists, coordinated the mission technology and science study efforts, respectively, and saw to the publication of this document.

J. David Bohlin, Chief
Solar & Heliospheric
Physics Branch

George P. Newton, Chief
Advanced Program and
Technology Branch

Solar Terrestrial & Astrophysics Division
Office of Space Science
NASA Headquarters

ABSTRACT

For several years, NASA has been studying the concept of a mission called STARPROBE which would send a spacecraft extremely close to the Sun (perihelion of 4 solar radii) to carry out scientific investigations in the three areas of solar internal dynamics and relativity, solar plasma and particle dynamics, and solar atmospheric structure. Three separate committees were convened by NASA to study the scientific rationale and instrumentation problems for each of these areas. The conclusions reached by these committees are presented in the first three chapters of this report. The fourth chapter summarizes the current mission and system design concepts responding to the recommendations of the study teams.

CHAPTER 1

GRAVITY AND RELATIVITY SCIENCE

R. D. Reasenberg, Chairman, Massachusetts Institute of Technology
J. D. Anderson, Jet Propulsion Laboratory
D. B. DeBra, Stanford University
I. I. Shapiro, Massachusetts Institute of Technology
R. K. Ulrich, University of California, Los Angeles
R. F. C. Vessot, Harvard-Smithsonian Center for Astrophysics

1.0 INTRODUCTION

The Starprobe Ad Hoc Gravity and Relativity Committee met on 20 and 21 October 1980 at JPL. The findings of that committee are summarized in this report, which disregards other possible scientific aspects of STARPROBE. The STARPROBE Mission is capable of making a significant contribution to our understanding of the laws of gravitation and to our knowledge of the internal structure of stars in general and of the Sun in particular. A possible contribution to neutrino physics is also identified.

To be successful, this mission requires the development of some new technology. An opportunity exists to augment the success of the mission if additional technological advances are made and incorporated. Sections 1.1 and 1.2 provide a summary of applicable material from two areas of astrophysics: stellar structure and experimental relativity. These sections provide the scientific basis for Section 1.3, in which we consider the scientific objectives under three categories: A, established; B, possible; C, secondary. Section 1.4 is devoted to a discussion of technological considerations and Section 1.5 contains the recommendations of the committee.

1.1 SOME PROBLEMS IN SOLAR AND STELLAR PHYSICS

Stellar structure was one of the earliest fields of astrophysics where a direct confrontation between theory and observation was possible. During the 1960s, stellar structure and evolution were studied using computer codes and opacity tables developed to model thermonuclear devices. By the early 1970s, it was generally believed that the principal aspects of this subject had been understood. Plausible models had been constructed to match the sparse set of available data.

The models were tested by comparing Hertzsprung-Russel (H-R) diagrams from various star clusters with theoretical models for main sequence stars and isochrones. The earliest versions of such diagrams were introduced by Hertzsprung and by Russell using spectral class and magnitude. Modern versions attempt to transform the observables, photometric color and photometric magnitude, to the theoretically needed effective temperature and bolometric magnitude. This transformation can be uncertain and we will generally refer to all such diagrams as H-R diagrams. Such observational data as those summarized by Sandage (1975) and Arp (1958) and theoretical wor' by Schwarzschild (1958), Iben (1967), and others formed the basis for the tests. The results were satisfactory in a broad sense; the theory was not found to be grossly out of line. In a more detailed sense, however, the theory was not tested. The comparison was not very precise; errors of 10% would not have been noticeable. The lack of measured stellar masses introduced a degree of freedom which could obscure an error that would alter all stellar models in a similar way.

The success of stellar theory in reproducing cluster H-R diagrams has led many astronomers and physicists to take an overly sanguine view of our understanding of stellar structure. Today there is evidence that the standard models are insufficient. We first consider problems encountered with solar data and then turn to evidence from stellar studies.

1.1.1 Sources of Data for Solar Models

Because of its proximity, and thus the relative ease with which it can be observed, the Sun serves as a particularly important test case for models of stellar evolution and structure. It appears to be a stable star evolving along the main sequence; thus it should be relatively easy to model. Constraints on models of the internal structure of the Sun have traditionally come from a small set of externally measurable parameters including the mass, radius, luminosity, and surface composition. An additional datum comes from the solar neutrino experiment of Davis et al. (For example, see Bahcall and Davis, 1976.) More recently, solar oscillation measurements have become available to test the models of solar structure.

1.1.2 Canonical Theory of Stellar Structure Versus Experiments

Much of the evaluation of the theory of solar and stellar structure has revolved indirectly about the "theorem" due to Russell and Vogt which states that, for a specified mass and chemical composition, there is a unique stellar model. Since the present solar internal composition is uniquely determined by

nuclear physics and the Sun's initial composition (assumed uniform), and since the time-dependent terms are negligible for the Sun, we should be able to calculate unique theoretical predictions for each of the four tests below. The status of the "canonical theory" is summarized in Table 1-1.

The solar neutrino flux and solar oscillations, both of which are discussed further below, are the subjects of the four "canonical theory" predictions. The eigenfunctions of solar oscillation are described by their three indices: n is the mode order (i.e., the number of nodes in the radial direction), and ℓ and m define the surface harmonic that describes the angular distribution, $Y_\ell^m(\theta,\phi)$. The tests show that (1) about four times as many neutrinos are predicted as are observed with a Cl detector; (2) the eigenfrequencies of highly nonradial modes of oscillation ($500 \leq \ell \leq 2000$), observationally known as the "five-minute oscillations," are in good agreement with theory; (3) with the possible exception of the spacing between $\ell = 0$ and $\ell = 2$, the spacings of the frequencies of these five-minute oscillations, as observed from the South Pole, agree with theory for the lowest degree modes ($\ell = 0,1,2,3$) and successive values of mode order n; and (4) the values of the frequencies of these lowest degree modes, as opposed to their spacing, may not agree with observation. However, the frequency theory is subject to unusual absolute accuracy requirements (i.e., the observed frequencies have fractional uncertainties of about 10^{-3}, hence a 0.3% error in the theory is significant), and thus the failure of this test is less significant than the failure of other predictions.

As of a few years ago, the standard models predicted a neutrino flux 3 times larger than that observed (Bahcall and Davis, 1976). Over the last few years, there have been small changes in both theory and experimental results, but these have not significantly altered the disparity. The calculation of the "expected" neutrino flux includes several difficult steps, and depends critically on the cross-sections of some low-energy nuclear reactions. Some of these cross-sections are too small to measure and therefore must be obtained by theoretical extrapolation from other cross sections. Other cross-sections, including those from which the extrapolations are made, are measurable only with great difficulty.

Recently, particle physics theories have predicted a "neutrino oscillation" which may be able to reduce the apparent neutrino flux discrepancy (Bahcall, 1978; Bahcall et al., 1980). This explanation is highly speculative, however, and should not be relied upon for an understanding of the internal workings of the Sun. Rather, the measurement at Earth of the solar neutrino flux may prove to be an important test of the "neutrino oscillation" theories. Before such a test is considered useful, however, there must be a substantial increase in the reliability of the prediction of the flux of neutrinos generated by the Sun.

1.1.3 Noncanonical Assumptions to Reconcile Experimental Data

A variety of noncanonical assumptions have been suggested in the past to account for the lack of solar neutrinos. Four of the most interesting of these are listed in Table 1-2. The "low Z model" (Joss, 1974) probably cannot be tested with the STARPROBE Mission and is not discussed further here.

Table 1-1. Stellar theory tutorial

Canonical theory says that solar structure is uniquely defined.
Russel-Vogt Theorem.

Tests of canonical theory:

- Solar neutrinos
- Solar oscillations
- Binary stars
- Cluster diagrams

Successes of canonical theory:

- Can match effective temperature and luminosity for binary stars, cluster diagrams and the Sun
- Can match frequency spacing of low degree modes of oscillation
- Can match high degree frequencies and spacing

Problem areas:

- Too few neutrinos
- Possible problems with low degree oscillation frequency values
- Blue stragglers
- Extension above zero-age main sequence

Summary:

- Canonical theory is in a bit of trouble

Table 1-2. Noncanonical assumptions

Nonuniform initial composition (low Z model)

Mixing: fast, slow, episodic
- Causes: meridional circulation, waves

Primordial magnetic field
- Decay times of 3 longest lived modes (10^9 years)[a]
  - 25
  - 10
  - 6

Rotation in the core

[a]See Ulrich (1974) and references therein.

Canonical theory assumes that no "mixing" of envelope material into the core takes place. Mixing would lead to a hydrogen-enhanced core which would be cooler and produce a smaller neutrino flux than the core of a comparable unmixed star. The solar models with mixing are influenced by the possibility of rapid core rotation. Although existing limits on the solar oblateness are sufficient to rule out centripetal acceleration as a cause for the difficulties of the canonical solar model, a variety of mixing processes becomes possible in the presence of strong differential rotation. Thus detection of J_2 at a level above that required by uniform rotation would provide a strong impetus to the further study of rotation-driven mixing. Such processes as Eddington-Sweet circulation, Ekman pumping, and Goldreich-Schubert instability are examples of mechanisms which could prove significant for a rapidly rotating core.

Magnetic fields are perhaps the most intriguing of the noncanonical assumptions. If they are important to solar structure, they can significantly change the solar oscillation spectrum (Tassoul, 1978, p. 425, and references therein). Although magnetic fields can introduce more free gravitational parameters than one could hope to estimate with STARPROBE, these configurations which decay most slowly as a result of ohmic dissipation are close to dipoles in structure. A small dipole field would necessitate the addition of only a few gravitational parameters, although no circulation is yet available which gives the relation between the field strength and J_2 (in a coordinate frame defined by the dipole axis). The existence of strong fields in some neutron stars suggests that a significant field in the solar interior is not impossible.

If the Sun has a large centered dipole magnetic field, the induced distortion of the gravitational potential will be indistinguishable from that caused by rotation as long as the axes of rotation and magnetic dipole are aligned. Such alignment is unlikely; if the J_2 axis turns out to be displaced from the solar rotation axis, a magnetic dipole field can be inferred. If this were detected by the STARPROBE Mission, it would be a result of major importance. In fact, such an off-axis oblateness signal has been suggested by Dicke (1980) through an analysis of the Dicke and Goldenberg (1967) data.

Numerous other, more highly speculative models have also been advanced to explain the apparent shortage of solar neutrinos. Among these are:

(1) The core is in a transient state in which it does not produce neutrinos; the surface does not reflect this state because of the Sun's long energy diffusion time. (Fowler, 1972. See also Dilke and Gough, 1974.)

(2) A small black hole at the center of the Sun would produce energy without neutrinos. Some thermonuclear burning would provide all the observed neutrinos. (Clayton et al., 1975.)

(3) If the Sun formed in stages, the composition of the core could be different from that of the surface. If the core were low in helium and high in metals, it would be convective and have reduced neutrino emission (Hoyle, 1975).

Short-period solar oscillations have been reported by Hill et al. (1979) and Grec et al. (1980). The excitation mechanisms for these oscillations need to be explained. Since some of the oscillations are able to transport a large amount of energy from the interior to the surface, they may lower the effective opacity and lead to a cooler interior and a lower neutrino flux than would otherwise be expected. Calculations by Johnson et al. (1979) and by Christensen-Dalsgaard and Gough (1979) indicate that:

(1) The frequency spectrum of these oscillations is a useful probe of the solar interior.

(2) The time varying solar quadrupole moment may be as much as 30% of the static quadrupole moment expected from uniform rotation. However, this conjecture is based on the reported amplitude of the 160-minute oscillations. The optical determination of this amplitude is quite uncertain; even the detection of the oscillation has been questioned, although the estimated amplitude is 7 times the formal standard deviation (Scherrer et al., 1980).

(3) The ratio of the amplitude of the visual and the gravitational time-dependent quadrupole moments provide a useful constraint on the structure of the solar interior.

1.1.4 Solar Luminosity Variations and Climate Questions

The classical theory of stellar evolution requires the Sun's luminosity to have been 25% smaller some 5 billion years ago when it joined the main sequence. Sagan and Mullen (1973) calculate that this could have led to frozen oceans which, because of the high albedo of ice, would not have melted. (See also Newman and Rood, 1977.) Of course, conditions in the distant past were different from those of today. An altered continental distribution implies a different pattern of ocean circulation and heat transport. Even a modest change in the composition of the atmosphere could alter the greenhouse effect. Thus there may not be a contradiction between a cooler Sun in the past and the presence of life on Earth today. Here, as in the case of the neutrino oscillations discussed above, a reliable determination of the behavior of the Sun would be of value to another branch of science.

1.1.5 Sun Spot Cycle Questions

Two other questions should be addressed. The 22-year sun-spot cycle, and the Maunder minimum (Eddy, 1976), if it exists, both need to be explained. Barnes et al. (1980a, b) have shown that these phenomena can be modeled by a nonlinear process driven by band-limited white noise. However, neither a physical basis for the narrow-band response nor a source of the driving noise has been identified.

1.1.6 New Tests of Stellar Structure

In the past 10 years, new tests of stellar structure theory have been developed based on the canonical theory discussed above which makes predictions about stars and stellar populations. Some of these predictions are now at variance with observations. The long-term study of eclipsing binary stars carried out by Popper (1980) has now yielded enough objects with known mass M, radius R, and luminosity L that a meaningful comparison between theory and observation is possible. The L versus M comparison with binary stars is good to within observational error, but the R versus M relation predicts stars too small by 10% at $M = 1.4\ M_{\odot}$.

1.1.7 Blue Stragglers

A prediction of the canonical theory is that all stars that have the same initial composition and mass should exhaust their hydrogen simultaneously; more massive stars are shorter lived. It is generally assumed that all of the stars in a cluster are the same age. Some clusters contain stars which are on the main sequence but are more massive than the stars which are currently exhausting their core hydrogen and are moving off the main sequence. These stars, which are called blue stragglers (Wheeler 1979a, b), occupy an anomalous position in the cluster H-R diagram -- to the blue of the cluster turnoff. Thus they appear to be less evolved than the other cluster members and their existence may contradict the canonical theory. One possible explanation of this phenomenon is that these stars have an extended main sequence lifetime due to mixing of hydrogen into the core. Other evidence for mixing is provided by the observations of Maeder and Mermilliod (1980), who found that the main sequences of 34 clusters extended much too far above the zero-age main sequence. They proposed that the zone of mixing in stellar interiors is more extended than was previously thought.

1.1.8 The Contribution of STARPROBE Gravity Data

The most predictable result of the STARPROBE gravity study will be a measurement of J_2 and an inference about the state of rotation of the solar interior. Kraft (1970) has summarized the observational data concerning stellar rotation and finds a break in the dependence of rotation rate on mass. Figure 1-1 shows these data. Clearly a rapidly rotating solar core is within reason.

The measurement of J_2 will be of fundamental importance in the study of the process of star formation. It would be useful to know how the angular momentum of the protosolar cloud was distributed between the Sun and its planets. As a first step toward this understanding, we should determine the present angular momentum of the Sun, which may be inaccurately inferred from the solar surface rotation. Young stars often have equatorial surface rotation rates in the range 15 to 30 km/s (cf. the Sun at 2 km/s). Figure 1-2 shows the distribution of absorption line widths in a sample of young stars. These stars are a factor of 2 to 5 times larger than they will be on the main sequence and some of them have masses near $1\ M_{\odot}$. Thus it is possible that the Sun began its life on the main sequence with a rotation rate as much as 30 times faster than the present apparent rate.

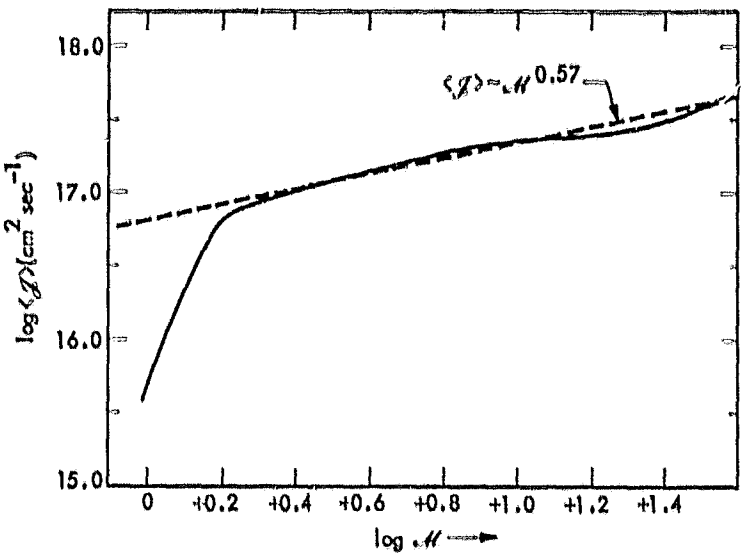

Fig. 1-1. $\langle I(M) \rangle \equiv \langle J(M)/(M) \rangle$ as a function of log M for main-sequence stars, where J(M) is the angular momentum per unit mass

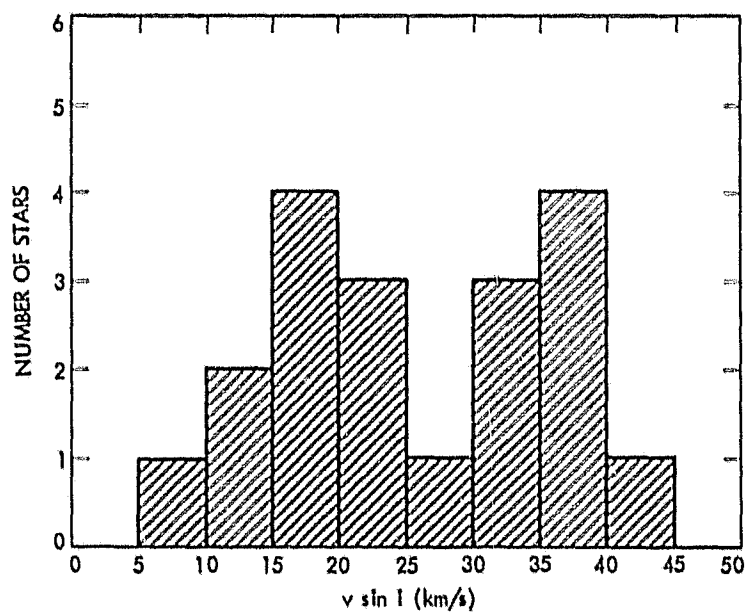

Fig. 1-2. Rotation velocities of pre-main sequence stars with absorption lines (Ulrich/Knapp survey)

The decay of the rapid rotation of young stars may be responsible for the activity typically observed in these objects. Magnetic braking through the solar wind is usually appealed to as the mechanism responsible for the current slow surface rotation rate. The relationship between the strength of chromospheric activity and cluster age observed by Wilson and Skumanich (1967) supports this view. However as Kraft (1970) has emphasized, there is considerable doubt about many of these conclusions because of a variety of observational uncertainties. Even if the solar core does not rotate quite this rapidly, there is an excellent chance that the value of J_2 is well above that expected on the basis of uniform rotation.

The evidence presented in this section was discussed in terms of the present standard theory of stellar structure and evolution. This canonical theory, although able to fit the older kinds of data, is now at variance with some modern high-accuracy data. Perhaps we have entered into a new phase of stellar theory development. If so, then the experimental evidence suggests that the new theories should be able to include the effects of differential rotation. The Sun, the best observed star, will continue to play an important part in testing new theories. By measuring the solar quadrupole moment, STARPROBE could contribute to the advance of stellar and solar physics.

1.2 SOME PROBLEMS IN EXPERIMENTAL RELATIVITY

1.2.1 The Parameterized Post-Newtonian Formalism of Gravitational Relativity

In addition to general relativity, there now exist several relativistic theories of gravitation that are consistent with available experimental results. In order to compare theories with experiments, a parametric "super theory" has been developed. Known today as the Parameterized Post-Newtonian (PPN) formalism, this approach is applicable in the solar system where the dimensionless gravitational potential ϕ and typical velocities v are small ($|\phi| < 2 \times 10^{-6}$ and v^2 is of order ϕ). In a post-Newtonian formalism, terms are grouped according to the combined powers of ϕ and v^2. The first-order terms are Newtonian; second-order, post-Newtonian. Higher order terms are neglected. An early version of the PPN formalism was given by Eddington and Robertson, who introduced three ad hoc parameters (α, β, and γ) into a power series expansion of the general relativistic metric in isotropic form. From the empirical definition of the unit of mass and the gravitational constant, $\alpha = 1$. However, it is often convenient to ignore this and use α as a parameter that describes the gravitational redshift. Heuristically, β is a measure of the nonlinearity of the superposition law for gravity and γ is a measure of the curvature of space produced by mass. (For example, see Misner, Thorne, and Wheeler, 1973, p. 1072.) The complete PPN formalism has 10 parameters, but our discussion will be restricted to the three original ones.

1.2.2 Relation of Gravity to Other Fundamental Interactions

Interest in estimating the PPN parameters goes beyond a desire to distinguish among current theories. Gravitation is the weakest of the four fundamental interactions and by far the most difficult to study experimentally. Because it is long range and because its "charge" is proportional to inertial mass, gravitation is able to dominate the large-scale structure of the universe.

The strong, electromagnetic, and weak interactions show promise of being unified in the near future. However, gravitation has thus far managed to remain distinct. There is a body of opinion that holds that the current class of theories of gravitation will manifest their weaknesses on the cosmological scale or at the subatomic scale or both. However, the opportunity to detect the failure of such theories is limited to those domains in which experiment is possible. Thus solar-system tests of relativity assume an important place in contemporary physics.

1.2.3 Advance of the Perihelion of Mercury

One of the classical tests of general relativity is based on the advance of the perihelion of Mercury. Excluding planetary perturbations, the secular advance is given by

$$\delta\phi = \frac{3\pi r_\odot}{p}\left|\frac{2+2\gamma-\beta}{3}+J_2\frac{R_\odot^2}{r_\odot p}\right|\ \frac{\text{radians}}{\text{revolution}}$$

where $p = a(1-e^2)$ is Mercury's semilatus rectum; $r_\odot \approx 3$ km is the gravitational radius of the Sun; and $R_\odot \approx 7 \times 10^5$ km is its physical radius. The uncertainty in the estimate of γ from the Viking relativity experiment is 0.2% (Reasenberg et al., 1979); further improvement is expected from the refined analysis of an enlarged Viking data set. The separation of β and J_2 with currently available data is unsatisfactory. (For example, see Reasenberg, 1980.) A determination of J_2 by the STARPROBE Mission would make possible the direct and relatively accurate determination of β from observations of Mercury.

1.2.4 Gravitational Redshift Experiments

The gravitational redshift is another of the predictions of general relativity that was subject to early experimental study. It was first reliably detected by the Mössbauer experiment of Pound, Rebka, and Snider. They reported an uncertainty of 1.0% in a measurement of the redshift of photons "falling" 20 meters.

The gravitational redshift is now not thought of as a test of general relativity, per se, but rather as a manifestation of the principle of equivalence which is a foundation stone of all relativistic theories of gravity. Should any aspect of the principle of equivalence fail an experimental test, the current ideas about the nature of gravitation would have to be replaced.

In a recent experiment, Gravity Probe "A" (GP-A), by Vessot et al. (1980), a hydrogen maser was flown in a spacecraft on a suborbital trajectory. A multilink doppler tracking and communication system was used to compare the flying clock with its counterparts on the ground. This experiment served to test the predictions of general relativity for the combined effects of the second-order Doppler shift and the gravitational redshift. The predicted

composite relativistic effect was confirmed with an uncertainty of 70 parts per million.

1.3 GRAVITY AND RELATIVITY SCIENTIFIC OBJECTIVES

1.3.1 Established Scientific Objectives - The Measurement of J_2

A primary scientific objective of the Starprobe Mission would be to determine J_2 through the analysis of spacecraft tracking data. Optical measurements of the visual oblateness of the Sun made by Dicke and Goldenberg (1967) are inconsistent with the more recent optical measurements made by Hill and Stebbins (1975). These measurements bear in a somewhat model-dependent fashion on the J_2 components of the spherical harmonic expansion of the solar potential.

1.3.2 Possible Scientific Objectives

We next consider four scientific objectives which, although possible, either require further theoretical analysis or special equipment on the spacecraft or spacecraft and tracking performance beyond the nominal mission specifications.

1.3.2.1 Other Zonal Gravitational Harmonics

For a uniformly rotating Sun it has generally been accepted that J_3 is approximately zero and that J_4 is similar to J_2^2; $J_2 \approx 2 \times 10^{-7}$. By using a particular parametric model of solar internal rotation, Ulrich and Hawkins (1981) have shown that solar differential rotation can lead to J_4 smaller than J_2 by a factor of only about 10 and thus much larger than J_2^2. Thus a measurement or constraint on the magnitude of J_4 would become a worthwhile scientific objective of this mission if it is shown through sensitivity studies that J_4 can be estimated with an uncertainty of no more than 10^{-8}. It also seems plausible that other even zonal harmonics, particularly J_6, may also be large for a differentially rotating Sun compared to what would be expected for a uniformly rotating Sun. However, this conjecture has not been tested, and the STARPROBE Mission is unlikely to be able to measure J_6 even if it is as large as $10^{-2}J_2$.

1.3.2.2 Variability of J_2

There is evidence that there are mechanical (both acoustic and gravity wave) oscillations of the Sun, and corresponding periodic changes in the gravitational potential are expected. The ratio of the amplitudes of corresponding optical and gravitational oscillations is a probe of the internal structure of the Sun. Of particular interest is the 160-minute oscillation that is associated with a periodic variation of the solar quadrupole moment. The amplitude of the time-dependent J_2 term is estimated to be of order 7×10^{-8} (Christensen-Dalsgaard and Gough, 1980) and thus measurable by STARPROBE. The simultaneous observation of the optical variations from the ground and the gravitational variations from STARPROBE is an attractive possibility.

1.3.2.3 Total Angular Momentum of the Sun

General relativity predicts a phenomenon known as the dragging of inertial frames, of which there are many potential manifestations. For example, the time required for light to propagate around (or past) a rotating body is different depending on whether the propagation is with or against the direction of the rotation of the body. It is hoped that frame dragging will be demonstrated during the 1980s by the Stanford Gyroscope Experiment (Gravity Probe B). Since the effect is proportional to the angular momentum of the rotating body, the precision radio tracking data from the STARPROBE Mission may permit a determination of the Sun's angular momentum. If successful, this would be the first measurement of a classical quantity in the solar system by means of a relativistic effect.

1.3.2.4 Redshift Experiment

The STARPROBE will experience a change in gravitational potential of 0.5×10^{-6} (in the usual dimensionless units for which $G = c = 1$). This change will be 1.2×10^{3} larger than the change in potential experienced by GP-A. A redshift experiment based on the STARPROBE Mission could provide a test of the predictions of general relativity to second order in the solar potential ϕ, where $\phi = 2 \times 10^{-6}$ at the surface of the Sun. For the next 10 years, there seems little hope of doing a second-order redshift experiment that uses Earth's gravitational potential.

1.3.3 Secondary Scientific Objectives

The radio tracking data of the STARPROBE Mission could be used to achieve a number of secondary objectives in the areas of relativity and gravitation physics. Data for these secondary objectives should be obtained on a "best efforts" basis.

1.3.3.1 Parameters of the Jovian System

The encounter with Jupiter (a brown dwarf star), although not unique, could provide useful additional measures of several important parameters of the Jovian system. The radio tracking data will be sensitive to Jupiter's mass and to some of the lower order coefficients of the spherical harmonic expansion of the Jovian potential. Further, it should be possible to arrange for the Jovian segment of the flight to include a close encounter with at least one of Jupiter's satellites, thus providing an improved measure of the satellite mass. The data obtained from the Jovian flyby should, of course, be combined with the tracking data from previous Jovian encounters. The combined data set will offer the advantages of reduced degeneracy and increased redundancy. Ranging observations made near the time of Jupiter encounter would be reduced to a single ranging normal point. A small set of these normal points, one of which may be obtained at each spacecraft encounter, can be used to substantially improve the ephemeris of Jupiter.

The combined Jupiter encounter data set would be used to estimate the mass and low order even zonal harmonics (e.g., J_2, J_4, and J_6) of Jupiter. These and the radius are the principal data constraining models of the interior of the planet. At present, the available mass, radius, and harmonic data for Jupiter and Saturn are inconsistent with our understanding of the equation of state of a hydrogen-helium mixture. (See Hubbard et al., 1980, especially p. 5915.) The situation calls for further investigation, both theoretical and experimental.

1.3.3.2 Gravity Wave Detection

During interplanetary cruise, the spacecraft might be used as one end of a free-mass gravity wave detection system. Since the spacecraft will have independent coherent doppler links with the ground in two different frequency bands (e.g., both S-band up and down links and X-band up and down links), the sensitivity and the immunity to plasma phase noise of the radio tracking system for detecting gravity waves will be increased as compared to a purely X-band system (which is better than a purely S-band system), provided only that the link margins are sufficient. The mission would offer an extended period during which the search for gravity waves could be conducted. Improved noise immunity may be achieved by the use of the proposed onboard hydrogen maser clock, possibly in conjunction with onboard doppler extraction, as will be discussed below, but the theoretical basis for these approaches to noise immunity need to be demonstrated in detail.

1.3.3.3 Estimates of β and γ

Covariance studies have shown that the STARPROBE tracking data are sensitive to the metric parameters β and γ. The physical effects which leads to these sensitivities are, respectively, the relativistic perihelion advance and time delay. From these sensitivity studies, it appears that although the STARPROBE Mission cannot provide estimates of β and γ with smaller uncertainties than are available from other sources, STARPROBE can come close to matching these earlier accuracies. However, these sensitivity studies were based on the tracking and drag compensation systems as they were perceived several years ago. Should these systems perform to higher standards, the metric parameters β and γ might be usefully determined by the Starprobe Mission.

1.4 TECHNOLOGY CONSIDERATIONS

In this section we consider three areas of technology which are of particular importance to the relativity and gravitation physics aspects of the STARPROBE Mission. The radio tracking and drag compensation systems are essential for most of the objectives discussed in Section 1.3. An onboard hydrogen maser would make possible a gravitational redshift experiment and might aid in achieving other objectives including a search for gravitational waves. Other items, such as the thermal shielding, although critical to the mission and requiring technological development, are not considered here.

1.4.1 Tracking System

All of the objectives discussed in Section 1.3 depend directly on the radio tracking system. For most of the mission objectives, including the J_2 estimate, the critical data must be taken when the spacecraft is near the Sun, and the radio signals must therefore pass through the solar corona. The coronal plasma causes the tracking signals to experience a frequency-dependent delay. Plasma inhomogeneities cause multipath interference and fading of the signal.

The STARPROBE encounter with the Sun is a unique and brief event. The tracking system must be designed not only to provide the required accuracy but to be robust and reliable. Advantage should be taken of the opportunity to perform in-flight pre-solar-encounter tests of all systems. These tests are particularly important at Jupiter encounter; this will be the first test of the drag compensation system in the presence of radiation. The tests should be performed even if (contrary to our present expectation) they degrade the Jupiter encounter science.

1.4.1.1 Doppler Tracking

The current standard NASA doppler tracking system uses phase-coherent electronics and operates at S-band. An additional downlink at X-band has been available on a few spacecraft (Viking orbiters, Voyager, etc.). When the Earth-spacecraft path is far from the Sun, the typical S-band tracking noise corresponds to 0.2 mm/s of equivalent velocity noise for a one-minute cycle-counting interval. This noise level increases precipitously as the ray path approaches the Sun. Under "fair to good" tracking conditions, the system slips only rarely (i.e., it gains or loses a cycle less often than once per hour); phase coherence is maintained.

The "baseline" STARPROBE doppler tracking system would use two two-way phase-coherent links operating simultaneously: one at S-band with an uplink frequency of 2.1 GHz and one at X-band with an uplink frequency of 7.1 GHz. If plasma effects were small and if the transponder turnaround ratios for these two bands were the same, then the system would be able to eliminate first-order (i.e., $\propto f^{-2}$ but not those parts $\propto f^{-4}$) plasma-induced noise in the measured round-trip phase path. Unfortunately, neither of these assumptions is correct. Coronal scintillation will cause the phas locked loops of the ground station receiver to go in and out of lock intermittently. Substantially different spacecraft transponder turnaround ratios will cause an incomplete cancellation of the coronal contribution to the phase delay. (At S-band the turnaround ratio is $240/221 = 1.085$; at X-band the ratio is $880/749 = 1.175$.)

It is estimated (Koerner, 1980) that the baseline tracking system would provide a velocity measurement error of $\sim$0.3 millimeters per second near close encounter with the Sun. However, this performance should not be compared directly with the 0.2 millimeter-per-second tracking accuracy ordinarily achieved with S-band and spacecraft for which the ray path does not pass close to the Sun. The important difference is in the phase coherence of the usual tracking; phase coherence substantially enriches the information content of the resulting data.

The analysis of the tracking system accuracy that was presented at the October 1980 meeting was based on the assumption that the spacecraft was 1 AU behind the Sun. This assumption contributes in two significant ways to mismodeling:

(1) Signals transponded by STARPROBE when it is in front of the Sun at encounter will have passed through less plasma than those transponded by a spacecraft at the same Sun-Earth-spacecraft angle and 1 AU behind the Sun.[1]

(2) Signals transponded by STARPROBE at the Sun see essentially the same plasma on the uplink as they do on the downlink. Signals transponded by a spacecraft at 1 AU behind the Sun see different parts of the inhomogeneous plasma near the Sun because of changes that take place during the 1000 second Sun-spacecraft-Sun propagation time: the plasma moves radially at about 100 km/s, and Earth moves around the Sun at about 30 km/s.

The first-order plasma-induced delay is proportional to Nf^{-2}, where N is the columnar electron content of the signal path and f is the signal frequency. Thus the use of higher frequencies is desirable. Within K-band there are two frequency spans allocated to space communications. These are in the K_u (15.35 to 17.25 GHz) and K_a (33 to 36 GHz) sub-bands. The use of signals in one of these sub-bands makes possible several attractive tracking systems. Some of these are listed in Table 1-3. Unfortunately neither spacecraft equipment nor ground-based (i.e., DSN) equipment is currently available for these bands. The difficulty (cost) of adding such equipment has not yet been assessed.

1.4.1.2 Ranging

The second standard radio observable is ranging, i.e., the group delay of a signal returned to a tracking station by a spacecraft transponder. The present S-band system has an uncertainty of less than 2 m under "good" conditions. (By convention, when units of distance are used they refer to one way distance and when units of time are used they refer to round trip — i.e., two-way — propagation time.) It has been found during solar conjunction experiments that the ranging system produces useful data under propagation conditions somewhat worse than those that cause the Doppler system to fail. Thus ranging can add robustness to the STARPROBE Mission for which the tracking is marginal for the critical encounter phase.

---

[1] If we assume a model corona with density $\rho = ar^{-n}$, where r is the distance to the solar center, then the path from Earth to the spacecraft behind the Sun contains 4 times as much plasma as the path to STARPROBE for a simple model with $n = 2$. For a more realistic model with $n > 2$, the ratio is larger.

Table 1-3. Possible tracking configurations

Configuration	Bands[a]	
	Uplink	Corresponding downlinks
1	S	S
	X	X K
2	X	X S
	K	K
3	X	X
	K	K S
4[b]	X	X K
	K	K

[a] K band is assumed to be K_u. If K_a were also available, it could be used to [b] advantage.
Configuration 4 may violate DSN constraints.

A wider bandwidth system for use at X-band and above is now being considered. (The system cannot be used at S-band because of limits on the total bandwidth available for space communication in that part of the spectrum.) This new system would have substantially greater accuracy. Thus one can envision the proposed X-band high-accuracy system being used along with the old S-band system. From the S-band range τ_S and X-band range τ_X, one can form a linear combination τ_0 that is the vacuum-equivalent range, free (to first order) from the effect of the plasma:

$$\tau_0 = A\,\tau_x + B\,\tau_s$$

where $A = (1-\alpha^2)^{-1}$, $B = 1-A$, and α is the ratio of the S-band and X-band carrier frequencies. For $\alpha = 3/11$, $A = 1.08$ and $B = -0.08$. Similarly for the uncertainties, we find

$$\sigma_0^2 = A^2\,\sigma_x^2 + B^2\,\sigma_s^2$$

if the measurement errors are independent. Thus the measurements at the two frequencies make equal contributions to σ_0 at $\sigma_S/\sigma_X = \alpha^{-2} = 13.5$; a system with a single measurement uncertainty of 20 cm is reasonable. (The ranging system suffers from the same problems as does the doppler system as a result of the difference between the frequency multiplication ratios used by the spacecraft transponder for the two bands. The same solutions are applicable.)

A partially published study (Reasenberg and Shapiro, 1978) showed that ranging data (σ = 10 ns = 1.5 m) may be more useful than doppler data (σ = 0.1 mm/s) for the estimation of J_2 from STARPROBE tracking. It also showed a synergy between the two observables. However, this early study neglected spacecraft process noise (nongravitational acceleration) and thus should be repeated.

1.4.2 Drag Compensation System

The drag compensation system is the second of the technologies that are critical to the gravity and relativity physics aspects of the STARPROBE mission. At solar encounter the non-gravitational acceleration of an uncompensated STARPROBE spacecraft would be of order 10^{-4} m/s^2 = 10^{-5} g. By comparison, sensitivity studies have shown that the nominal objectives can be reached if the nongravitational acceleration is compensated, leaving a white acceleration noise with variance corresponding to $(10^{-10}\ g)^2 \cdot 60$ s. Although the white noise assumption is convenient for preliminary studies, eventually it must be replaced by a realistic model of the spacecraft process noise.

The nominal spacecraft design is three-axis stabilized and, of course, solar pointing. An alternative under consideration is a spinning solar-oriented spacecraft. The latter poses some problems which require evaluation:

(1) The attitude control system must precess the spacecraft as it passes through perihelion.

(2) Either the dish antenna must be despun, which would lose some of the advantages that were to be gained by spinning the spacecraft, or the antenna must be replaced by an electronically steerable array.

(3) The proof mass used by the drag compensation system must be housed in a sufficiently large cavity that it can "orbit around the spacecraft center of mass." A hydrogen maser on board the spacecraft would not be adversely affected by rotation rates as great as 150 rpm.

In the near solar environment it is expected that ionizing radiation will cause the proof mass to develop a charge. Several means have been proposed to mitigate this problem: (1) bathe the proof mass in UV light to promote discharge; (2) bathe the proof mass in visible light and coat it with a material whose work function is sufficiently low that discharge will be promoted; (3) include the unknown proof-mass charge in the estimation algorithm, apply low frequency ac to the housing electrodes, and detect the corresponding proof-mass acceleration.

Regardless of the details of the drag compensation system, it appears that there will be a class of estimation and control calculations which could either be done in real-time on board the spacecraft or after the fact on the ground. It is a choice between a feed-back and a feed-forward system. From the point of view of the experimenter, it is of course more convenient to have these calculations done on board and thus for them to be "transparent" in the data analysis. However, this choice is more reasonably based on an evaluation of other factors: (1) spacecraft simplicity, (2) total mission cost, (3) communications channel reliability, and (4) impact on communications of additional engineering data required to support the ex post facto analysis of errors or biases in the real-time drag compensation system.

1.4.3 Hydrogen Maser

A scientifically important redshift experiment could be conducted by STARPROBE if the spacecraft carries a hydrogen maser clock. However, such a clock would have to be designed to work unattended for an extended period of time. Ordinarily hydrogen masers are maintained at intervals short compared to the Earth-Jupiter-Sun transit time for the proposed mission.

The benign environment of space should in principle permit the clock drift rates to become stable; some sources of noise will be absent. However, our cumulative experience with hydrogen masers in orbit is about 2 hours, and comes from Gravity Probe A as discussed in Section 1.2. Prelaunch orbital simulations provide a considerable extension of this experience. Finally, the effects of solar encounter need to be considered. Although the solar environment does not appear to pose a problem for a hydrogen maser clock, further analysis seems warranted.

In hydrogen masers intended for laboratory use, there are several components or systems that have had to be redesigned to function in space. Among these are (1) the hydrogen dissociator, (2) the cavity thermal control system, and (3) the waste-hydrogen scavenger. Recently, the physical dimensions and power requirements have been reduced also. The integration of all of the recent design improvements into a single maser and the long-term test of that maser is needed.

1.5 RECOMMENDATIONS

We find that the STARPROBE Mission offers the opportunity to achieve several significant scientific objectives. Our preliminary examination shows that the prime objectives can probably be achieved by implementation of a design similar to that already discussed. Further scientific benefit both in accuracy and in breadth of subject matter investigated would come from improved systems performance. Below we discuss briefly 11 recommendations for further investigations and studies in support of the proposed mission.

1.5.1 Sensitivity Studies with Ranging Data

New sensitivity studies should be performed to investigate the use of ranging data in addition to Doppler data. These studies should include ranging data that would be obtained from both the present system and more advanced systems that could be available. A realistic model of the effects of the solar corona would be an important tool for such a study. For the results to be useful, it is essential that the sensitivity study be performed with a large parameter set such as would be used in the analysis of real data: an abridged parameter set will yield deceptive results.

1.5.2 Sensitivity Studies for the Detectability of Physical Effects

A study should be performed to determine the sensitivity of the data to the following quantities in addition to those that have previously been included in such studies: spherical harmonic coefficients C(2,2), S(2,2), C(2,1), S(2,1) and J_4; J_2 (periodic), assuming the frequency and phase are known; L, the angular momentum of the Sun; and a coefficient for the gravitational redshift.

1.5.3 K-band Tracking

Investigate the feasibility of a K-band downlink from (or K-band uplink to) the STARPROBE spacecraft.

1.5.4 Spacecraft Doppler Extractor

The nominal dual-band tracking system fails to completely cancel the effect of interplanetary plasma because the S-band and X-band transponder turn-around frequency ratios are different. However, more clearly complete cancellation could be achieved if the spacecraft were equipped with a Doppler extractor which would measure F_p, the uplink contribution from the plasma: $F_p = F_S - \alpha F_X$, where α is the ratio if S-band to X-band frequencies at the DSN transmitter.

1.5.5 Coronal Model

Develop a model of the effect on the telecommunications links of the solar corona for a spacecraft near but in front of the Sun, corresponding to the planned STARPROBE geometry. A suitable statistical model could be used not only to calculate the plasma contribution to a single link, but also to estimate the uplink-downlink correlation as a function of doppler integration time. The study should include fading and cycle slipping; the latter should be evaluated as a function of receiver loop stress, since the loop stress can be relieved by programming the DSN transmitter frequency to yield a constant frequency at the spacecraft.

1.5.6 Proof-Mass Charging Effect

Unmodeled charge on the drag-compensation proof mass would result in biased spacecraft acceleration. Such a charge may develop as a result of ionizing radiation in the solar vicinity and could be the principal source of process noise. This phenomenon should be modeled and the model tested as realistically as possible by exposing a "mockup" of the system to radiation.

1.5.7 Spinning Spacecraft Option

If the spinning spacecraft option is to be given further consideration, the effect of spin on the gravity experiments needs to be considered. Of particular importance is the effect of rotation on the characteristics of a hydrogen maser clock.

1.5.8 Long-Term Behavior of Hydrogen Masers

Although it is believed that a hydrogen maser clock can be constructed to run unattended for a period of years, this feat has not yet been accomplished. Funding should be provided to construct one or more clocks and to observe clock behavior over a period of years. In addition to testing the long-term survivability of unattended clocks, the study could address aging processes and the evolution of the clock's stability.

1.5.9 Effect of Hydrogen Maser on the Detectability of Physical Effects

A hydrogen maser on the spacecraft would make possible high-quality "one-way" observables, both delay and Doppler. An evaluation should be made of means by which these observables can be implemented without interference with the usual tracking system. The noise characteristics of the new observables should be determined. A sensitivity study should be performed to determine the utility of the proposed new data for estimating such quantities as J_2, J_4, β, γ, and L.

1.5.10 Alternate Spacecraft Trajectory Options: A One-Year Orbital Period

The nominal mission design does not include a second solar encounter. However, there are three ways in which the spacecraft could be put in a one-year solar orbit: (1) a drag chute could be used during solar approach; (2) a Solar Electric Propulsion system could be used both before and after (but not during) encounter; and (3) a chemical propulsion system could be used shortly after encounter. A multiencounter mission offers many advantages including redundancy of data, a reduction of the reliability requirement of the tracking system, and a chance to distinguish between normal and transient solar behavior.

1.5.11 Sensitivity Studies for the Detectability of the Parameters of the Jovian System

These studies should include an investigation of the options to encounter one or more of the satellites. It should also be determined whether the mission requirements for ΔV at Jupiter permit any degrees of freedom to be specified by considerations of Jupiter science.

1.6 ACKNOWLEDGMENT

The authors gratefully acknowledge suggestions and contributions from J. Barnes, P. Callahan, N. Cohen, G. Colombo, T. Croft, F. Estabrook, P. Joss, P. Morrison, K. Nordtvedt, J. Underwood, and A. Zygielbaum.

1.7 REFERENCES

Arp, H. C., In: Handbuch der Physik, Ed. S. Flugg, Vol. 51, Springer-Verlag, Berlin, 75, 1958.

Bahcall, J. N., Comments on Astrophysics, 8, 37, 1978.

Bahcall, J. N., and Davis, R., Science, 191, 264, 1976.

Bahcall, J. N., Lubow, S. H., Huebner, W. F., Magee, N. H., Jr., Merts, A. L., Argo, M. F., Parker, P. D., Rozsnyai, B., and Ulrich, R. K., Phys. Rev. Lett., 45, 945, 1980.

Barnes, J. A., Sargent, H. H., III, and Tryon, P. V., "Sunspot Cycle Simulation Using a Narrowband Gaussian Process," NBS Technical Note 1022, U.S. Government Printing Office, Washington, 1980a.

Barnes, J. A., Sargent, H. H., III, and Tryon, P. V., In The Ancient Sun, Ed. R. O. Pepin, J. A. Eddy, and R. B. Merril, Pergamon, New York, 1980b.

Christensen-Dalsgaard, J., and Gough, D. O., In: Nonradial and Nonlinear Stellar Pulsation, Ed. H. A. Hill and W. A. Dziembowski, Springer-Verlag, New York, 1980.

Dicke, R. H., and Goldenberg, H. M., Phys. Rev. Lett., 18, 313, 1967.

Dicke, R. H., and Goldenberg, H. M., Ap. J. Suppl., 27, 131, 1974.

Dicke, R. H., Proc. Nat. Acad. of Sci., 78, 1309, 1981.

Eddy, J. A., Science, 192, 1189, 1976.

Gree, G., Fossat, E., and Pomerantz, M., Nature, 288, 541, 1980.

Hill, H. A. and Stebbins, R. T., Astrophys. J., 220, 471, 1975.

Hill, A. H. and Caudell, T. P., Mon. Not. R. Astr. Soc., 186, 327, 1979.

Hubbard, W. B., MacFarlane, J. J., Anderson, J. D., Null, G. W., and Biller, E. D., J. Geophys. Res., 85, 5909, 1980.

Iben, I. Jr., Ann. Rev. Astron. and Astroph., 5, 571, 1967.

Johnson, W. W., Winget, D. E., Douglass, D. H., and VanHorn, H. M., Nonradial and Nonlinear Stellar Pulsation, Ed. H. A. Hill and W. A. Dziembowski, Springer-Verlag, New York, 1980.

Joss, P. C., Astrophys. J., 191, 771, 1974.

Koerner, M., results presented at the SPAHGRC meeting, October 1980.

Kraft, R. P., in Spectroscopic Astrophysics, Ed. G. H. Herbig, UC Press, Berkeley, 385, 1970.

Maeder, A., and Mermilliod, J. C., Astron. Astrophys., 93, 136, 1981.

Misner, C. W., Thorne, K. S., and Wheeler, J. A., Gravitation, Freeman, San Francisco, 1973.

Newman, M. J. and Rood, R. T., Science, 198, 1035-1037, 1977.

Popper, D. M., Ann Rev. Astron. and Astroph., 18, 115, 1980.

Reasenberg, R. D., in Cosmology and Gravitation, Ed. P. G. Bergmann and V. De Sibbata, Plenum, New York, 1980.

Reasenberg, R. D. and Shapiro, I. I., in A Close-up of the Sun, Ed. M. Neugebauer and R. W. Davies, Jet Propulsion Laboratory, Pasadena, 19, 1978.

Reasenberg, R. D., Shapiro, I. I., MacNeil, P. E., Goldstein, R. B., Breidenthal, J. C., Brenkle, J. P., Cain, D. L., Kaufman, T. M., Komarek, T. A., and Zygielbaum, A. I., Astrophys. J. Lett., 234, 219, 1979.

Sagan, C. and Mullen, G., Science, 177, 52-56, 1972.

Saio, H., and Wheeler, J. C., Astrophys. J., 242, 1176, 1980.

Sandage, A. R., Ap. J., 125, 435, 1957.

Scherrer, P. H., Wilcox, J. M., Severnyi, A. B., Kotov, V. A., Tsap, T. T., Astrophys. J., 237, L97-L98, 1980.

Schwarzschild, M., Structure and Evolution of Stars, Princeton Univ. Press, Princeton, 1958.

Tassoul, J.-L., Theory of Rotating Stars, Princeton Univ. Press, Princeton, 1978.

Ulrich, R. K., Astrophys. J., 188, 369, 1974.

Ulrich, R. K., and Hawkins, Astrophys. J., in press, 1981.

Vessot, R. F. C., Levine, M. W., Mattison, E. M., Blomberg, E. L., Hoggman, T. E., Zystron, G. U., Farrell, B. F., Decher, R., Eby, P. B., Baugher, C. R., Watts, J. W., Teuber, D. C., and Wills, F. D., Phys. Rev. Lett., 29 Dec. 1980.

Weinberg, S., Gravitation and Cosmology, Wiley, New York, 1972.

Wheeler, J. C., Astrophys. J., 234, 569, 1979.

Wheeler, J. C., Comments on Astrophysics, 8, 133, 1979.

Wilson, O. C., and Skumanich, A., Astrophysics. J., 140, 1401, 1964.

1.8 MEMBERS OF THE STARPROBE AD HOC GRAVITY AND RELATIVITY COMMITTEE

John Anderson (JPL)
Giuseppe Colombo (CfA, JPL, U. of Padua)
Daniel DeBra (Stanford)
Kenneth Nordtvedt (Montana State U.)
Robert Reasenberg (MIT), Chairman
Irwin Shapiro (MIT)
Roger Ulrich (UCLA)
Robert Vessot (CfA)

CHAPTER 2

PARTICLES AND FIELDS SCIENCE

F. L. Scarf, Chairman, TRW
B. E. Goldstein, STARPROBE Study Team, Jet Propulsion Laboratory
A. Barnes, Ames Research Center
W. C. Feldman, Los Alamos National Laboratory
L. Fisk, University of New Hampshire
G. Gloeckler, University of Maryland
S. M. Krimigis, Johns Hopkins University (Applied Physics Laboratories)
K. N. Ogilvie, Goddard Space Flight Center
C. T. Russell, University of California, Los Angeles

2.0 INTRODUCTION

Our present understanding of the Sun is based largely on analysis of remote observations of the solar surface and corona. Extremely important local measurements of the solar wind plasma, the interplanetary magnetic field, the energetic particle population and associated wave-particle interactions are also available, but none of the spacecraft that provide these direct observations have yet traversed the region within the 0.3 AU perihelion distances of Helios 1 and 2. Thus, from the solar surface out to a distance of about 60 solar radii, our present knowledge of coronal plasma processes essentially consists of a set of indirect extrapolations and model-dependent theoretical inferences.

This unexplored region is an extremely important one, however, and *in situ* measurements are needed to provide critical information on the coronal energy balance and the origin of the solar wind and solar cosmic rays. Some of the problem areas that are already known to be of great significance are summarized in Fig. 2-1 and discussed briefly below, but it is important to note the proposed STARPROBE mission is truly exploratory, so that we cannot expect to be able to anticipate the complete science return beforehand. Nevertheless, we consider a nominal mission with a perihelion distance of 4 $R_\odot$, we tabulate several primary science goals, and we indicate in Fig. 2-1 where the related critical measurements should be obtained.

2.1 PARTICLES AND FIELDS SCIENTIFIC OBJECTIVES

2.1.1 Coronal Processes: Origin of the Solar Wind

STARPROBE will provide an opportunity to answer several unresolved fundamental questions about the origin and acceleration of the solar wind. This general problem has been a focus of theoretical activity ever since the solar wind concept was established by Parker, and it has a significance that ranges far beyond the specialty of solar wind studies. The solar wind process typifies the escape of matter from a large class of stars, and probably other objects as well. There would seem to be little hope of understanding the general problem of astrophysical mass loss until we understand what causes the expansion of the solar wind. In addition, it now seems quite likely that the complex changes in solar wind activity are related to variations in Earth's weather and climate. For example, it appears that solar activity was depressed during the Maunder minimum. We have no good idea of what the solar wind was doing at that time, in large part because we do not yet really understand how the solar wind is accelerated.

The mechanisms of acceleration and heating of the solar wind remain elusive because observations from only two relevant regions are available: the inner corona, and the asymptotic coasting region of the wind ($r \geq 60\ R_\odot$, the perihelion of Helios). Therefore, theoretical models are constrained by data at essentially only two points, and several models with quite different assumptions about the acceleration mechanisms are equally consistent with the available

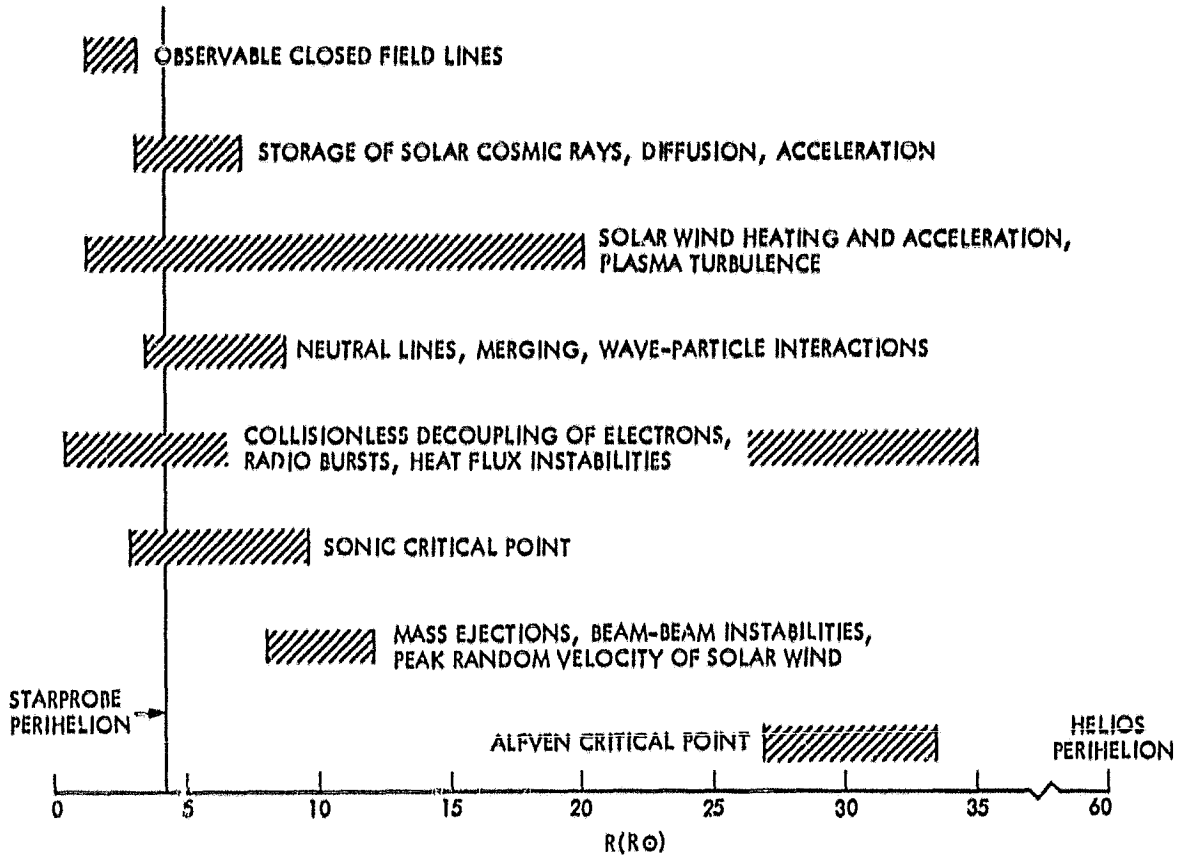

Fig. 2-1. STARPROBE science objectives, fields and particles phenomena

observations. Generally speaking, all models give flat velocity profiles beyond about 20 $R_\odot$, and, in fact, typical day-to-day variations in speed observed near 1 AU are larger than the variation between 0.1 and 1 AU predicted by any model. Thus, velocity measurements outside of, say, 20 $R_\odot$ will not be of primary value for determining the acceleration mechanisms.

In contrast, plasma measurements for r between 4 and 20 $R_\odot$ will yield velocity data of extreme significance. Because in a single encounter the measurements will be a convolution of variations in heliocentric distance, latitude, and longitude, as well as temporal variations, and because the outer corona is likely to be very inhomogeneous, STARPROBE measurements of velocity alone will not yield a simple radial profile v(r), and by themselves, they probably will not give a definitive picture of solar wind acceleration. However, even these partial measurements should restrict the alternatives in an important way. For example, at present it is not at all clear where the flow makes the transition from subsonic to supersonic. Conventional spherical models place the sonic "critical point" somewhere between 2 and 10 $R_\odot$. Other models, which suggest that the wind may come from rapidly diverging "magnetic nozzles," place the critical point almost at 1 $R_\odot$. Some of these uncertainties are indicated in the "critical point" boxes of Fig. 2-1. On the other hand, studies of scattering of radio waves from the Viking lander (Taylor et al., 1980) during superior conjunction suggest

that the solar wind speed may remain low, possibly subsonic, out to beyond 10 $R_\odot$. In situ measurements of velocity by STARPROBE will clarify which of these disparate pictures is most typical of the Sun, thereby placing a major new constraint on acceleration mechanisms.

We expect that the region inside 20 $R_\odot$ will be highly turbulent and nonuniform. These characteristics are extremely important properties of the corona; however, it is also important to note that the turbulence, as well as the temporal variations associated with mass ejection (see Fig. 2-2) and the variations associated with spatial nonuniformities (see Fig. 2-3), can seriously complicate the hydrodynamic interpretation of velocity measurements. We anticipate a fluctuating component of the flow velocity of order 100-200 km/sec near perihelion, and measurements of bulk plasma parameters may not distinguish true turbulence from apparent fluctuations due to the sampling of a number of steady streams of varying speed. However, comprehensive measurements of the local state of the plasma (magnetic field, thermal characteristics, suprathermal particle population)

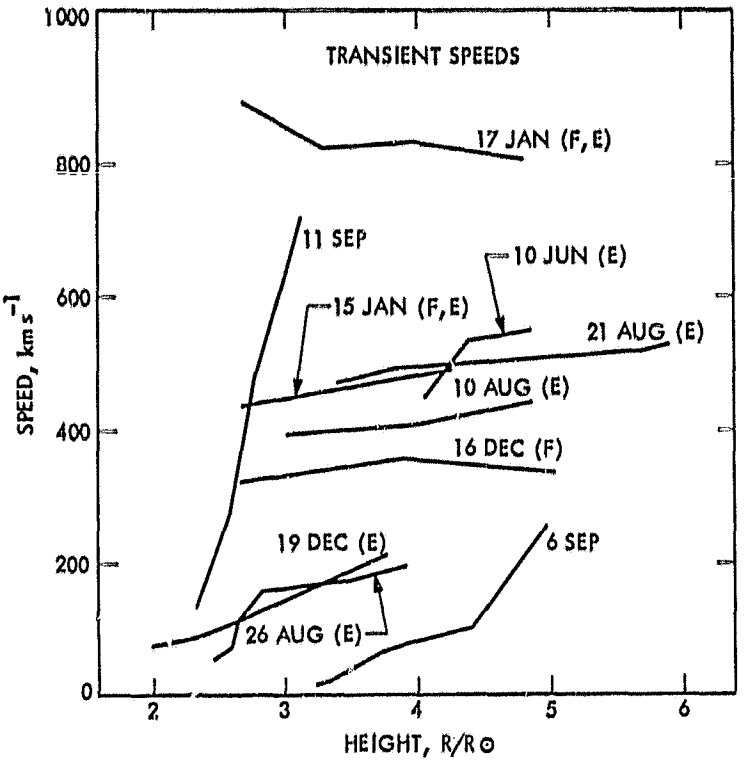

Fig. 2-2. Speeds of loop transients' leading edges versus distance from Sun center. Each point is plotted at the mid-height of the interval used to determine it. The points for each event are connected to guide the eye. All but the January (1974) events occurred in 1973. An F or E after the date indicates that the ejection was associated with a flare or eruptive prominence, respectively. (From "Mass Ejections," D. M. Rust et al., pp. 273-339, in Solar Flares, ed. P. A. Sturrock, Colorado Associated University Press, 1980.)

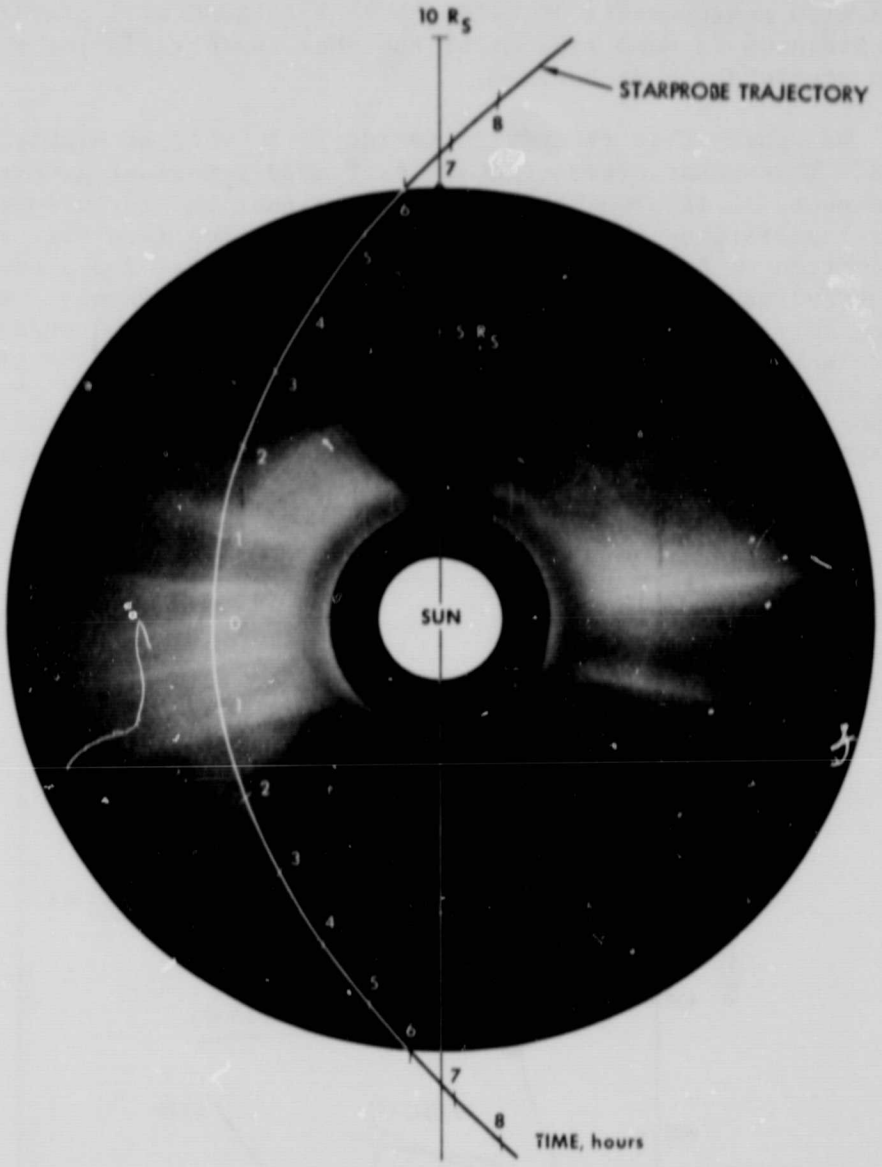

Fig. 2-3. STARPROBE, near perihelion, 4 R_S trajectory, view perpendicular to orbit

will allow us to identify streams of varying speed and help to differentiate between spatial and temporal variations.

Theoretical studies suggest that the proton temperature profile is especially sensitive to the main heating and acceleration processes that drive the wind. The extreme cases that can be imagined are (1) extended heating out to 20 $R_\odot$ or beyond, and (2) essentially adiabatic expansion beyond a coronal base near the solar surface. If either of these extremes obtains, it should be apparent in STARPROBE temperature data, and for intermediate cases, the range of possible alternate models will be severely restricted.

Correlated plasma, magnetic field, and plasma wave measurements will also provide an opportunity to confirm or deny some of our ideas about extended heating and acceleration by hydromagnetic turbulence and wave-particle interactions. Two extreme mhd models would be that the turbulence is entirely Alfvénic or entirely magnetoacoustic. Alfvénic turbulence is known to be present far out in the solar wind, but its intensity in the acceleration region is unknown. Magnetoacoustic and plasma wave turbulence are both strongly dissipative and could exist at very significant levels only inside about 20 $R_\odot$. It should be fairly straightforward to distinguish the two kinds of mhd turbulence on STARPROBE, both because their spatial distribution and decay are qualitatively different, and because their local properties (polarization, cross-correlations, etc.) are distinctive and well understood. These data would tell us whether there is a turbulent mhd envelope, and whether it consists mainly of Alfvénic or magnetoacoustic fluctuations, or a mixture of both, or something else entirely. Plasma wave measurements will also tell us about beam-beam and beam-plasma instabilities, wave-particle interactions associated with magnetic merging, collisionless decoupling of electrons, and heat-flux instabilities.

Although the problem of the acceleration of the solar wind is fundamental for progress in the field of coronal and interplanetary physics, many other extremely important problems can only be resolved with STARPROBE. These include a determination of (1) the character of the expansions within streamers and above active regions, (2) the sharpness of boundaries between flows close to the Sun which evolve from different coronal regions, (3) the origin of various slow speed flows including those density-enhanced flows observed at 1 AU which do not appear to result from a compression in interplanetary space, (4) the extent of heavy element fractionation as well as the mix of physical processes causing spatial and/or temporal abundance variations, and (5) the scale sizes of inhomogeneities. The STARPROBE mission can also provide important new information on the solar wind angular momentum flux and the subsequent solar spin down rate.

2.1.2 Energetic Particle Phenomena

The study of solar energetic particle phenomena is of primary importance not only because these particles produce very significant geophysical effects and associated flares generate many secondary solar phenomena, but also because these energetic particles offer the opportunity to study processes of central importance to astrophysics and the physics of plasmas. The solar flare processes, in particular, include energy storage and its sudden release in magnetized plasmas, particle acceleration, explosive heating and evaporation, mass ejection and shock waves, generation of radio noise, and formation of high temperature plasmas. Studies of the energy spectra and composition of energetic particles from the Sun provide essential information on mechanisms responsible for their acceleration and on the regions where they are accelerated and confined and released.

The present inferences from measurements made beyond 60 $R_\odot$ suggest complicated pictures such as that shown in Fig. 2-4, which is adapted from a discussion by Roelof (1974). Energetic particles are presumably stored in magnetic bottles, and they escape along neutral lines as coronal conditions vary. For the region within 10 $R_\odot$, important questions that require direct

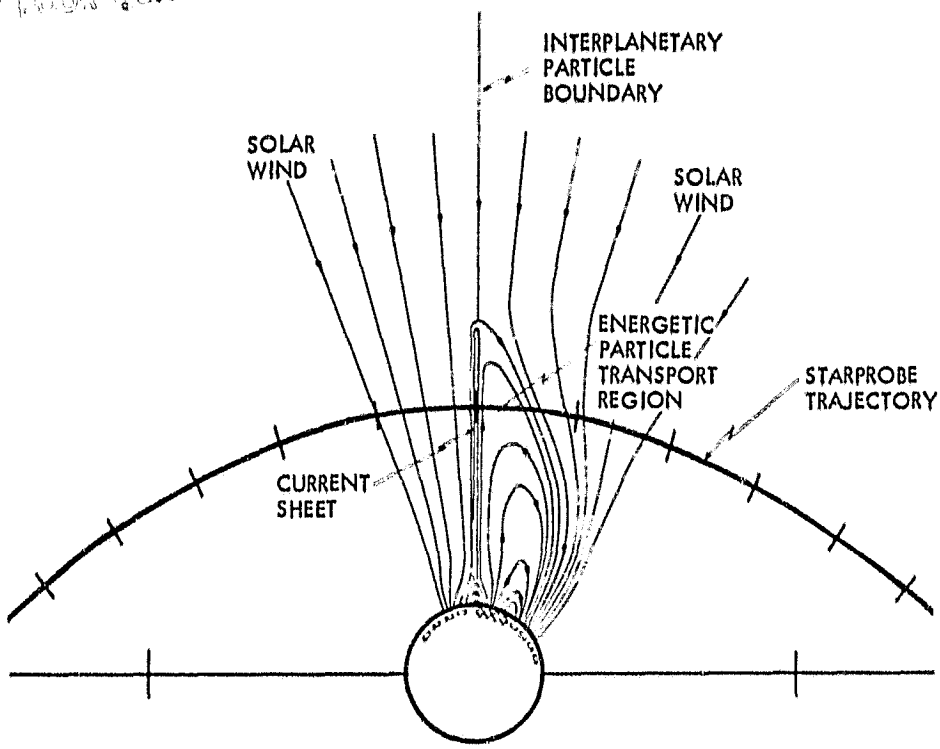

Fig. 2-4. Coronal structure and the solar wind (from E. Roehof, 1974)

measurements involve the determination of the locations of and conditions in the acceleration regions, the proximity to open field lines, the associated wave-fields, the scale sizes of the inhomogeneities, and the compositional variability in the surrounding corona. The STARPROBE trajectory plot in Fig. 2-4 shows that the spacecraft will pass directly through the acceleration/storage region, so that local information on these fundamental processes will be obtained.

Additional new first-order information on shock acceleration, energy losses and solar radio bursts, interplanetary propagation, and diffusion will also be provided on the mission segment from 10 $R_{\odot}$ to 60 $R_{\odot}$.

2.2 MEASUREMENTS AND TECHNIQUES: PLASMA PHYSICS AND ENERGETIC PARTICLES

2.2.1 Baseline Requirements

The Committee on Solar and Space Physics of the Space Science Board recently discussed the need for a program of measurements close to the Sun. In the 1980 NAS report, Solar System Space Physics in the 1980s: A Research Strategy, the committee noted that

> The first in situ determinations of the density, temperature, velocity, and composition of the solar wind near its subsonic-supersonic transition region: the large-scale weak magnetic field, coronal electron and hydromagnetic wave heat fluxes; energetic particle energy, angular, and mass spectra; and plasma-wave turbulence will provide qualitatively new information critical to understanding the coronal energy balance, solar-wind generation, and solar cosmic rays.

This brief statement clearly indicates that the science payload for the STARPROBE mission must include solar wind plasma probes and energetic particle detectors capable of providing complete information on ion composition as well as angular distributions for ions and electrons. The payload must also include a magnetometer and a plasma wave instrument with full coverage for anticipated field variations and changes in characteristic frequencies over the primary measurement range from perihelion out to at least $r \approx 60\ R_\odot$.

For a perihelion distance of $4\ R_\odot$, we expect the local wind speed to be no less than 50 km/sec, the electron and ion temperatures to be no greater than about 10^7 K, and the local plasma density and local magnetic field strength to be less than 10^6 electrons/cm^3 and 10^5 gamma, respectively. These numbers provide inner coronal bounds for the ranges of the plasma probe and magnetometer, and they also yield a suitable upper bound near 20 MHz for the plasma wave spectral coverage (f(MAX) is on the order of two times the electron plasma frequency f_{pe}, where $f_{pe} = 9000\sqrt{N}$ Hz). The $60\ R_\odot$ parameters set the other ends of the instrument ranges; Table 2-1 contains a summary of the baseline measurements in the space plasma physics area, and Table 2-2 shows the associated spacecraft requirements.

The instrumental requirements in the energetic particle area can be specified in somewhat greater detail based on extrapolations from our present fairly detailed knowledge of measurements beyond 0.3 AU. The baseline requirements are summarized in Table 2-3.

2.2.2 Field of View Considerations

2.2.2.1 Measurement Program

The measurements to be performed on STARPROBE will lead to canonical numbers to be used to test theories of coronal structure, solar wind acceleration,

Table 2-1. STARPROBE required measurements: space plasma physics

Quantity	Range	Precision	Time Resolution
Magnetic field[a]	1 γ - 1G	2%	20 meas/sec
Solar wind - 3D			Few sec/meas
Speed	50 - 100 km sec^{-1}		Few sec/meas
Density	1 - 10^6 cm^{-3}	10%	Few sec/meas
Electron temp	10^5 - 10^7 K	2%	Few sec/meas
Ion temp	10^5 - 10^7 K	2%	Few sec/meas
Ion composition	H - Fe	1 AMU up to C	Few sec/meas
Suprathermal particles			
Electrons	5 keV - 250 keV		Few sec/meas
Ions	5 keV - 500 keV		Few sec/meas
Plasma waves			
E	1 Hz - 20 MHz	3%	Few sec/meas
M	1 Hz - 20 MHz	3%	Few sec/meas

[a]High data rate burst mode recordings are desirable.

charged particle propagation, turbulence, and many other subjects for years to come. Because of the danger of error, every possible effort must be made to conduct the best measurement program possible at the time when the experiments are designed. For the plasma experiments, this means three-dimensional measurements of the velocity distribution functions must be carried out as frequently as possible on as many plasma species as possible throughout the mission. Because of its importance for solar wind theory, the region between 10 and 60 solar radii is as crucial as the one between 4 and 10 solar radii. One of the most serious constraints put upon the spacecraft for this mission is that it must provide for the plasma instrument's field of view to allow the required measurement program to be carried out.

Table 2-2. Spacecraft requirements

Quantity	Requirement
Look angles	Solar wind instruments must look in solar direction outside 10 $R_\odot$. Most of 4 π should be covered, especially for electrons.
Magnetic field	Spacecraft field should be no more than 1% of magnetometer range in use at any time in mission.
Spacecraft potential	Should be an equipotential with $\Delta\phi$ less than 10 eV.
Telemetry requirements	10 kb/sec at closest approach; larger at other distances for readout of tape recorder. Waveform burst mode should be available.
Electromagnetic and electrostatic cleanliness	Voyager-class EMC and ESC controls should be imposed.

2.2.2.2 Supersonic and Subsonic Flow

An important aspect of the STARPROBE mission is that it will be required to measure accurately in both sub- and supersonic flows. In the solar wind near Earth, for example, because of their high thermal speeds, the electrons are subsonic, and they remain in this regime all the way to 4 solar radii. The ions, however, are characterized by a Mach number of approximately 5 to 8 at 1 AU, but become subsonic at a distance (not precisely known) of perhaps 5 to 10 solar radii (see Fig. 2-1). This situation is considerably complicated by the fact that, close to the Sun, the speed of the spacecraft with respect to the Sun is comparable to or exceeds the solar wind speed, resulting in large aberration (see discussion below).

In general terms, because particles in a subsonic stream may approach the spacecraft from all directions, exclusion of part of the solid angle of a detector by part of the spacecraft (such as the heat shield) may not be too serious a matter, provided the excluded part is not large. However, the situation is reversed in supersonic flow, and obscuration of a relatively small part of 4π may be fatal if it is in the direction of the relative velocity of the solar wind with respect to the spacecraft at any time during the mission.

2.2.2.3 STARPROBE Situation

Since the purpose of the sunshield is to provide shelter for the spacecraft, the instruments must be situated behind it with respect to the Sun. Supersonic flow from the solar direction, which occurs for ions beyond a

Table 2-3. Energetic particles experiment complement for STARPROBE

Detector designation	Energy range	Particle species	Resolution	Geometry[a] factor cm^2sr	Field of view, deg	Bit[b] rate, kbs
Charge-energy mass spectrometer	20-300 keV/Q	ions	$\frac{\Delta M}{M} \sim 0.2$	2×10^{-3}	7×55	1
			$\frac{\Delta E}{E} \sim 0.1$			
			$\frac{\Delta Q}{Q} \sim 1$			
Medium energy particle analyzer (MEPA)	0.05-10 MeV/nuc	ions	$\frac{\Delta M}{M} \sim 0.5$	2×10^{-2}	20	1
			$\frac{\Delta E}{E} \sim 0.5$			
	0.01-1 MeV	electrons	$\frac{\Delta E}{E} \sim 0.2$	1	40	1
High energy particle analyzer	10-100 MeV/nuc	ions	$\frac{\Delta M}{M} \sim 0.2$			
	1-10 MeV	electrons	$\frac{\Delta E}{E} \sim 0.2$			

[a]Geometry factors depend on solar particle environment model.

[b]These refer to instruments with single detector heads on a spinning platform. A minimum of two will be required for the spectrometer even on a spacecraft with a spinning platform: one to view the solar direction through an electrostatic deflector, and one for all other directions.

heliocentric distance of a few solar radii, will appear to be "centered" about the aberrational direction (Fig. 2-5). According to the best presently available information, solar wind flow will be sufficiently aberrational so as to be observable from behind the sunshade near closest approach, but a region occurs between the limit of present knowledge, at 80 $R_\odot$, and about 10 $R_\odot$ where plasma ions can only be detected by one of the following methods:

1. By observing through holes in the heat shield.

2. By extending a platform so that the instrument "sights" over the edge of the spacecraft.

3. By deflecting the ions behind the sunshade by an electrostatic deflection system.

It must be noted that this requires that, in the first two cases, the entrance aperture of the instrument, and, in the last case, part of the deflection system must be exposed to a large heat load. We note that if the experiment can observe through a hole in the heat shield, it is not subject to the full heat load to which the heat shield is exposed. Since the deflection system may be made of perforated or mesh material and need not be attached to the experiment, this solution is attractive at first sight.

2.2.2.4 Field of View Using Apertures in the Heat Shield

Due to the distance from the hole to the sensor (≈1M) and the restrictions placed on the hole diameter by thermal considerations, this method does not provide adequate viewing for distribution function mapping at low and moderate Mach numbers and will not be considered further.

2.2.2.5 Field of View Provided by Viewing Around the Heat Shield

This method entails mounting the experiment on a moving platform whose position is adjusted during the flight to provide an adequate field of view. The technical problems (weight, cg, cost, etc.) would be a significant constraint on the spacecraft, but can be overcome. The principle is shown in Fig. 2-6. It will be seen that a single sensor is markedly inferior to two sensors in terms of coverage when the spacecraft is between 0.3 AU and the distance at which aberration makes the extension unnecessary. Thus, despite the complexity of platforms, this method has to be considered as one alternative.

2.2.2.6 Field of View Provided by a Spinning Extendable Platform

This solution requires that the experiment be mounted on an extendable boom, spinning about the axis of the heat shield, and be gradually withdrawn as the Sun is approached, in such a way as to provide an adequate field of view for the expected supersonic ion flow (Fig. 2-6).

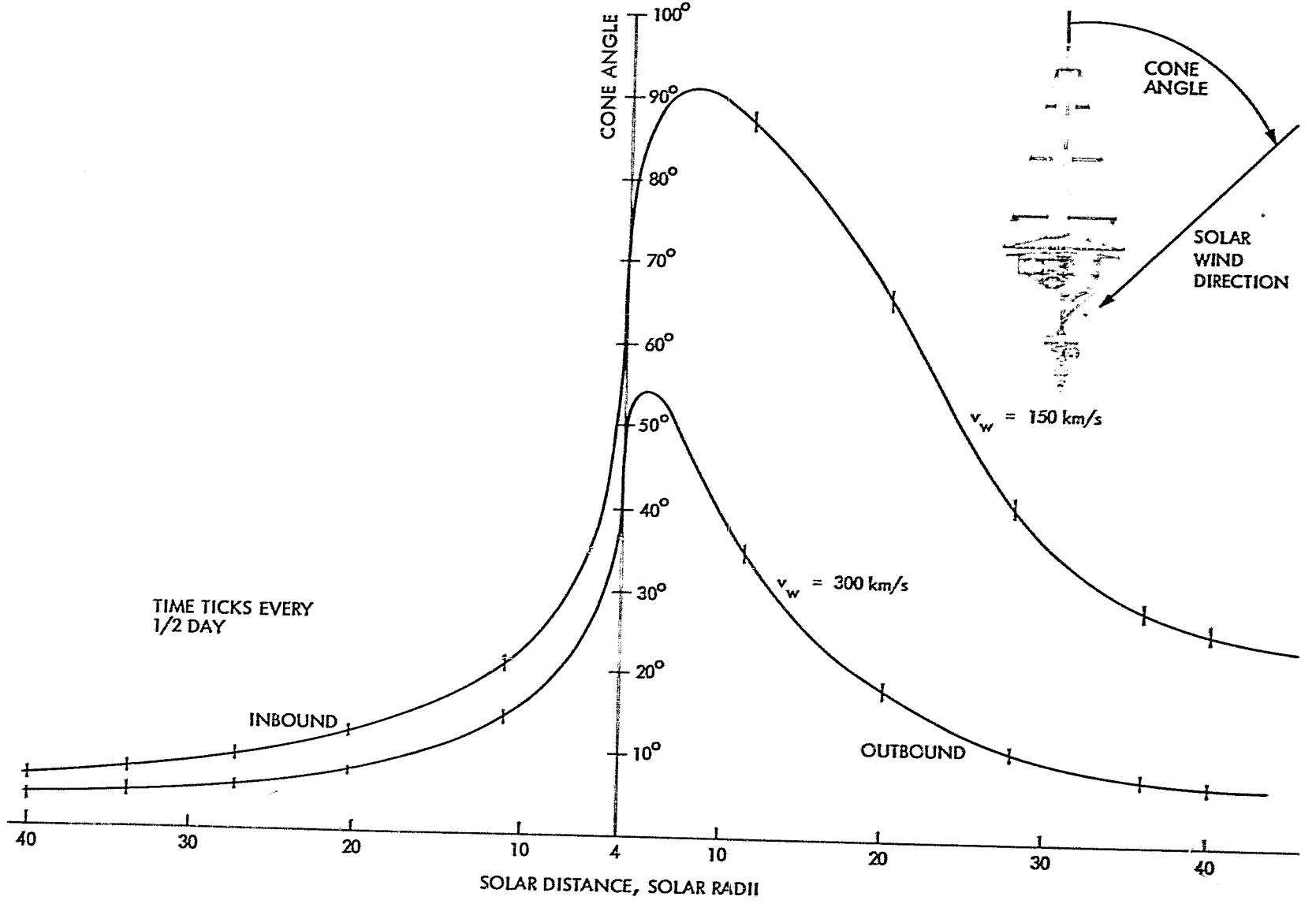

Fig. 2-5. Apparent direction of solar wind from STARPROBE

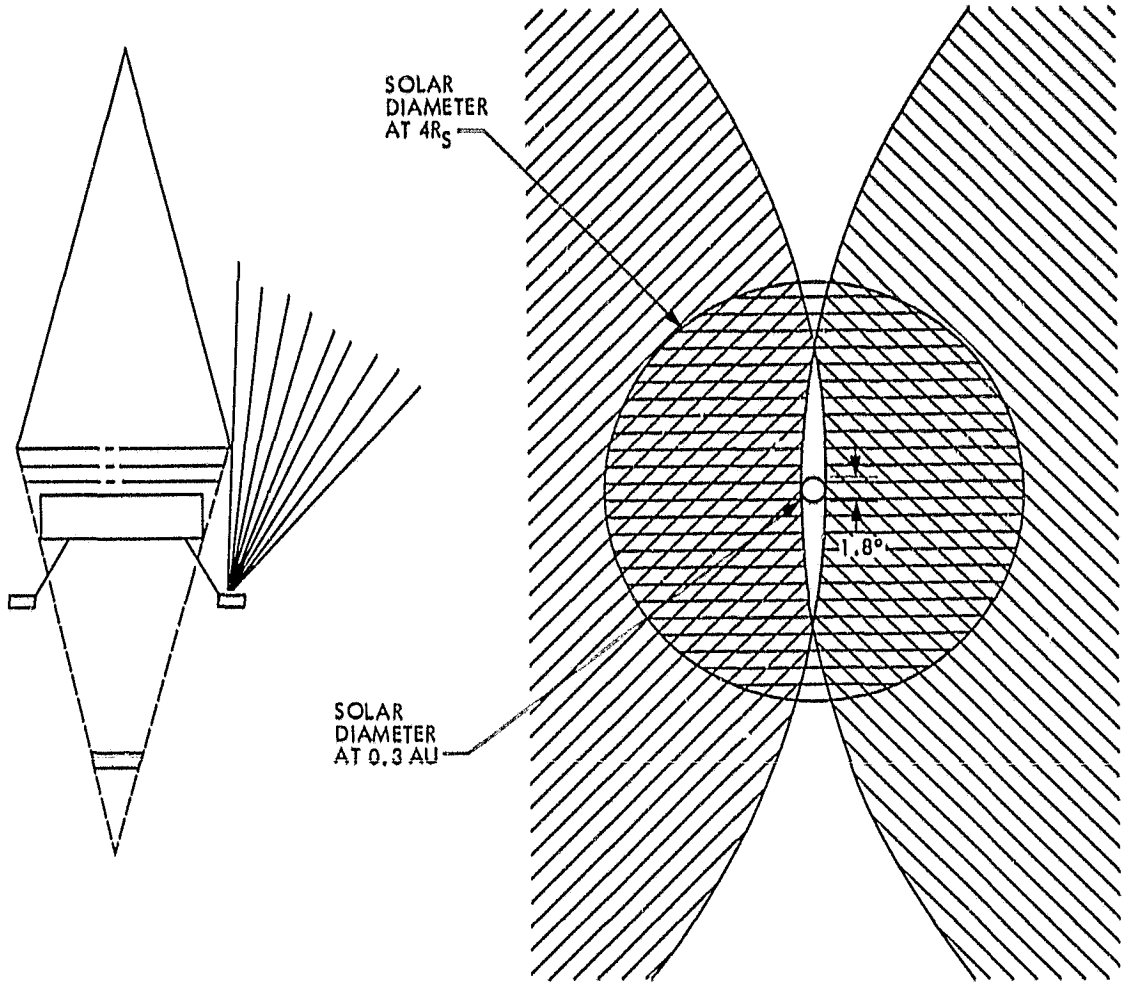

Fig. 2-6. Field of view provided by viewing around the heat shield: (a) instrument on platform beyond umbra, (b) field of view coverage for two instruments

2.2.2.7 Electrostatic Deflection

For this solution, an electrostatic deflection system (made of tungsten) causes a sample of the solar wind ions to be observable by an instrument mounted behind the shield (Fig. 2-7). The technology required for this solution exists but has never been used in space heretofore. Since the deflection suffered by an ion is a function of the potential supplied to the deflector, the latter becomes a part of the instrument. One can imagine a single deflection system that has a number of output slits, each of which supplies ions to a detector, so that faster measurement cycling can be achieved. Close collaboration between experimenters and spacecraft design staff would be required, since a very good knowledge of the precise properties of the deflector is required to convert ion distribution functions measured at the output of such a device back to the ambient medium. However, measurements during cruise under relatively well-known conditions would be possible. There are several potential problem areas, including thermionic emission, scattering, and outgassing, and the thermal and

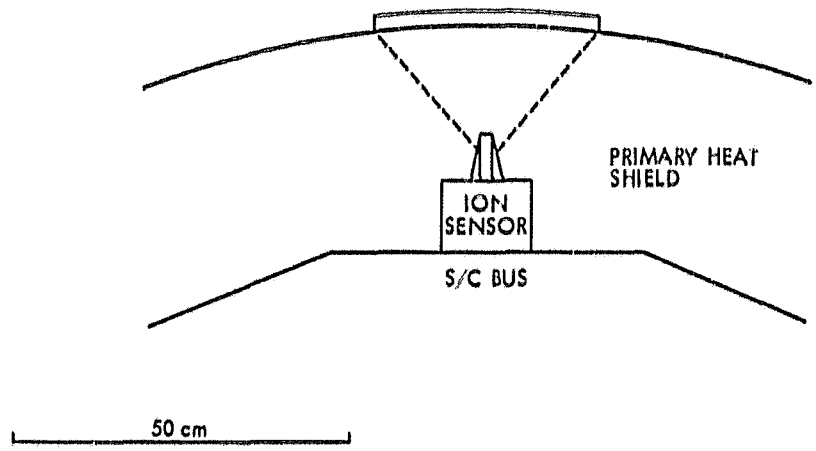

(a) VIEW TOWARD SUN

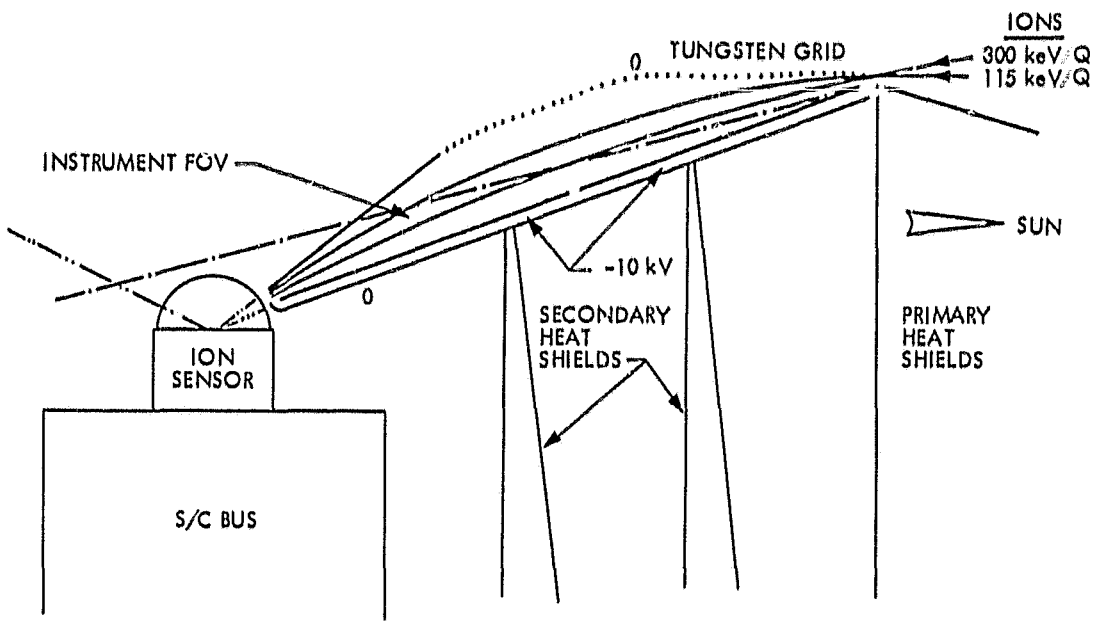

(b) SIDE VIEW

Fig. 2-7. Electrostatic deflection system schematic

mechanical design. Potentially the most satisfactory solution, this method of ensuring an adequate solid angle requires considerable development work.

Besides the adoption of one of the methods outlined above, electrons which can be measured adequately from a point which remains always in the umbra of the heat shield should be used to deduce plasma parameters using extensions of methods used on the ISEE and Voyager spacecraft. Indirect measurements of the plasma parameters should also be pursued, so that the maximum degree of certainty is obtained during this unique mission. This involves analysis of the plasma wave spectrum.

2.2.3 Measurements of Electric and Magnetic Fields

2.2.3.1 Frequency Coverage

Gurnett (1978) gave a preliminary assessment of the problems and prospects for a plasma wave investigation on the STARPROBE mission. He noted that the spectral coverage would have to extend up to about 20 MHz, based on a criterion that includes measurement of the peak value for twice the local electron plasma frequency. Figure 2-8, adapted from Gurnett's report, shows how the characteristic frequencies in the solar wind plasma should vary with radial distance from the Sun. Here, we include a model radial profile for the interplanetary (solar) magnetic field and a model profile of the solar wind density (scales on right-hand side).

The low-frequency measurements are of particular interest because, as indicated in the lower-left-hand side of Fig. 2-8, these waves, which will be measured by the dc magnetometer and the plasma wave instrument, are thought to be directly related to processes involved in coronal heating. It has been suggested that acoustic waves could heat the corona by steepening into shock waves as they propagate outward from the photosphere. However, recent evidence of the large density inhomogeneities of the corona and the probable importance of the magnetic fields suggest that the damping of ion cyclotron waves may be a significant source of coronal heating. In Fig. 2-9, we show the variation of the H^+, He^{++}, and He^+ ion cyclotron frequencies near the Sun (assuming a surface field strength of 1.0 gauss and a radial dependence of r^{-2}). The cyclotron frequencies of heavy ions are related to the f_c-value protons (H^+) by the ratio of charge to mass numbers (Z/A) as indicated in the table of Fig. 2-9. In the region of closest approach for STARPROBE (4-10 $R_\odot$), the ion cyclotron frequencies span the range of about 1-100 Hz, a range that is most adequately sampled for magnetic field fluctuations by a magnetometer-search coil instrument combination. However, since ion cyclotron waves have low phase velocities near a resonance, doppler shifts may affect the observed frequencies in any variation in the ion composition. Thus, detailed spectral measurements of the magnetic field, in conjunction with ion composition and other plasma measurements, can reveal the importance of ion cyclotron resonances as a source of coronal heating. Heating may also occur due to hybrid frequency waves, i.e., lower hybrid and ion-ion hybrid waves. These waves have frequencies between the electron and ion cyclotron frequencies and are also shown in Fig. 2-9.

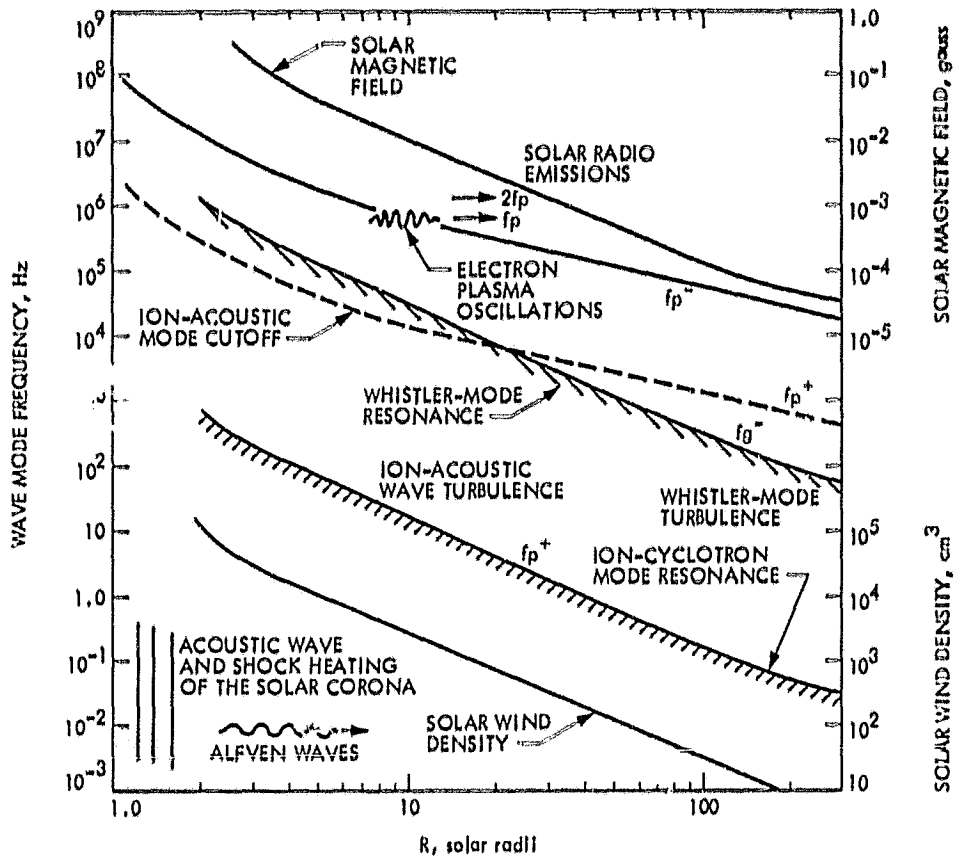

Fig. 2-8. Variations of various characteristic frequencies in solar wind plasma (from D. Gurnett, A Close-Up of the Sun, JPL Pub. 78-70, p. 285)

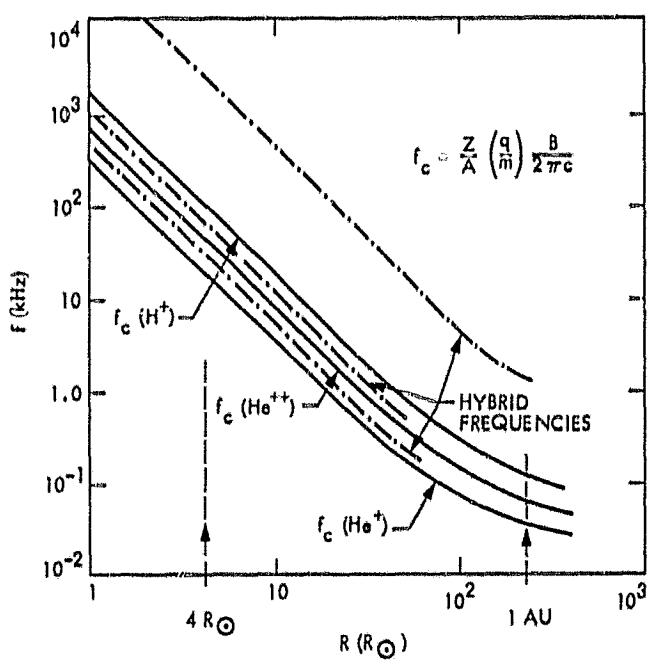

ION	Z A
H^+	1.0
He^{++}	0.5
He^+	0.25
C^{6+}	0.5
C^{5+}	0.42
C^{3+}	0.25
N^{5+}	0.36
O^{6+}	0.38
O^{5+}	0.31
Na^{9+}	0.39
Na^+	0.04
Mg^{10+}	0.42
S^+	0.03

Fig. 2-9. Interplanetary ion cyclotron frequencies

2.2.3.2 Burst Mode Telemetry

The measurements of low-frequency wave modes are complicated by the presence of the many ionic species shown in Fig. 2-9, along with the varying nature of the wave phase speeds. Near the Sun, the doppler shifts for the ion cyclotron waves will add to the difficulty of resolving and identifying the wave modes. It is extremely important to have available a high sampling rate capability that will allow bursts of the complete E or B waveform for transmission to Earth. Detailed ground-based spectral analysis of these waveforms can then lead to reconstruction of the wave modes in the coronal frame of reference.

2.2.3.3 Plasma Wave Antenna Length

Gurnett (1978) pointed out that the plasma conditions change drastically as the STARPROBE spacecraft moves inward from 60 $R_\odot$ to 4 $R_\odot$. Near the perihelion of Helios, the nominal Debye length for quiescent conditions is of the order of three meters, and $(2\pi\lambda_D)$, the minimum wavelength for ion sound waves, is near 20 meters. However, at r = 4 $R_\odot$, most models give $2\pi\lambda_D$ (nominal) in the range of a fraction of a meter, and a very short antenna is needed to ensure accurate E-field amplitude measurements. Thus, an optimum plasma wave instrument will have a short antenna ($\ell \approx 1$ meter) for the inner corona and a long antenna ($\ell \gtrsim 20$-30 meters) for the more distant solar wind.

2.2.3.4 Magnetometer Boom Length

The requirement for a spacecraft field contribution less than 1% of the magnetometer range in use (Table 2-2) is readily implemented without a boom near perihelion when the ambient field is very strong. However, at 60 $R_\odot$, where $B \approx 20\text{-}40\gamma$ (Fig. 2-8), a fairly long boom is needed, assuming that normal spacecraft magnetic cleanliness specifications are imposed. The present concept for a magnetometer boom that can meet the 60 $R_\odot$ requirement has the boom deployed in the spacecraft shadow directly along the antisolar direction. As the spacecraft approaches the Sun, the shadow zone shrinks while the ambient field becomes larger. Solutions that meet both the varying thermal problem and the magnetic contamination requirement involve programmed retraction of the boom as r approaches 4 $R_\odot$. Figure 2-10 shows two versions of the retraction plan; for a nadir-pointing spacecraft the retraction is linear, but if imaging scanning requires tilting of the spacecraft, the more severe retraction plan would be implemented.

2.2.4 Mass Loss and Spacecraft Equipotential Requirements

The mass loss requirements for the STARPROBE spacecraft during solar encounter have been determined to have important consequences for the design of the thermal shield and the spacecraft. The most stringent criterion for mass loss results from the rapid ionization of neutrals lost from the spacecraft; the mass loss plasma must not have sufficient number density or energy density to interfere with either plasma or plasma wave observations. A scientific advisory group, the STARPROBE Mass Loss Requirements Group (SPMLRG) met at the Jet Propulsion Laboratory on September 29 and 30, 1980, to discuss this issue. The requirements for spacecraft potential were also considered by this group.

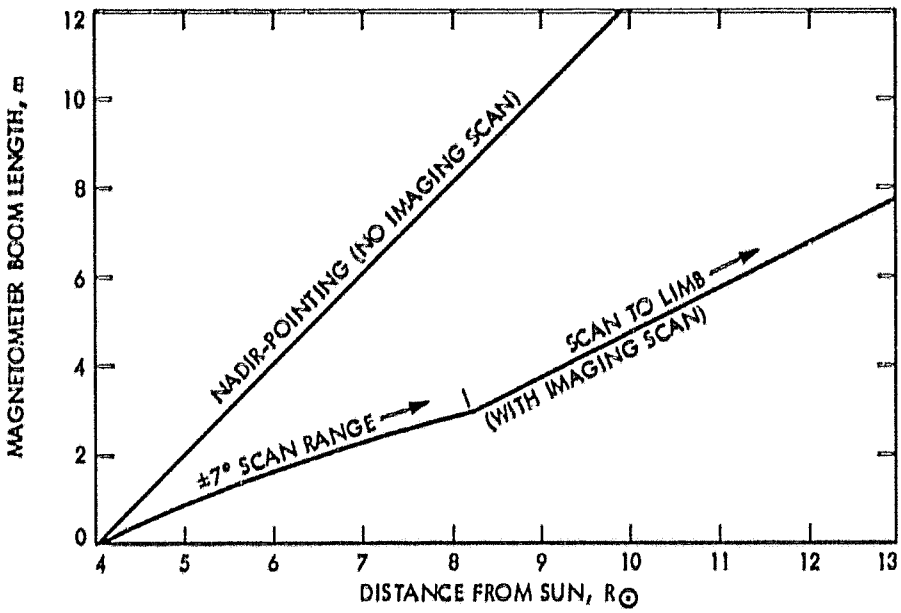

Fig. 2-10. Retraction plan for magnetometer boom

A pictorial description of the interaction is provided in Fig. 2-11. Newly created ion-electron pairs will be separated by the solar wind electric field; the consequent space charge creates a shielding electric field that opposes the solar wind electric field. Additionally, the increased density of plasma near the spacecraft and the high electron thermal speeds will result in an electric field that accelerates positive ions away from the spacecraft; this electric field is the mechanism by which the electron pressure gradient affects the ions.

SPMLRG developed a model of the plasma interaction that is likely to overestimate the effects of the mass loaded plasma; such a conservative approach was considered necessary in view of the many uncertainties in the situation. Acceleration of the mass loaded plasma by the solar wind electric field was ignored; the only effect considered was the mass loss plasma pressure gradient. Neutrals were assumed to leave the spacecraft with a radially symmetric distribution; consequent ionization by electron impact and solar UV results in a lifetime for neutral C_2 molecules of about 60 seconds at 4 solar radii. (This rate could be an underestimate if multiple stage excitation mechanisms affect polyatomic carbon molecules; the mass loss requirement described below would be further constrained in this case. Mass loss requirements for tungsten heat shields have not been determined, as an estimate for the ionization rate of tungsten in the near solar environment is needed.) It was assumed that the electron temperature associated with the mass loaded plasma would be the same as that of the solar wind. The resulting pressure gradient can be used to calculate the electric field; the science requirement imposed was that perturbations in the electric potential due to the mass loaded plasma not exceed 20 volts. Allowing a factor of 5 for uncertainties, the maximum allowable loss rate on this basis is 3.0×10^{-3} gm/sec. A worst case estimate for the local

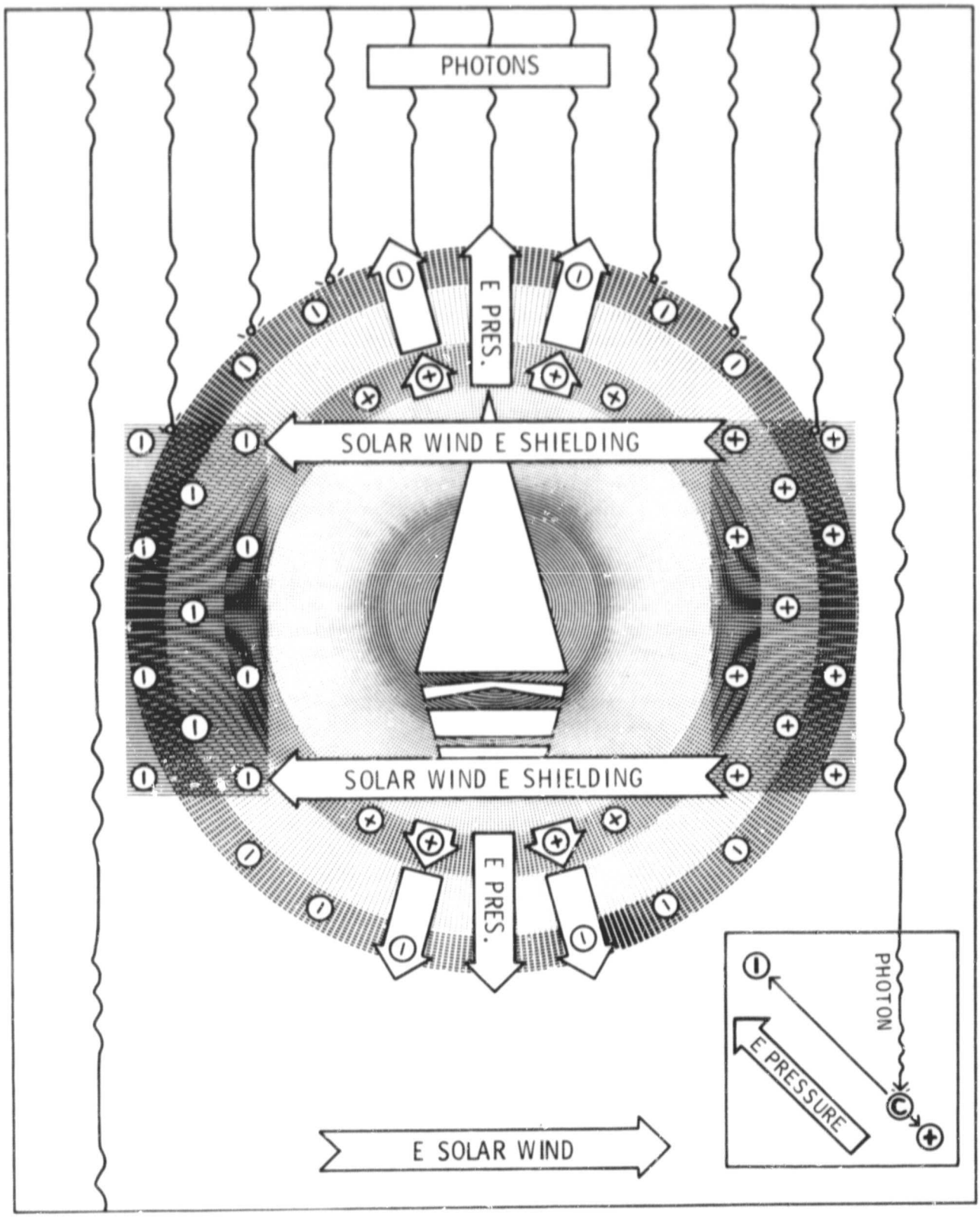

Fig. 2-11. Shield mass-loss effects on solar wind measurements

density would be based on the assumption that the mass loss photoelectrons are not replaced by solar wind electrons so that the carbon ions escape with their initial thermal velocities. In this case, the maximum potential perturbation is not increased but the density of the mass loss plasma could be as large as 1.3×10^4 cm^{-3} in the vicinity of the spacecraft. If, instead, it is assumed that the ions are swept away by the solar wind electric field, the maximum density is 2.8×10^3 cm^{-3}. For the purposes of comparison, the nominal solar wind density at perihelion is about 5.0×10^4 cm^{-3}.

The spacecraft has an unusual geometry to allow radiative cooling of the heat shield; the shield surface is a cone with an area much larger than the cross-sectional area normal to the solar direction. For this reason, there was concern that charging due to solar wind electron fluxes might drive the spacecraft to an unknown negative potential. A preliminary investigation indicated that such a negative spacecraft potential is not likely to occur in any typical solar wind environment encountered during the mission. However, further investigation to increase the reliability of this conclusion was considered desirable. It is also scientifically desirable for interpretation of plasma data that the exterior surface of the spacecraft be approximately an equipotential; requirements for grounding and/or conductivity of spacecraft surfaces were therefore specified. Wake effects were considered, and it was felt that problems due to the wake should not be worse than on other solar wind missions.

In summary, a mass loss requirement of less than 3.0×10^{-3} gm/sec of C_2 was determined. It was recommended that the spacecraft exterior surfaces be approximately an equipotential and that this potential be positive. Further study of the plasma interaction that leads to the mass loss requirement was also recommended. To the extent that the solar wind electric field can be coupled into the mass loss plasma on a small scale size (Goertz and Boswell, J. Geophys. Res., 84, 7239, 1979), the effects of the mass loss would be reduced. The mass loss requirement might in this case be relaxed, with important consequences for heat shield and spacecraft design. Additionally, at lower mass loss densities the likelihood of successful studies of short wavelength waves such as ion acoustic waves and electron gyroharmonics is increased. Other areas of required research are models of the spacecraft potential and ionization rates of C_2 and tungsten. A detailed report of the work and recommendations of the SPMLRG is published as JPL internal report 715-100 ("Spacecraft Mass Loss and Electric Potential Requirements for the STARPROBE Mission", B. E. Goldstein, W. C. Feldman, H. B. Garrett, I. Katz, L. Linson, K. W. Ogilvie, F. L. Scarf, and E. C. Whipple).

2.3 PARTICLES AND FIELDS SUMMARY

2.3.1 Strawman Payload/Spacecraft Configuration

The subcommittee considered a large number of spacecraft configurations, including simple spinners. However, we were never able to find a suitable mission concept using a spin-stabilized spacecraft. The very serious problems included the following:

(1) The spin axis must be precessed 180° in 12 hours during closest approach (see Figs. 2-3, 2-4), and the thrusters would have to

fire almost continuously. This would lead to nearly continuous plasma contamination and unacceptably high levels of boom vibrations.

(2) All spin-stabilized configurations yielded unacceptably low telemetry rates. Moreover, in many cases, spacecraft booms would pass through the antenna pattern once per spin, and this would seriously endanger the overall telemetry link concept.

The selected configuration is a 3-axis stabilized nadir-pointing spacecraft with a deployable spinning platform, a magnetometer boom that can be deployed and retracted, and thermally protected plasma wave antennas that emerge into sunlight. A strawman payload devised primarily to satisfy the plasma science requirements of our subcommittees is shown in Table 2-4, and the spacecraft configuration is shown in Fig. 2-12. We include here the electrostatic ion deflection system for measurements in the solar direction.

2.3.2 Supporting Research and Technology Needs

The ion deflection system must be developed further. Questions involving thermionic emission from grids and wire antennas, and other aspects associated with the need to look in the solar direction, must be addressed with SR/T funds.

Table 2-4. Strawman payload: 3-axis stabilized spacecraft

	Mass, kg	Power, w	bits/ sec	bits storage
Plasma spectrometer	15	7	4,000	2×10^8
Magnetometer[a]	5	4	1,000	4×10^7
Plasma wave	9	5	4,000	10^8
Energetic particles	15	17	4,000	1.6×10^8
Ion composition	6	3	2,000	10^8
Dust impact	4	3	100	2×10^5
Coronal light detector	4	3	4,000	4×10^8
High speed camera[b]	10	5	10,000	10^9
	68	47	29,100	2×10^9

[a]Mass of boom not included.

[b]Nadir-viewing; no pointing capability.

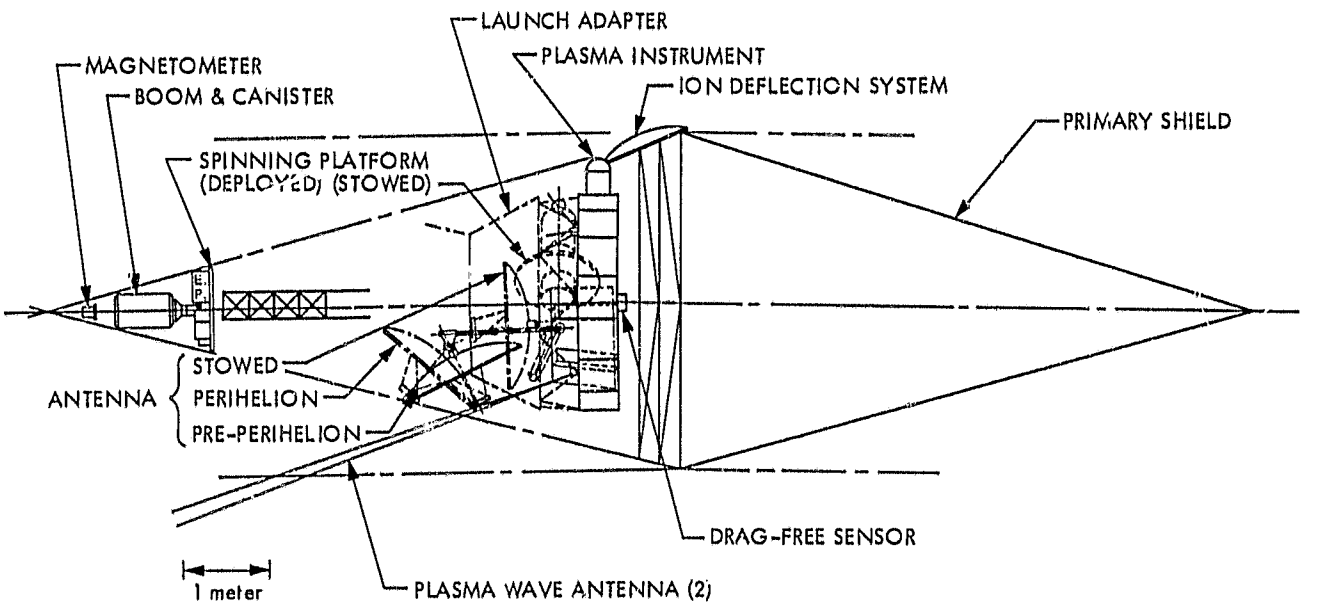

Fig. 2-12. Fields and particles plus gravitation spacecraft configuration (side view)

CHAPTER 3

IMAGING SCIENCES

A. B. C. Walker, Jr., Chairman, Stanford University
A. Title, Lockheed Palo Alto Research Laboratories
A. Kreiger, American Science and Engineering
J. Kohl, Harvard-Smithsonian Center for Astrophysics
H. Zirin, California Institute of Technology
J. Underwood, STARPROBE Scientist, Jet Propulsion Laboratory
E. Frazier, The Aerospace Corporation
R. Munro, High Altitude Observatory, Boulder
G. Timothy, Laboratory for Atmospheric and Space Physics, Colorado
G. Withbroe, Harvard Observatory
J. Davis, American Science and Engineering
E. Rhodes, University of Southern California

3.0 INTRODUCTION

Our understanding of the phenomena that occur in stellar atmospheres is based in large part on the study of the solar atmosphere, since the Sun is the only star for which we can resolve individual structures within the atmosphere and study these phenomena at the level of the basic plasma physics processes which underlie them. The complexity of these phenomena is demonstrated by Fig. 3-1, which illustrates the upward flowing gas jets, called spicules, associated with the boundaries of large-scale convection cells (supergranulation cells) in the solar atmosphere. The spicules are an example of a phenomenon which we believe plays a central role in the solar atmosphere, specifically, in this instance, in the dissipation of mechanical energy generated by convective processes in the photosphere and in the exchange of mass between the chromosphere and corona, but which operates on a scale too small to allow the use of observations obtained with present instruments to test detailed physical models. Other examples of phenomena in the solar atmosphere that operate on a scale beyond the resolving power or sensitivity of present instruments are (1) the physical processes that determine the flow velocity, composition, and ionization structure of the solar wind, (2) the role of the fine structure of the solar photosphere (the granulation cells) in the convective transport of energy, (3) the nature of the physical processes responsible for heating the chromosphere and corona, and (4) the detailed physical processes responsible for explosive phenomena such as flares and coronal transients.

The exploitation of the unique opportunities presented by the Space Shuttle will allow solar physics to develop a comprehensive solar observatory in near-earth orbit (the Advanced Solar Observatory) which should provide a factor of 3-10 (depending on wavelength) improvement in resolving power compared to present capabilities. Even this dramatic improvement in resolution will not, however, be sufficient for critical tests of physical models of many of the most important processes that operate in the solar atmosphere; such tests will demand another order of magnitude improvement in resolution. Imaging experiments on the STARPROBE Mission, a unique and exciting program which envisions an interplanetary probe which will execute a close solar encounter (to within 3 solar radii of the surface), can achieve this improvement in resolving power of nearly 2 orders of magnitude compared with our present capabilities by virtue of its close approach to the Sun's surface at solar encounter. Furthermore, the STARPROBE mission will allow observations from within the region in which the solar wind is accelerated, permitting uniquely sensitive and accurate measurements of the global properties of the solar wind, as well as in situ measurements of solar wind velocity, composition and ionization structure. These unique encounter observations, and the stereoscopic observations that will be possible during the STARPROBE cruise phase, in concert with the comprehensive observational program which will be possible with a Shuttle-supported Advanced Solar Observatory in near Earth orbit, form the core of the program of solar research for the next decade recommended by the Solar Physics Working Group of the Astronomy Survey Committee.

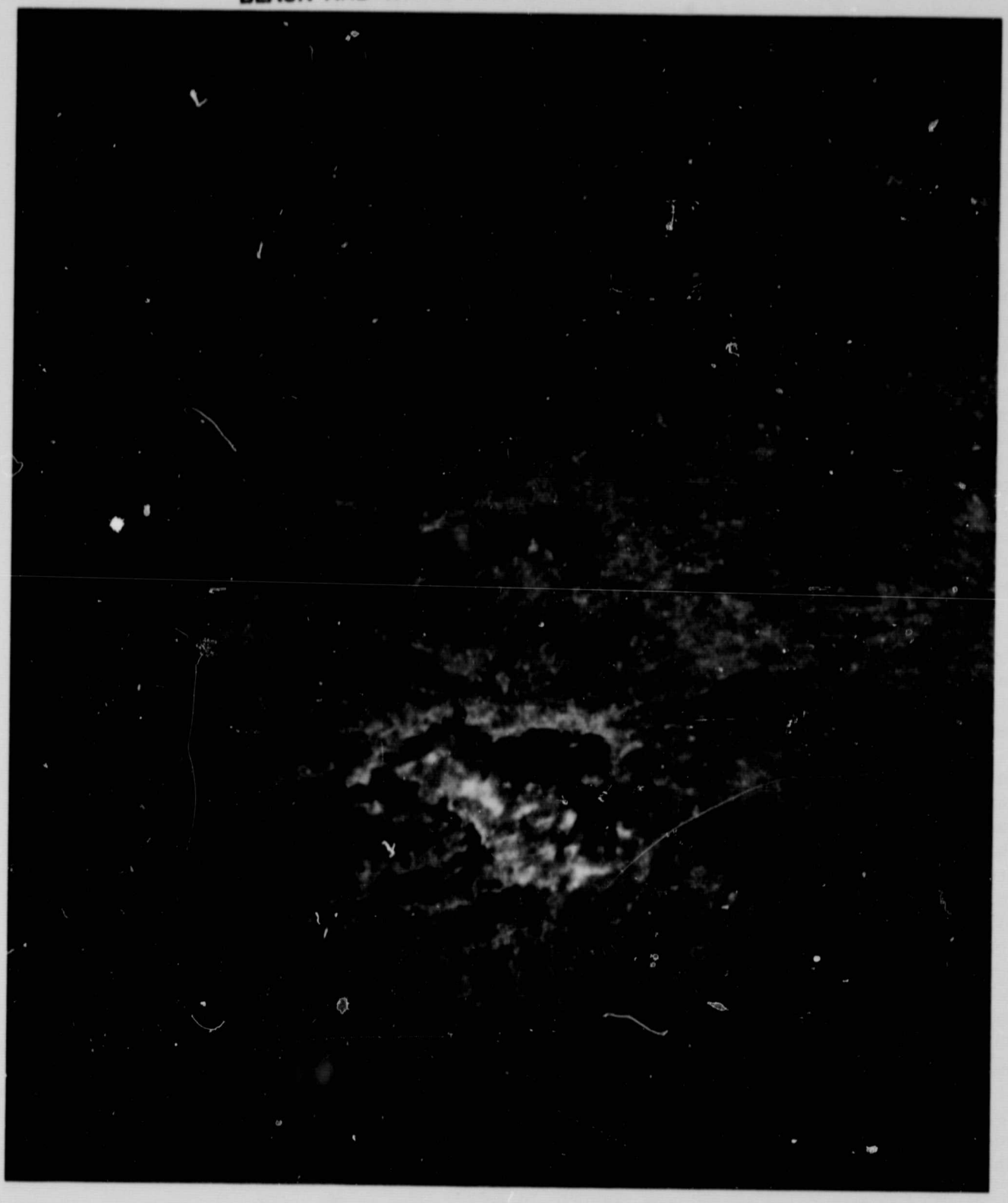

Fig. 3-1. Field of spicules on the surface of the Sun. Photograph taken in the light of the H-α line of hydrogen at 6563A (Courtesy of the Sacramento Peak Observatory)

In the following report, we review the conclusions reached by the STARPROBE Ad Hoc Imaging Subcommittee, which met on three occasions during the past 24 months. In Section 3.1, we review the role we anticipate the STARPROBE Imaging Experiments will play in addressing the major objectives of Solar Physics in the next decade and briefly discuss the relationship of STARPROBE to other major proposed space missions. In Section 3.2 and 3.3, we discuss the major scientific questions which the STARPROBE imaging package will address, and present the strawman payload and mission concept which the Committee has developed. In Section 3.4, we briefly discuss a number of issues which might be addressed in subsequent studies.

3.1 THE ROLE OF THE STARPROBE IMAGING INSTRUMENTS

In the recent report of the Solar Physics Working Group (SPWG) of the Astronomy Survey Committee (ASC), solar physics was defined as "a fundamental inquiry into the physics of the remarkable large-scale behavior of ionized gases in gravitational and electromagnetic fields." The Working Group singled out three major themes of this inquiry:

(1) The study of the structure, composition, and evolution of the solar interior.

(2) The study of active phenomena in the solar atmosphere, including the chromosphere and corona, the generation of the solar wind, solar flares, and the sunspot cycle and the associated magnetic cycle.

(3) The study of the structure and dynamical behavior of the corona, solar wind and heliosphere.

The close connection between solar physics and astrophysics on one hand and between solar physics and space physics and heliospheric physics on the other hand is implicit in the three themes enumerated above. We have already mentioned the key role played by solar observations in the study of stellar atmospheres in the Introduction; the role of solar observations is no less critical to the theory of stellar structure and evolution. In an even more direct way, solar physics is critical to heliospheric physics. The large-scale solar magnetic field and the solar wind together dominate the heliosphere and its interaction with planetary ionospheres, magnetospheres, and atmospheres; consequently, studies of the large-scale structure and dynamical behavior of the corona and solar wind are central to the programs of these disciplines.

Each of the imaging instruments which the Committee has identified as candidates for STARPROBE addresses one or more of the major themes we have enumerated above in a unique and critical manner, with observational programs that cannot be achieved by alternative techniques. The objectives of the STARPROBE Imaging instruments encompass all of the major themes of solar physics:

(1) To study at ultrahigh resolution (7-10 km, equivalent to 0.0$_4$ arc sec from earth orbit) the structure and dynamical behavior of the photosphere, chromosphere, and corona.

(2) To study the global properties of the corona and heliosphere in concert with the STARPROBE in situ particle and field experiments, with particular emphasis on the mechanisms responsible for the acceleration and the variable flux, composition and ionization structure of the solar wind.

(3) To study the principal modes of the radial and nonradial oscillations of the Sun in order to determine the structure and dynamical behavior of the solar convection zone and interior.

(4) To obtain stereoscopic observations of the evolutionary and transient behavior of photospheric and coronal structures during cruise, in collaboration with the Advanced Solar Observatory.

The STARPROBE Mission is an integral component of the scientific strategy developed for solar physics by the SPWG of the Astronomy Survey Committee for the next decade; it is useful to think of this strategy in two phases. In the first phase, the four principal objectives listed above will be addressed by Shuttle Attached instruments such as the Solar Optical Telescope, by the International Solar Polar Mission (ISPM)[1], and by two explorer class missions, the Solar Coronal Explorer (SCE) and the Solar Interior Dynamics Mission (SIDM). Although each of these observatories will have the capability to address more than one objective, the principal focus of each program is indicated in Table 3-1.

Table 3-1. Focus of principal solar programs currently under study

Principal scientific objective	Phase I	Phase II
Atmospheric structure and dynamics	Shuttle attached instruments	STARPROBE/ASO
Global structure and dynamics	ISPM	STARPROBE/ASO
Structure and dynamics of the solar interior	SIDM	STARPROBE/ASO
Evolution of the structure of the atmosphere and corona (solar cycle)	SCE	STARPROBE/ASO

[1] At the time of this writing, the NASA ISPM spacecraft has been cancelled, leaving only the ESA spacecraft at present. NASA is currently studying a modified ISPM spacecraft as a candidate for a new start in 1983.

In the second phase, two powerful observatories, STARPROBE and the Advanced Solar Observatory (ASO), each capable of unique and highly complementary observing programs, will be able to make observations which should provide critical tests of physical models of solar phenomena at the level of basic plasma processes such as magnetic reconnection, wave propagation, the generation and dissipation of mass and current flows, and the transport of energy by convective processes. The STARPROBE's role, as the first man-made instrument to visit a star, is crucial to this scientific program; for only by directly traversing the corona and making in situ measurements of particle populations and flows, simultaneously with global measurements of the faint corona from the inside, and by approaching sufficiently close to the solar surface to allow observations with resolution approaching a few kilometers, can we unravel the role of the many complex structures and processes occurring in the solar atmosphere.

3.2 SCIENTIFIC OBJECTIVES OF THE IMAGING INSTRUMENTS PROPOSED FOR STARPROBE

From the point of view of the imaging instruments, the STARPROBE mission can be divided into two phases, the cruise phase, which we might define as those periods, both before and after encounter, when the spacecraft is more than 20 solar radii from the Sun, and the encounter phase itself. It is then convenient to divide the instruments defined by the Committee into two groups -- direct viewing instruments and umbral instruments, the latter name being used because these instruments do not look directly at the Sun, but rather above the limb in the shadow formed by an occulting element. The direct viewing instruments are the Visual Magnetograph/Tachometer (VM/T), the EUV Spectroheliograph (EUVS) and the Soft X-Ray Heliograph (SXH), and their primary objective is to achieve ultrahigh resolution (~7-10 km) imaging of the physical structures which dominate the solar atmosphere at encounter and to relate these structures to the global properties of the corona and solar wind which will be observed by the umbral instruments and the in situ measurements. The secondary objective of the direct viewing instruments is to carry out a synoptic program of stereoscopic observations with the ASO during cruise.

The umbral instruments are the Coronal Lyman-Alpha Spectrometer (CLAS), the Coronal Light Detector/Magnetometer (CLDM), and the Coronal EUV Spectrometer (CES). The primary objective of the umbral instruments is to relate the global properties of the corona directly to the in situ observations of the particles and fields instruments during encounter and, therefore, ultimately to the structures and dynamic processes occurring in the lower atmosphere. The secondary objective of the umbral instruments is to study the evolution of the large-scale structure of the corona and coronal transients in collaboration with the ASO during cruise. In this section, we describe how the observing program that can be undertaken with this complement of instruments can address the scientific objectives we have identified.

3.2.1 Structure and Dynamical Processes in the Photosphere, Chromosphere and Low Corona

With present techniques, we have been able to distinguish the structures which dominate the solar atmosphere, but we have not been able to provide observational guidelines to models of their internal dynamics. Shuttle attached or space platform supported instruments in near-Earth orbit such as SOT, operating at the highest attainable resolution (∿70 km on the Sun at wavelength of 5000 A), will be able to resolve structures such as magnetic flux tubes and spicules into at most 2 or 3 resolution elements. Instruments operating as part of the ASO, in the EUV and X-ray portion of the spectrum, will be limited (because of fundamental optical polishing processes) to a resolving power of 300-500 km on the Sun, which will not be adequate to resolve in detail structures such as magnetic tubes or coronal bright points, which are loops of total length ∿10,000 km, and with cross-sectional diameters probably approaching a few hundred km. Thermal gradients in such structures will almost certainly occur on smaller scales. The STARPROBE imaging instruments, which can achieve resolving power of 7-10 km in the visible, and 10-20 km at EUV and X-ray wavelengths during encounter (both are limited only by telescope diameter), will be able to distinguish the structure of features such as spicules, granules and coronal loops in sufficient detail to determine such parameters as temperature and density gradients and mass flow velocities and how these parameters relate to the detailed configuration of the magnetic field.

Some of the principal scientific questions which will be addressed at encounter are discussed below. (We indicate in parentheses which instrument has each question as a major objective.)

- What is the size and field strength of the individual flux elements which make up the solar magnetic field? How does the fine structure of the field differ in sunspots, in bright points, in granule boundaries, in coronal holes, and in emerging flux regions? (VM/T)

The structure of the magnetic field is the most important factor in regulating the transport of mass and energy in the chromosphere and corona. Central to understanding the generation and evolution of the solar magnetic field is the universal, and at present inexplicable, property of magnetic fields in the photosphere to become quantized in separate flux tubes with field strength in excess of 1000 gauss. These flux tubes appear to be fundamental elements, aggregating in active regions and sunspots to form extended regions of strong fields; but they are present both in regions of large-scale strong fields, such as sunspots (Fig. 3-2), and in regions in which the large-scale field is weak. The balance between cool low density gas in regions of strong field, and the surrounding regions of hotter material and weak field which is observed on a large scale in sunspots, must be repeated on the very small scales associated with the fundamental magnetic flux tubes. The complexity associated with these phenomena is illustrated in Fig. 3-2. With present techniques, such phenomena are barely resolved in a sunspot of 10,000-km diameter; the characteristic size of the fundamental flux tubes is expected to be less than a few hundred kilometers; clearly, resolving power of ∿10 km will be necessary to determine the structure and dynamical behavior of these elements. Furthermore, we expect considerable structure within the central region (umbra)

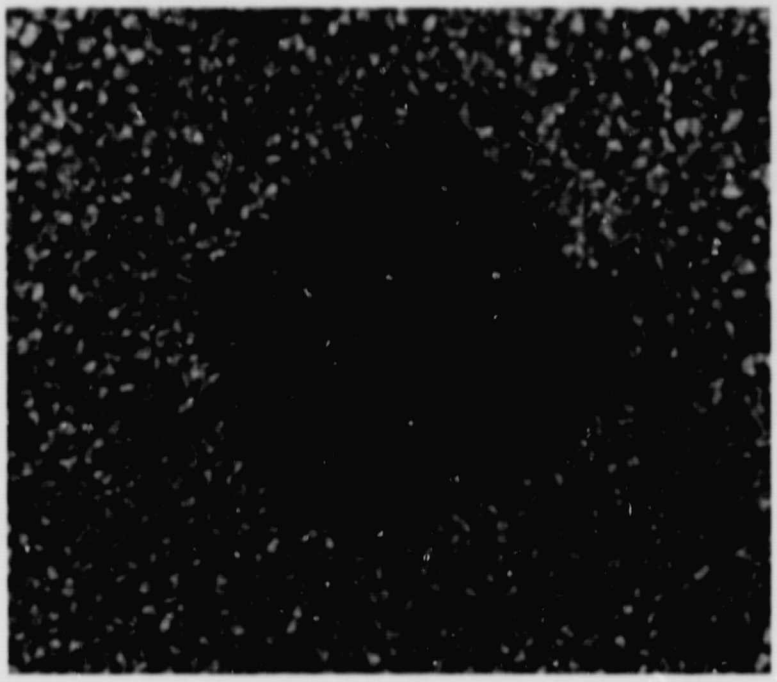

Fig. 3-2. Photograph of a small sunspot, surrounded by the granulation field (Courtesy of Sacramento Peak Observatory)

of sunspots, which can be resolved by STARPROBE. The dark granule boundaries (clearly visible in Fig. 3-2 but completely unresolved) are themselves only a few hundred kilometers across, but may contain considerable magnetic structure. The very best ground-based photographs begin to show 0.15 arc sec bright elements in the granulation boundaries. The clarification of our understanding of the magnetic configuration of the ubiquitous structures in the solar atmosphere is the single most important problem faced by the solar atmospheric model builder.

- What is the latitude distribution of the basic field elements? What is the strength of the polar field? (VM/T)

The STARPROBE Mission, with its polar orbit at encounter, is in an ideal and unique position to answer this fundamental question, which has important implications for models of the solar activity and magnetic cycles.

- What is the fine structure of the turbulent motions within the solar granulation? What factors determine the growth of instabilities, and how do these factors affect the efficiency of convection? What acoustic wave modes are excited by convection and what is their role in chromospheric heating? How and where are these waves dissipated? (VM/T)

Convection is a fundamental mechanism of energy transport in stars; however, we do not as yet have a fundamental theory of convection. The scale of features such as the solar granulation (see Fig. 3-3), assumed to represent fundamental convection cells, must be put into present theories as a parameter. Although granulation cells have been studied for many years, we have no observations which can specify the magnetic, density, temperature and velocity profiles of the cells and dark lanes in detail. Such phenomena as "exploding granules" have been observed at the limits of resolution, but the observation of possible fine structure within granules is beyond our present capabilities. With STARPROBE, such observations will be possible, as well as the possible determination of vertical structure within granules by limb observations. Such observations will provide the guidance needed to develop a fundamental theory of convection in stellar atmospheres.

- What is the fine structure of the chromospheric network and of spicules? What is the structure of the chromosphere-corona transition region, and how does it mediate the exchange of mass and energy? Is the transition region different in large coronal loops, in bright points, and in coronal holes? (EUVS, VM/T)

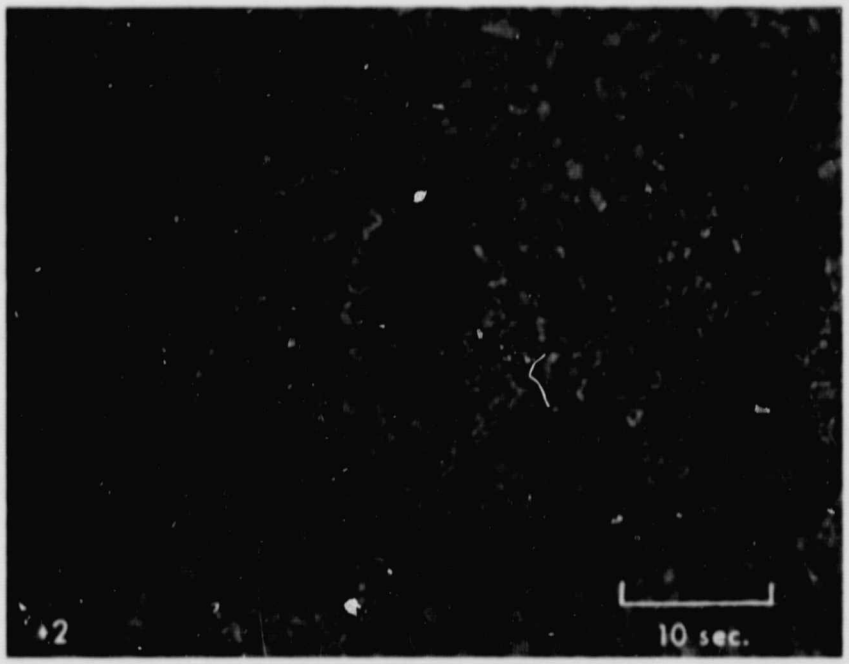

Fig. 3-3. Solar granulation seen in the red wing of the H-α line, emphasizing the dark lanes between granules. Note the bright filamentary structure (called filigree) believed to denote the foot points of magnetic flux tubes rooted in the photosphere (Courtesy of Sacramento Peak Observatory)

The chromospheric network traces out the boundaries of the large-scale convection cells called supergranules, which are typically 30,000 km across. The network is a region of strong field and presumably higher dissipation of non-thermal energy. The network is visible in the cores of absorption lines (such as the Mg Bl observations shown in Fig. 3-4), which correspond to levels in the

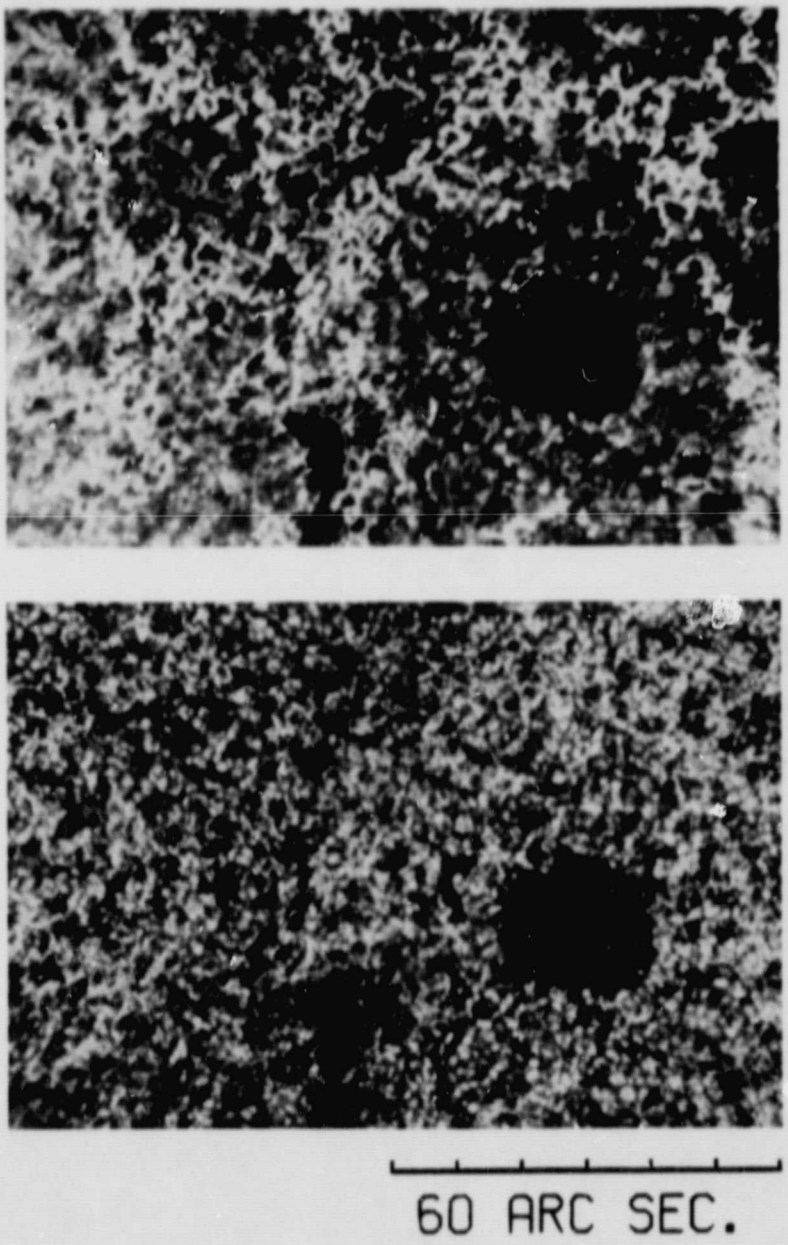

Fig. 3-4. The chromospheric network is visible in the upper figure, which is an image near the line core (+0.4A) of the Mg Bl line. It is less prominent lower in the atmosphere where the temperature is lower. Lower figure taken at +0.8A from line center (Courtesy of the Sacramento Peak Observatory)

atmosphere which are higher and hotter than the photosphere, and in EUV emission lines corresponding to excitation temperatures as high as 500,000 K. In cooler lines, such as Hα, the network is dominated by the upward moving gas jets called spicules; a field of spicules is visible in Fig. 3-5, which was taken at the same time and with the same field as Fig. 3-3, but in the blue wing of the line. Current models suggest that spicules are magnetic flux tubes containing upflowing cool material. At present, the quantity of upflowing material greatly exceeds that needed to supply the corona and solar wind. We do not know how or in what form this material returns to the photosphere. Nor do we presently know how the chromospheric network is heated, although present models suggest the dissipation of waves channeled by the magnetic field. These are fundamental questions for the theory of stellar atmospheres, since we know that all cool stars have chromospheres. We seek the fundamental processes involved in the transport and dissipation of energy, and in mass transport, and most importantly the configuration of the field which controls transport properties of the gas. These phenomena operate on scales beyond our present capabilities to observe. Only the superior resolving power of the STARPROBE instruments can provide the necessary observations.

- What is the thermal structure of coronal loops? How important is mass flow in loops, and how is mass exchange between the chromosphere and coronal loops accomplished? Can evidence for heating by current dissipation or reconnection be discerned from the thermal structure of loops? (EUVS, XRH, CLDM).

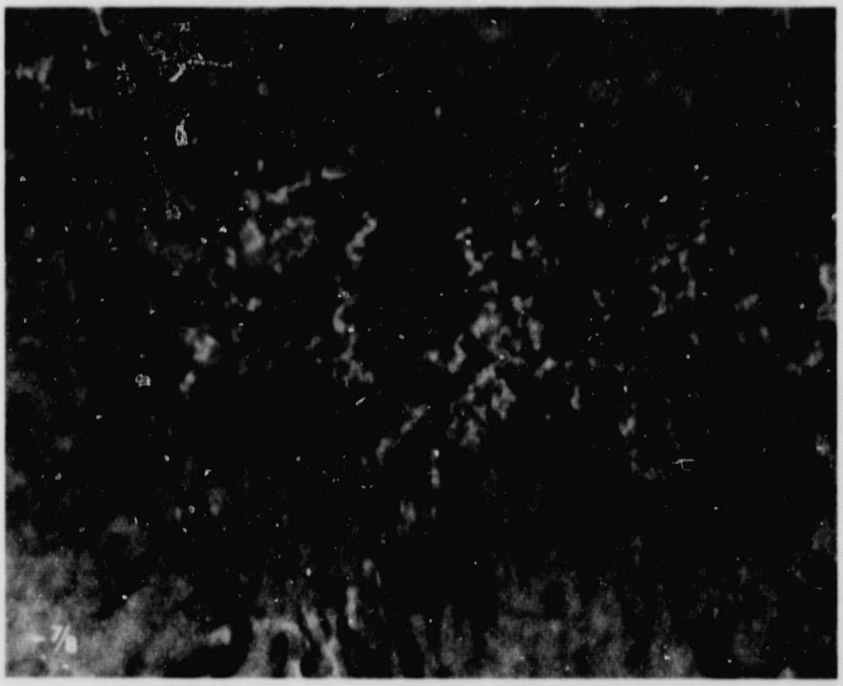

Fig. 3-5. The same view as Fig. 3-3, taken, however, in the blue wing of the line to emphasize upward moving material (Courtesy of the Sacramento Peak Observatory)

In the past decade, observations made at EUV, EUV and X-ray wavelengths have clearly demonstrated the fundamental role that magnetic fields play in determining the structure of the transition region and corona. The fundamental structure in the corona is the high-temperature magnetically confined loop. Loops are present in the atmosphere on a variety of scales, and encompassing a wide range of temperatures (ranging from about 100,000 K to 10,000,000 K (see Fig. 3-6).

Current models suggest that loops are isothermal over most of their length, due to the high conductivity of the plasma parallel to the magnetic field, but must have a very steep thermal gradient near their footprints. Loops of different temperatures may form arcades; however, the scale of temperature gradients across the field is not known. Although we can resolve individual loops, we cannot resolve their structure; certainly loops must be dynamic structures, with mass flow and one or more forms of energy dissipation and transport occurring on a fine scale within the loop structure.

Present observations can offer no guidance to theory in the detailed modeling of these ubiquitous structures. Technical limitations prevent the achievement of resolution better than a hundred kilometers[2] from earth orbit

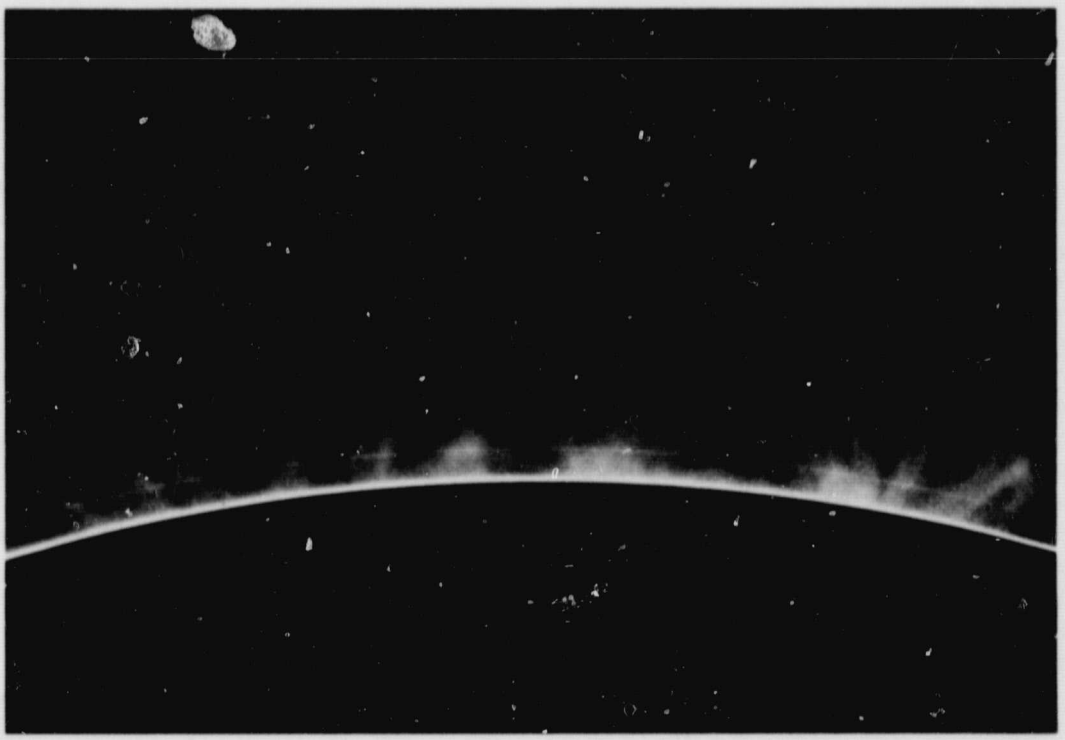

Fig. 3-6. Coronal loops in the light of the 5303Å coronal forbidden line of Fe XIV (~1,500,000 K) (Courtesy of the Sacramento Peak Observatory)

[2]Achieving even this level of performance will require the introduction of new technologies such as large aperture Fresnel zone plates.

at EUV and X-ray wavelengths in the foreseeable future. It is clear, however, that resolution of 10-20 km is required to determine the structure and dynamical behavior of loop structures. Only STARPROBE can achieve this performance, because again the limit is not surface quality but minor diameter.

- What is the structure of coronal bright points? What role do they play in the transport of mass into the solar wind, and in the emergence of magnetic flux? What processes are responsible for heating bright points and supplying the energy for their flare-like behavior? (EUVS, XRH)

Coronal bright points are small regions of intense EUV and soft X-ray emission that are associated with regions of emerging magnetic flux. They are observed to be distributed more or less uniformly over the solar disk (see Fig. 3-7). It is likely that bright points are small loop structures, of total size 10,000-20,000 km. It is believed that bright points may play an important role in transport of mass from the chromosphere to the corona, and ultimately to the solar wind. Among the important questions regarding bright points which STARPROBE can address are the relationship of bright points to chromospheric phenomena, such as spicules, and the source of heating and mass for the bright points.

- What is the transition region structure in coronal holes (open field regions)? What processes are responsible for mass transport? Are abundance gradients observable in the low corona in holes? (EUVS, XRH, VM/T)

One of the most fundamental discoveries of the past decade is that the corona is divided into strong closed magnetic field and weak open magnetic field regions. The strong field regions are dominated by coronal loop structures and are bright at X-ray wavelengths. The weak field regions are the source of the high-speed solar wind streams, and are dark at X-ray wavelengths. Figure 3-7 clearly demonstrates the dichotomy. Present instruments lack both the sensitivity and resolution to study the embryonic solar wind as it emerges from coronal holes. Many fundamental questions arise in connection with coronal holes. How is the material in the wind heated and transported from the chromosphere? Where and by what mechanism do the abundance anomalies observed in in situ measurements of the wind originate? Where is the ionization structure frozen in? The answers to these questions are important to the interpretation of the in situ measurements to be made by STARPROBE, as well as to the interpretations of the observations of chromospheric phenomena such as spicules and the chromospheric network.

- How does the energy budget of the corona differ in coronal holes, and in strong and weak field regions? (XRH, EUVS).

This is a fundamental question which can only be answered by detailed models of all important structures in the atmosphere, so that the role of mass transport and mass and current flows, as well as radiation losses can be properly included. Clearly, STARPROBE, as well as ASO, will play important roles.

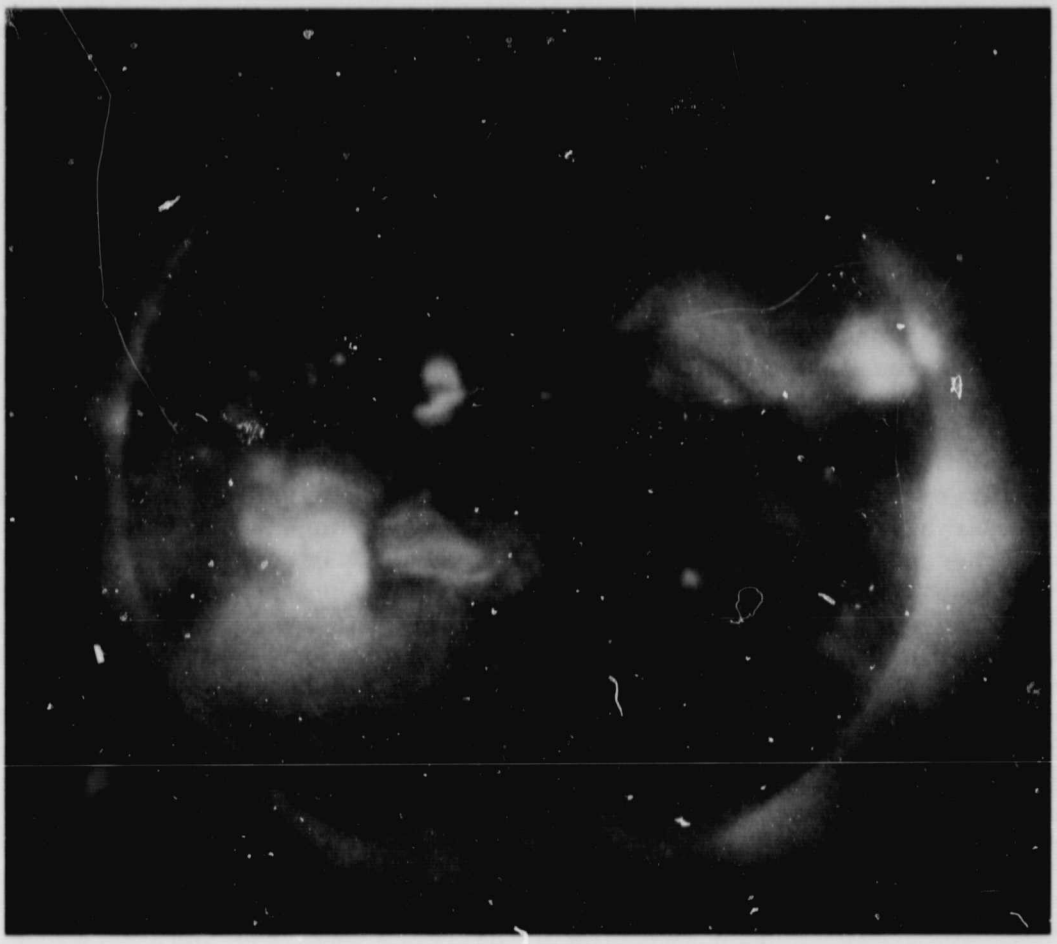

Fig. 3-7. The Sun photographed at soft X-ray wavelengths. Note the large coronal hole, extending to the North Pole, and the presence of a number of bright points, both in regions of high coronal emission and in coronal holes. Note also a number of large loop structures both on the disk and at the limb (Courtesy of American Science and Engineering)

3.2.2 The Global Properties of the Corona and Solar Wind

The in situ particle and field measurements on STARPROBE will provide an unprecedented opportunity to determine unambiguously the conditions in the far corona and in the region in which the acceleration of the solar wind is believed to occur. In order to attain the maximum benefit from these observations, it is essential to relate them to the structures and conditions in the inner corona and in coronal holes which are connected directly to the STARPROBE position by magnetic field lines and to the global properties of the magnetic field, solar wind, and corona at the time of solar encounter. The direct viewing instruments will play an important role here; however, the observational program of the umbral instruments will be especially critical. We discuss here the imaging observations which link most closely the scientific objectives of the imaging and in situ instruments.

- What is the global nature of the solar wind velocity distribution? (CLAS)

Thus far, we have been able to sample directly only the properties of the solar wind in the ecliptic plane. The ISPM (see footnote 1, page 3-4) will provide the first data on the properties of the solar wind outside of the ecliptic plane; however, the coverage will be limited, the measurement transient, and, of course, ISPM will measure only solar wind properties at 1-2 AU. The in situ measurements on STARPROBE will measure solar wind velocities directly into the acceleration region (believed to lie between 2 and 10 $R_{\odot}$), but only along a single track, and only transiently at each position. The Coronal Lyman-α Spectrometer can measure the global distribution of solar wind velocities, and so relate the in situ observations to global and transient phenomena and to structures at lower altitudes in the corona. Although observations of coronal velocity can be made from outside the corona, their resolution and sensitivity is limited, and their interpretation is ambiguous since these observations must integrate conditions over a line of sight encompassing a wide range of coronal heights and features. Because the STARPROBE Coronal Lyman-α Spectrometer can obtain outwardly directed observations over a variety of coronal heights directly, they may be interpreted unambiguously to obtain the solar wind velocity distribution as a function of height, and can attain the resolution and sensitivity necessary to distinguish structure in the solar wind which can be related directly to structures in coronal holes. The power of the STARPROBE observations is illustrated by Fig. 3-8, which shows the sensitivity of the line profile of the backscattered radiation to flow velocities. This sensitive indicator of the properties of the solar wind is only available to an observatory such as STARPROBE which penetrates into the corona.

- What are the composition and ionization structures of the solar wind as a function of distance from the Sun? (CES, EUVS).

The composition and ionization structures of the solar wind are known to be highly variable, but we do not have the observational data necessary to relate these variations directly to the structures or the conditions in the solar atmosphere which are their cause. The combination of the in situ observations and the observations by the coronal and direct viewing EUV spectrometers can uniquely provide a direct determination of these important parameters of the solar wind. Instruments in near-Earth orbit lack both the sensitivity and resolution to make these observations, and even if such observations became possible with an instrument of aperture much greater than any presently believed feasible, they would suffer from ambiguity of interpretation due to the long integration path in the solar wind. The power of outwardly directed observations from inside the corona, as in the case of velocity measurements, cannot be duplicated by remote observations from Earth orbit.

- What is the global configuration of the coronal magnetic field and the coronal plasma? (CLDM).

- What is the global distribution of the interplanetary dust? (CLDM).

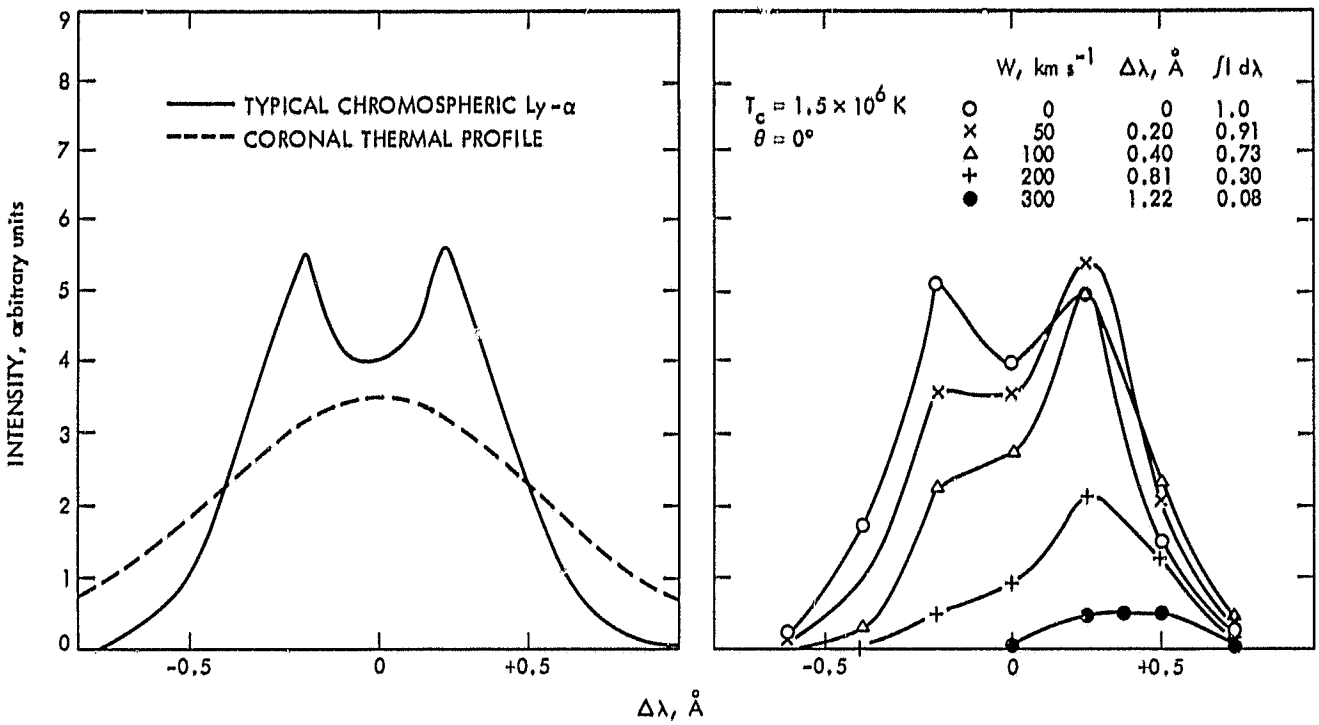

Fig. 3-8. Line profiles associated with resonant scattering of Lyman alpha radiation. The left side of the figure shows a typical emergent Lyman-alpha profile from the disk (solid line) and a 1.5×10^6 K thermal gaussian profile (dashed line). The right side of the figure shows the expected coronal profiles for resonant backscattering toward Sun-center for several different solar wind velocities. The corresponding doppler shifts of the coronal absorption profile and the integrated intensities (relative scale) of the backscattered profiles are provided also. Courtesy of John L. Kohl, Smithsonian Astrophysical Observatory

An important adjunct to the in situ measurements of the properties of the coronal plasma possible from the STARPROBE will be an imaging device capable of observing the coronal structures into and through which the probe passes. This instrument would then allow post-perihelion passage specification of the large-scale domain through which the probe penetrated (e.g., location and extent of streamers, coronal holes, etc.) by a means which is directly interpretable from past near-Earth or solar polar measurements.[3] Equally important, the CLDM would permit optical measurement of scale sizes in coronal structures for direct comparison with the in situ measurements, and provide for the first time observations of the small-scale (possibly turbulent) structure of the corona which has been inferred from radial (scintillation, phase lag) measurements.

[3] See, however, footnote 1, page 3-4. At the present time, the development of the Coronagraph and X-Ray/XUV Spectroheliograph instrument (CXX) on ISPM has been terminated, although studies for a revised CXX have been initiated.

The CLDM has important applications to interplanetary medium studies in addition to those relevant to the solar electron corona; specifically, such an instrument would be capable of observing outwardly through the zodiacal light with a variable line-of-sight, and thus would allow a direct deconvolution of the integral effects from the interplanetary cloud. Most importantly, the STARPROBE CLDM would permit observations of the F-corona relatively close to the Sun — a region which has been essentially unobservable. In fact, only such observations can fully characterize the dust scattering processes and define the spatial and size distributions and the albedo and other optical properties of dust near the Sun. Furthermore, if the CLDM is sensitive to infrared radiation in addition to visible light, the instrument would permit examination of the dust vaporization zone(s) of interplanetary material near the Sun in a direct and unambiguous way.

Finally, the inclusion of a capability to observe a magnetically sensitive coronal forbidden line provides a potential technique to measure the large-scale structure of the coronal magnetic field, an observational goal of enormous importance.

3.2.3 The Interior Structure of the Sun

The demonstration that the well-known 5-minute oscillations of the solar atmosphere are harmonics of the nonradial p-mode (pressure) acoustic oscillations of the Sun has opened up a new experimental window on the solar interior and ushered in a new subdiscipline of solar physics: solar seismology. It has already been possible to deduce some properties of the outer convection zone, such as the variation of rotational velocity with depth, from observations obtained on the ground. Although they have not yet been detected, low-order p-mode oscillations which involve the deep interior should also be present. In addition to the p-mode oscillations, theory predicts the existence of radial g-mode (gravity) oscillations that involve the entire Sun. Both oscillation modes can be used to probe the deep interior structure of the Sun, as well as that of the convection zone. During cruise phase, the Visible Light Magnetometer/Tachometer, observing in concert with the ASO, can provide a unique and precise record of the solar oscillations. We discuss the scientific objectives of this phase of the STARPROBE Mission below.

- What are the characteristics of the global modes of the solar oscillations, and what conclusions about the structure of the convection zone and solar interior follow therefrom? (VM/T)

The measurement of the oscillation modes of the Sun involves the recording of precise records of the velocity field of the photosphere. The large-scale field must be distinguished from the many microscopic and macroscopic effects present on the surface of the Sun, convection cells, differential rotation, circulation, etc. In order to deduce the oscillation modes from this complex velocity field, the observations should (1) be of long duration and (2) cover as large a portion of the surface as possible. Although the first criterion can be met by instruments in near-Earth orbit alone, the second cannot. The stereoscopic capability covering a wide range of viewing angles, which can be achieved by STARPROBE and ASO in concert, provides a truly unique opportunity to study the global oscillations of the Sun, and, therefore, the solar interior.

Such stereoscopic observations are essential to the detection of the lowest order modes, which is necessary to probe the deep interior of the Sun. This is the only method by which such fundamental parameters as the detailed variation of the rotation period and temperature with depth can be probed directly.

- How do the properties of the solar oscillations change with changes in the magnetic configuration of the Sun and with the solar cycle? (VM/T)

The interaction of the differential rotation of the Sun and the convective transport of energy is responsible for the solar dynamo which generates the solar magnetic field. Variations in the dynamic behavior of the convection zone underlie the solar magnetic and activity cycles. The STARPROBE provides an ideal platform from which to study the evolution of the structure and dynamical behavior of the convection zone, in concert with the ASO.

3.2.4 The Evolutionary and Transient Behavior of Photospheric and Coronal Structures

The award of the Nobel prize to the physicists who perfected the application of tomography to medical diagnostics has emphasized the importance of stereoscopic observations to the determination of the true nature of structures accessible only by remote sensing, especially optically thin structures. The ASO and STARPROBE observatories provide a truly classic application of this technique for solar structures because of the variable viewing angles which can be attained over the life of the mission for typical large-scale structures and during encounter for small-scale structures. (We note that the STARPROBE is especially effective in this mode during encounter since, due to its rapid motion along its track at perihelion, it can view the same structure from different angles.) Among the objectives which can be addressed during cruise are:

- The study of the evolution of the global distribution of the solar magnetic field. It should be noted that the full vector field can only be obtained unambiguously by stereoscopic observations. (VT/M, CLDM).

- The study of the evolution of the large-scale structure of the corona and of coronal loops. (SXH, CLDM, CES, EUVS).

- The study of the evolution of coronal holes, and their relation to the solar wind flow measured by the in situ STARPROBE instruments. Simultaneous coverage by STARPROBE and ASO will allow the regions on the Sun responsible for the solar wind sector structure, which STARPROBE will measure directly, to be identified. (SXH, CLDM, CLAS, CES, EUVS).

- The study of the role of coronal transients and other dynamic phenomena in the corona in determining the structure and dynamics of the solar wind flow. (CLDM, CLAS).

- Stereoscopic velocity field observations with ASO and STARPROBE (when it is near solar encounter and can attain high resolution). These observations can measure such phenomena as the full vector flow field in small structures such as granules and spicules. (VM/T)

- Stereoscopic magnetic observations with STARPROBE (again near solar encounter) and ASO. These can uniquely determine the vector field of structures such as spicules, sunspots, emerging flux regions, and cool loops. (VMT, EUVS).

- Stereoscopic observations of the magnetic structure and thermal structure of transient phenomena such as flares and prominences, in concert with ASO. An important objective is the study of magnetic and thermal structures which are likely sites of flares as close to encounter as possible, in order not only to determine how the structure of such regions evolves, but to maximize the opportunity for the stereoscopic study of the flare processes at the highest possible resolution. (VM/T, SXH).

There are many other observational programs which the unique stereoscopic capability of STARPROBE and ASO can achieve, both during the long cruise period, and for some programs during encounter when, especially at optical wavelengths, both ASO and STARPROBE will achieve resolution an order of magnitude greater than we can attain from the ground. We believe that the stereo capability of ASO and STARPROBE will present a truly unique opportunity, and that the scientific payoff which will be achieved will be truly stunning. And, we must emphasize that such an observational capability can be achieved in no other way, since a telescope able to match or exceed ASO performance elsewhere in the ecliptic plane than in near-Earth orbit would be prohibitively large for a deep space probe which did not approach very close to the Sun.

3.2.5 Some Remarks on Transient Phenomena

In the preceding discussion we have shown how the specific scientific questions raised by our major scientific objectives can be addressed by the observational program of the STARPROBE imaging instruments, in some cases jointly with the Advanced Solar Observatory.

This discussion is, however, not an exhaustive one. We wish to mention, in particular, transient phenomena such as flares, coronal transients and prominences. We have not made observational programs associated with such phenomena a formal part of the encounter science objectives, since it is difficult to assess the probability of such events occurring near solar minimum, which is the preferred time for encounter. However, we believe that it is important to build as much flexibility as possible into the STARPROBE imaging observing programs to maximize the possibility of studying a flare, or other transient phenomena, at ultrahigh resolution, should the opportunity present itself at or near the time of encounter.

3.3 BASELINE INSTRUMENT COMPLEMENT AND MISSION CONCEPTS

In Table 3-2, the physical characteristics and general performance specifications of the six imaging instruments which the Committee has identified are summarized. In the following discussion, we review the observational demands, configuration, operation modes, and anticipated performance of each of the baselined instruments. We also discuss the accommodation of each instrument on the spacecraft and the requirements which each instrument places on the spacecraft and mission characteristics.

3.3.1 The Visual Magnetograph/Tachometer (VM/T)

The Visual Magnetograph/Tachometer instrument has the strongest requirement for ultrahigh resolution imaging at encounter. Typical observational demands which determine the VM/T performance specifications are:

- The solar field is divided into individual flux tubes of field strength greater than 1000 gauss, and whose size has been estimated to be between 20 and 200 km, and are probably twisted.
- The details of the turbulent motions of the photosphere on scales from 10-100 km are crucial to models of convection and of the granulation.
- Observation of the velocity field associated with the solar oscillations and with large-scale circulation patterns will require velocity resolution of a few kilometers per second.
- The thermal gradient between the chromosphere and corona occurs on scales of less than a few hundred km even in large coronal loops. The chromosphere, which is controlled by the field, must have structure at the level of 10-20 km.

The baseline VM/T configuration which the Committee has developed is a Gregorian telescope of ~10- to 12-centimeter aperture, with blocking filters and polarizers, and a high-resolution interferometer, to allow line profile measurements in linear and circularly polarized as well as unpolarized light. The Gregorian configuration is chosen since a heat rejection mirror may be placed at the prime focus to reject the solar flux which is not within the primary field of view.

The VM/T may operate in either a magnetic or velocity mode, depending on the choice of polarizers. The use of an interferometer as the dispersing element insures the attainment of the resolution required to obtain sensitive magnetic velocity observations ($\lambda/\Delta\lambda \sim 50{,}000$). In Fig. 3-9, the optical resolution of the Solar Optical Telescope and the STARPROBE VMT Telescopes are compared (for a 10-cm VM/T aperture), illustrating the power of the STARPROBE concept.

Table 3-2. STARPROBE optical experiment strawman payload

Instrument	Mass,[a] kg	Power, W	Real-time data rate, bps	Onboard storage bits	Dimensions, cm	Wavelength coverage, angstroms	Resolution			Field of view
							Angular	Linear	Spectral ($\lambda/\Delta\lambda$)	
Direct Viewing Instruments										
Visual Magnetograph/Tachometer (VM/T)	10	5	0-500	8×10^8	20×20×100	1200-7000	1"	10 km	5×10^4	35'
EUV Spectroheliograph (EUVS)	5	3	0-500	7.5×10^8	10×10×100	300-1300	1"	10 km	5×10^3	35'
Soft X-ray Heliograph (SXH)	23	5	0-500	7.5×10^8	25×25×175	6-60	1"	10 km	10-15	10', 57'
Unbral Instruments										
Coronal Lyman-Alpha Spectrometer (CLAS)	6	10	50	2×10^7	20×10×110	1000-1300	10'-60'	4000 km	10^4	2π str
Coronal Light Detector/Magnetometer (CLDM)	6	4	20-150	3×10^8	20×10×100	4000-30000	10'-60'	4000 km	100^b	2π str
Coronal EUV Spectrometer (CES)	5	3	250	5×10^8	20×10×100	100-800	10'-60'	4000 km	10^4	2π str

[a]Does not include weight allowance for radiation shielding in all cases.

[b]For the coronal forbidden line observations 5×10^4.

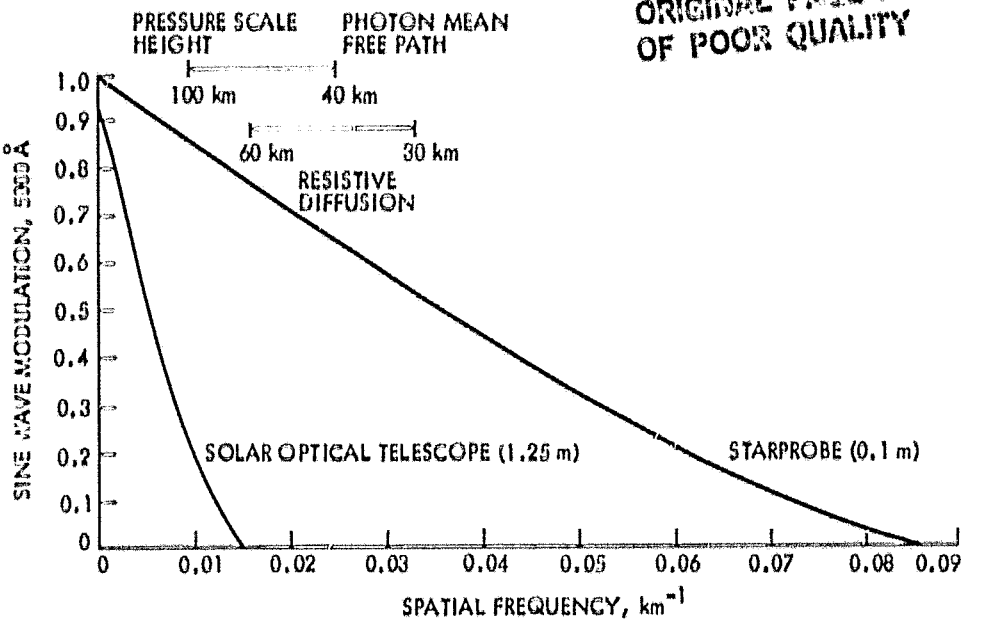

Fig. 3-9. Comparison of the modulation transfer function (MTF) of the 10-cm-diameter STARPROBE telescope (at closest approach) and the SOT telescope. The spatial frequency is expressed in km^{-1} rather than arc seconds to allow for the different distances at which the two instruments will operate. Some characteristic scale lengths, which might limit the size of features to be seen in the photosphere, are also indicated

3.3.2 The Soft X-Ray Heliograph and EUV Spectroheliographs

The observational demands on the Soft X-Ray Heliograph and the EUV Spectroheliograph are determined primarily by two factors: the small scale on which thermal gradients and heating mechanisms must occur in coronal loops, and the need to make observations over the broad range of temperatures, from 10^4 to 10^7K, which occur in the quiescent solar atmosphere. We summarize these demands below:

- Thermal gradients from coronal to chromospheric temperatures occur on scales of a few hundred kilometers, even in large loops.
- Manifestations of heating mechanisms in coronal loops and bright points must occur on scales of a few hundred km or less.
- The radiation characteristics of the structures which dominate the transition from chromospheric to coronal temperatures cover the wavelength range from a few angstroms to more than 1300 Å.

3.3.2.1 The Soft X-Ray Heliograph SXH

The resolution requirements for the SXH dictate a unique approach to a grazing incidence optical system. The objective of 1-arc-sec resolution, and the size of the individual elements in present or foreseeable array detectors, such as CCDs, require a plate scale of ∿15 microns/arc sec. With the ordinary Wolter Type I configuration, which is the most efficient X-ray imaging configuration for observations below 100 Å, this would require a telescope of 3-meter focal length, resulting in an instrument of 3.5 to 4.0 meters total length. An instrument of this size would impose intolerable demands on the STARPROBE heat shield. Recently, A. Krieger, J. Davis and K. Silk[4] have studied the use of secondary grazing incidence mirrors which, in a manner analogous to normal incidence optical systems, can result in an overall system magnification. Two configurations are possible, one in which the secondary element is placed in front of the primary focus (following a suggestion by J. Underwood; see Fig. 3-10), and a second in which the secondary element is placed behind the primary focus. One baseline SXH configuration which can satisfy the observational demands is an optical system consisting of a Wolter Type I primary mirror of ∿10-cm aperture and 0.5-meter focal length and a "Cassegrain" secondary hyperboloid mirror providing a magnification of 6. The overall length of this instrument is ∿1.75 meters; however, the focal length is 3 meters. Using a 800 × 800 CCD focal plane detector with 15 micron cells, this instrument can achieve ∿10-km resolution and a ten-arc-min field of view (which corresponds at encounter to 8.7 arc sec as viewed from the Earth). In order to obtain a larger-scale image for comparison with images from instruments in near-Earth orbit, the primary image (a 57-arc-min field of view which corresponds to a 50-arc-sec field of view from Earth) must be recorded as well.

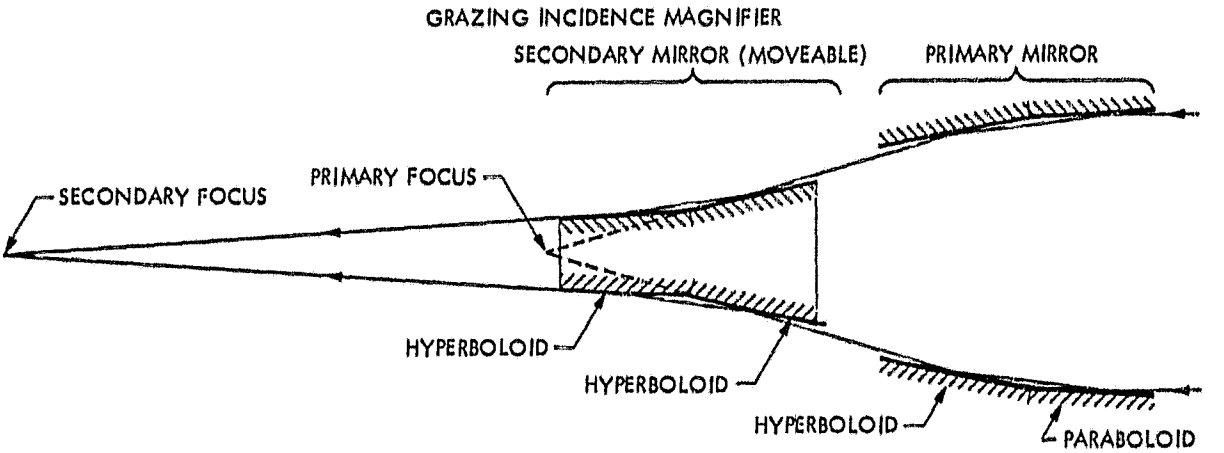

Figure 3-10. The configuration of the X-ray telescope, which utilizes primary and secondary grazing incidence mirrors to provide a magnified image

[4] See STARPROBE: A Design Study for an X-Ray Imaging Instrument, prepared by American Science and Engineering, ASE 4672 (JPL Reorder 81-12).

Spectral resolution is provided by broadband filters and Ross filters. The latter, which can achieve bandpasses of ~0.6-1.0 Å, can isolate individual line multiplets, allowing images to be obtained which correspond to material at temperatures ranging from ~1.5×10^6K (O VII, 21.6 Å) to >10^7K (Si XII, 6.64 Å or Mg XII 8.12 Å).

As is the case for the VM/T, the SXH will be placed behind a baffled collimating tube, which will reduce the irradiance on the telescope aperture to ~20 solar constants (as measured at 1 AU). The configuration of the combined SXH/EUV apertures is shown in Fig. 3-11. A critical element for the SXH is a pair of thin filters which must transmit only the X-ray spectral bandpass of interest (~6-60 Å) and reflect or absorb other wavelengths. Preliminary design studies indicate that a pair of 1500 Å aluminum films, or 3000 Å beryllium films with aluminum overcoat, supported by mesh grids, can withstand the expected ambient temperatures, and will transmit the desired radiation.

3.3.2.2 The Extreme Ultraviolet Spectroheliograph (EUVS)

There are several approaches to the design of the Extreme Ultraviolet Spectroheliograph. Figure 3-11 indicates how the EUVS and SXH may share a single optical precollimator. The grazing angle selected for the diagonal mirrors determines the short wavelength cutoff of the instrument. This could be made as short as 100 Å; however, the baseline provisionally adopted by the Committee was ~300 Å. The instrument approach currently regarded as the baseline configuration is a normal incidence Wadsworth which can stigmatically image 4-6 emission lines in the wavelength range from 300-1200 Å. Typical lines which might be selected are: H Ly α (1216 Å), He II (304 Å), O VI (1032 Å), Si XII (499 Å), Mg X (610 Å) and Fe XVI (335 Å). These lines encompass the temperature range from 10^4K to 3×10^6K in the atmosphere. There are, however, several other instrumental approaches which should be studied in more detail. For example, the use of a grazing incidence Wolter II optical system might allow observations down to 100 Å (although it might be limited to $\lambda \sim 800$ Å); an objective grating configuration might allow higher resolution, and the study of line profiles. The baseline configuration will, however, meet all of the observational criteria we have established.

The EUVS would primarily operate in a mode in which simultaneous spectroheliograms in 4 to 6 preselected emission line were recorded; however, observations could be obtained in any emission line in the spectral range of interest. The instrument may, therefore, obtain observations in any of a number of density sensitive line multiplets, such as those belonging to the beryllium isoelectronic sequence, or in the temperature sensitive line multiplets belonging to the lithium isoelectronic sequence (see, for example, Gabriel and Jordan, 1972[5], or Walker, 1976[6]). The EUVS can, therefore, carry out very powerful diagnostic studies of the corona/chromosphere transition region at very high angular resolution.

---

[5] Gabriel, A. H. and Jordan, C., in Case Studies in Atomic Collision Physics, Vol. II, p. 211

[6] Walker, A. B. C., Space Sci. Instr. 2, 9.

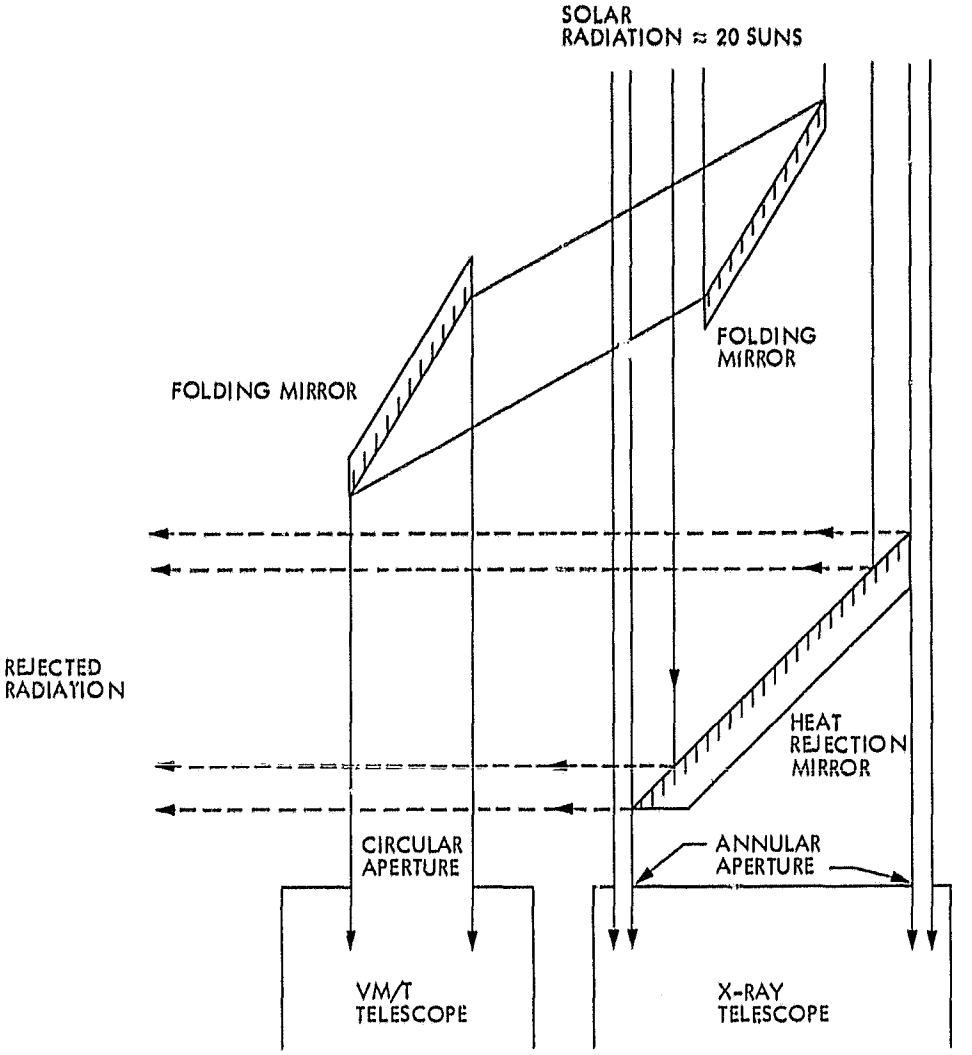

Fig. 3-11. Configuration of the combined SXH and VM/T apertures

3.3.3 The Coronal Lyman Alpha and EUV Spectrometers and the Coronal Light Detector

The three umbral instruments view the corona and, thus, are not subject to the thermal problems which must be resolved for the direct viewing instruments. The coronal viewing instruments must, however, use external (and, in some cases, internal) occulters, and must be able to scan over a very large angle (ideally $\sim 2\pi$ steradians). For the Lyman-α and coronal light instruments, scanning can probably be accomplished internally; however, it may be necessary to scan the entire EUV instrument. The unique observational capabilities of these instruments are summarized below:

- In order to determine the solar wind velocity with precision, it is necessary to make outwardly directed observations of back-scattered radiation. STARPROBE is uniquely suited to this

requirement. Lyman-α observations are most sensitive to velocities of 100-300 km/sec; to resolve smaller velocities, it is desirable to observe the profiles of other lines such as O VI (1032 A).

- Coronal measurements on the STARPROBE can be made much closer to the solar limb than would be possible with a conventional coronagraph from Earth orbit.

- The lower density of the plasma in coronal holes and in the solar wind requires much higher sensitivity than can be achieved from Earth orbit to study elemental abundances and ionization structure. The STARPROBE instruments can achieve the enhanced sensitivity which is necessary; furthermore the radial dependence of these parameters can be unambiguously unfolded from the sequence of outwardly directed observations to be taken during the encounter.

3.3.3.1 The Lyman-α Spectrometer (CLAS)

The baseline configuration of the Coronal Lyman-α Spectrometer consists of an off-axis parabolic telescope which feeds an Ebert-Fastie Spectrometer (Kohl, 1979, Kohl et al., 1980[7]). The desire for a wide field of view could be accommodated by using several telescope mirrors viewing in different directions, which could feed multiple spectrometer entrance slits. It would be desirable to observe the profiles of lines other than Lyman-α as well (i.e., O VI 1032); however, the additional complexity introduced must be weighed against the scientific advantages.

3.3.3.2 The Coronal Light Detector (CLDM)

The Coronal Light Detector will not have the stringent requirements for light rejection which the usual externally occulted coronagraph must meet; however, it must be carefully baffled internally. The CDLM will operate in two modes, utilizing filters in coronal intensity observations, or polarizers and a high-resolution interferometer for observations of coronal forbidden lines, to obtain coronal fields. The filters must cover a broad wavelength range, extending into the infrared.

3.3.3.3 The Coronal Extreme Ultraviolet Spectrometer (CES)

The Coronal Extreme Ultraviolet Spectrometer will utilize a Wolter Type II optical system, most probably combined with secondary optics in its

[7] Kohn, J. L., in A Closeup of the Sun, 1979, JPL Publication 78-70, Kohl, J.L., Withbroe, G. L., Weiser, H., MacQueen, R. M. and Munroe, R. H., The Spacelab Lyman Alpha and White Light Coronagraphs Program: to be published in Space Science Reviews.

spectrometer design; however, the details of the CES design are not yet well established. The 100-800 Å interval selected for the CES was chosen because the widest range of ionization stages of C, O, Ne, Mg, Si and Fe can be observed within this wavelength interval. It is anticipated that the CES will operate primarily in a spectrometer mode, scanning over select wavelength intervals in order to measure the abundance and ionization structure of the solar wind.

3.3.4 Accommodation of the Imaging Instruments

We comment briefly here on the most significant problem areas of instrument accommodation which the Committee addressed.

3.3.4.1 Physical Placement of Instruments

The basic philosophy adopted to accommodate the direct viewing instruments is to place them behind collimated baffles which reduce the incident heat flux to ∿20 solar constants (as measured at 1 AU) by limiting the field of view. This approach is illustrated by Fig. 3-12 (Fig. 3-12 does not necessarily represent the latest STARPROBE configuration, but it does illustrate the basic design philosophy). Recently, a study by Ball Aerospace[8] has indicated that separate collimation tubes for the VM/T and SXH/EUVS may be preferable, since this approach eliminates constraints on the VM/T and SXH apertures. Although it is not shown in Fig. 3-12, the EUVS may be easily accommodated with the same collimated baffle system as the SXH, as shown in Fig. 3-11.

The accommodation of the Coronal Light Detector and the Coronal Lyman-α Spectrometer in a single package is assumed in Fig. 12. The use of a spinning platform, coupled with the use of multiple apertures to allow observations at angles up to 90° from the spin platform axis, can accommodate the desired 2π steradian field of view.

The accommodation of the Coronal EUV Spectrometer presents a more difficult problem, since the use of reflecting flats is limited for an instrument operating at 100 Å in the EUV. Alternatively, limiting the short wavelength cutoff to 300 Å may ease this problem. Other approaches to meeting the CES view requirements are discussed in Section 3.4.

3.3.4.2 Thermal Control

With the adoption of the collimated optical baffles to reduce the radiative flux on the primary optical elements, and th prudent use of techniques

---

[8] Design Study of Imaging Techniques for the STARPROBE Mission, BASD Report F21-08, July 1981.

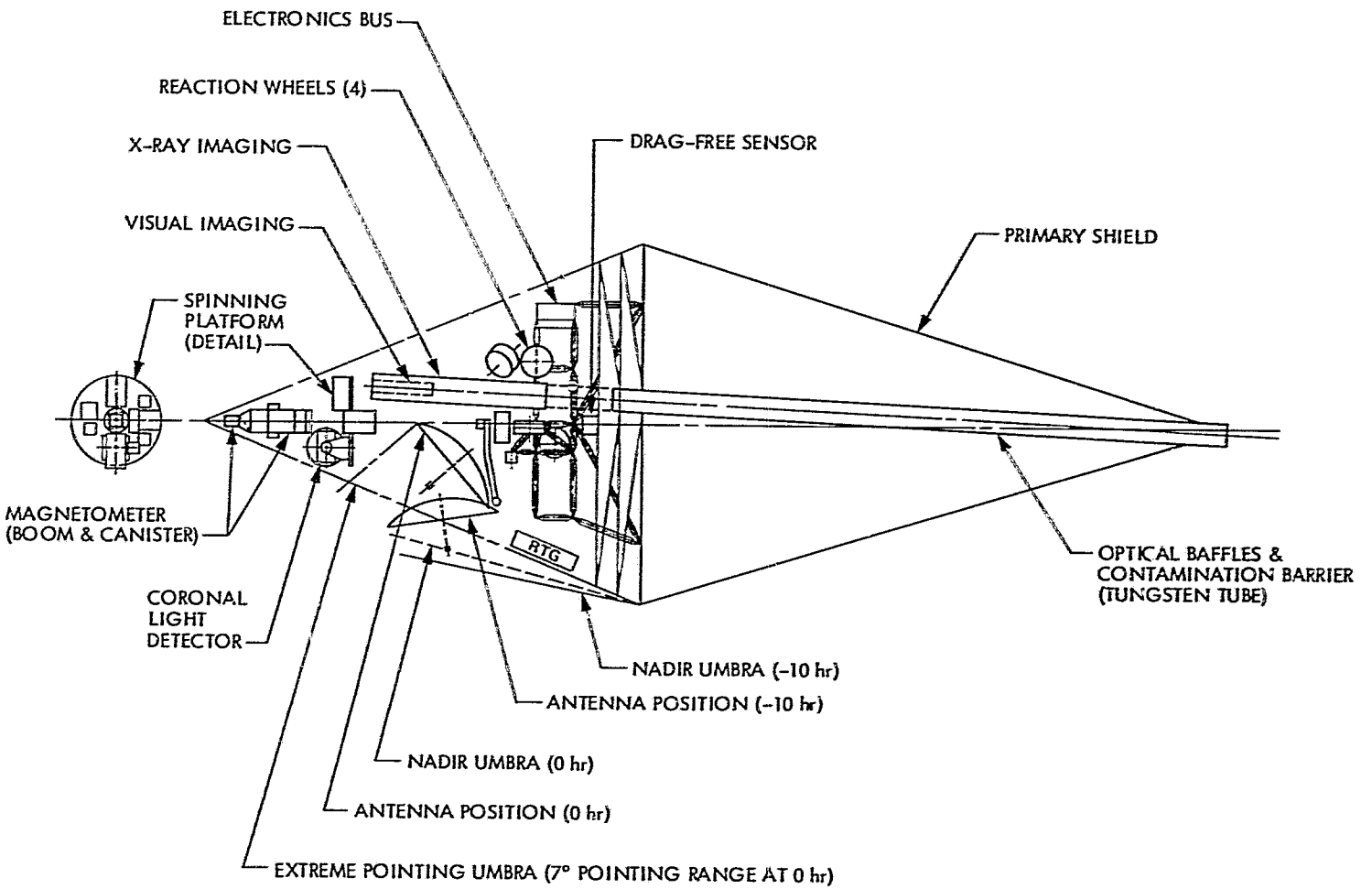

Fig. 3-12. Sideview of STARPROBE full science payload configuration. Note the use of an optical baffle to reduce the heat on the optical elements. The EUVS and CES are included in this configuration

such as the VM/T Gregorian design to reject surplus radiation, it appears that the direct viewing instruments can tolerate the thermal environment at encounter. Detailed studies have already been carried out for the SXH and VM/T, indicating that the performance specifications of Table 3-1 will not be compromised by thermal control measures. The coronal instruments are not expected to encounter severe thermal problems.

3.3.4.3 Imaging Data Storage

A rather critical issue from the point of view of the imaging experiments is the capacity to store data during the encounter phase, when the data link with the spacecraft will be severely limited. Table 3-2 indicates the requirements for onboard storage which the Committee has developed. These requirements are based on the fact that even with onboard data compression, a single image from, for example, the VM/T or SXH will contain more than 10^6 bits. When the requirements for multiple filters or multiple wavelength images and line profile determinations is taken into account, a single "observation" will require $\sim 10^7$ bits for most instruments. The importance of this capability to fully exploit the unique opportunity presented by the STARPROBE encounter cannot be overemphasized.

3.3.4.4 Contamination of Optical Surfaces

The flux of material sublimed from the heat shield during solar encounter is expected to be quite high. Since the optical surfaces of the various optical instruments will be cool compared to most other spacecraft systems, contamination of these surfaces presents a serious potential problem. Reflectivity in the EUV is especially sensitive to contamination; experience on OSO has shown that a factor of 100 in reflectivity can be lost due to contamination. This problem deserves very careful study.

3.3.4.5 Region of View

As the STARPROBE spacecraft passes over the solar meridian of 0° longitude (as viewed from Earth) it is necessary to have the capability to offset the viewing direction lateral to the spacecraft motion in order to view various features on the disk. This is accomplished by tilting the spacecraft axis; the degree of offset allowed depends on the configuration of the heat shield and payload. The current configuration, assuming an X-ray telescope of less than 2 meters length (the current baseline is 1.75 meters) will allow a scan range of ±7.5°. Figure 3-13 indicates the quite excellent coverage which can be achieved.

3.3.5 Mission Profile

The Committee has agreed that the preferred period for STARPROBE solar encounter is near solar cycle minimum, somewhat toward the ascending phase; and that the spacecraft orbit should cross the Sun's poles. This will ensure that

OPTICAL POINTING RANGE BOUNDARIES

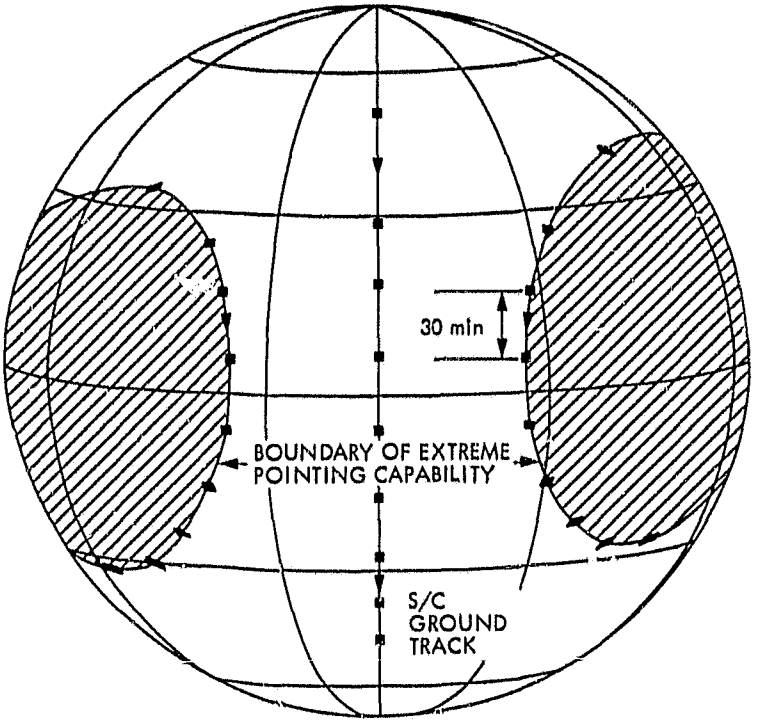

Fig. 3-13. The unshaded regions indicate the area on the disk which may be viewed. Note the rapid motion of the subsatellite point

the spacecraft will pass through polar coronal holes, and that the solar wind related objectives can be achieved. The encounter should be timed so that the spacecraft approaches the Sun from behind, as viewed from Earth, so that the features to be observed at perihelion are observable from Earth, and a comprehensive observing program can be developed and implemented. Preliminary studies of solar activity levels of previous solar cycles early in the ascending phase suggest that there is a very high probability that examples of all features of interest, such as sunspots, coronal loops, etc., will be present for encounter.

3.4 SOME TASKS FOR FUTURE STUDIES

There are a number of questions relating to the imaging instruments which require more detailed study. Among those which appear to be most urgent are the following:

- The extreme Ultraviolet Spectroheliograph should be more clearly defined. In particular, the thermal problems associated with the optical flats, should be addressed. Furthermore, there are several basic approaches to the EUVS; each has its advantages and disadvantages, both scientifically and technically. If possible, each should be studied to the depth which has already been achieved for the SXH and VM/T.

- The Coronal Light Detector/Magnetometer has not been fully defined. In particular, the concept of including a capability for high-resolution observations of coronal forbidden lines to determine the coronal field is fairly recent.

- The Coronal EUV Spectrometer is the least well defined of the imaging instruments. One serious issue which must be addressed is how to obtain the desired wide field of view without scanning the entire instrument. Such approaches as the use of layered synthetic microstructures as EUV mirrors or optical elements should be carefully investigated.

- An element common to many of the imaging instruments is the desire to utilize a CCD array as the imaging element. This will require the use of radiative coolers since these detectors must operate at ∿170 K for the most effective performance. The impact of this requirement for radiative coolers to provide the necessary thermal environment should be studied.

3.5 IMAGING SCIENCES SUMMARY

In summarizing the work of the Ad Hoc Imaging Committee, the following points can be made:

- The Committee has concluded that the scientific objectives which can be addressed by imaging instruments on STARPROBE are critical to Solar Physics, and can be accomplished in no other way.

- The Committee has defined six baseline instruments, each of which has a unique set of objectives and capabilities. The measurements to be taken are highly complementary to one another, and to the in situ observing program of the particles and fields instruments.

- Collaborative observations between STARPROBE and the Advanced Solar Observatory throughout the STARPROBE Mission (including the cruise phase) will greatly enhance the scientific return of both observatories.

- The technical challenges, such as thermal control, which the STARPROBE mission presents to the imaging instruments are formidable; however, they all appear solvable.

- The accommodation of all six imaging instruments on the current all-science spacecraft design appears feasible. Field of view requirements can be met. Important issues which remain to be resolved are the onboard data storage requirements (∿3.5×10^9 bits are desired) and the extent of the danger of contamination of optical surfaces presented by mass loss from the heat shield during encounter.

3.6 ACKNOWLEDGEMENTS

The Committee wishes to express its thanks to the JPL engineering staff for extraordinary insight and responsiveness. The concept of the imaging package has been developed and refined in remarkable detail, given the constraints of time and resources under which we worked. We also wish to thank Bruce Goldstein and Jim Underwood, the Project Scientists, and Jim Randolph, the Project Manager, for their help and encouragement. The individual members of the Committee look forward to a continued close working relationship with the JPL staff, and the STARPROBE project in particular.

CHAPTER 4

STARPROBE MISSION AND SYSTEM OPTIONS

J. E. Randolph, Jet Propulsion Laboratory

4.0 INTRODUCTION

The STARPROBE mission concept has been under study at JPL and its history is reported elsewhere (Refs. 4-1, 4-2). The current study included five mission and system design options satisfying five scientific mission concepts. This is a report of the results of this study including a summary of the scientific objectives, design requirements, and specific designs satisfying these five concepts.

The mission involves targeting a shielded spacecraft to pass through the outer solar corona. With this proximity to the Sun, fundamental investigations of the local surface and interior characteristics of the Sun are possible and are detailed in chapters 1 through 3. Trajectories require large energies which are currently only possible with a Jupiter gravity-assist delivery. A spacecraft is delivered on a trajectory over the pole of the Sun and to a perihelion radius of four solar radii ($4R_s$)

Depending on the scientific objectives and payload, the spacecraft can have various appearances which are characterized by the design of the thermal shield. A research program is underway at this time to determine the shield design. The details of this program and the design are discussed in Ref. 4-4. The drag compensation requirements (Refs. 4-3, 4-5, 4-6) also influence the configuration design and affect the system and subsystem design requirements (Ref. 4-8). Incorporation of a "drag-free" sensor and associated onboard computational complexity is necessary to provide the high drag compensation accuracy for the mission options with gravitational experiments (Refs. 4-3, 4-5, 4-6, 4-7).

STARPROBE may become an official NASA project in the late 1980s with the earliest launch opportunity probably in 1988. Current trajectory design concepts consider only this launch opportunity but similar opportunities exist about every 13 months.

4.1 SCIENCE SUMMARY

The scientific justification for the STARPROBE has been reviewed periodically. A typical question asked is, "What can STARPROBE do that other missions cannot?" The following points attempt to summarize the answers.

(1) Measure the solar J_2 to the <u>accuracy</u> ($\sim 10^{-8}$) required to:

   (a) Determine the rotation rate(s) of the solar internal structure yielding the solar mass distribution and total angular momentum (see Sections 1.1.3 and 1.1.8).

   (b) Determine the value of the PPN parameter β providing one of the most accurate experimental tests of general relativity (see Section 1.2.3).

(2) Observe in-situ the dynamics and heating of the solar wind in the unexplored region between $4R_s$ and $60R_s$ (see Section 2.1.1)

(3) Determine the mass loss mechanisms of a stellar object (see Section 2.1.1).

(4) Measure the energy spectra and composition of solar energetic particles to determine their storage, release and acceleration histories (see Section 2.1.2).

(5) Image the sun at a resolution at least an order of magnitude better than the most advanced proposed solar observatories, yielding details about structure in the photosphere, chromosphere and corona which would never be visible by other techniques (see Section 3.2.1).

Details of the scientific objectives and requirements for the three STARPROBE scientific disciplines are discussed in chapters 1 through 3 and by Underwood (Ref. 4-3). The fields and particles (F&P) discipline includes the following typical instruments:

Plasma Spectrometers (PS)

Magnetometers (MAG)

Plasma Wave Spectrometer (PW)

Energetic Particle Detector (EP)

Dust Impact Detectors (DI)

Ion Composition Analyzer (IC)

Coronal Light Detector (CLD)

Figure 4-1 illustrates the regions of each of the phenomena expected near perihelion (see Section 2.0) and the instruments used to measure each of the phenomena. Note that a STARPROBE perihelion of $4R_S$ would pass through all of the regions with the exception of the region of closed field lines. This region could only be observed with remote sensing instruments.

The Imaging scientific discipline consists of the remote sensing experiments which rely on optical instruments in two classes as discussed in chapter 3. The first class would utilize direct viewing instruments including:

Visual Magnetograph/Tachometer (VM/T)

EUV Spectroheliograph (EUVS)

Soft X-Ray Heliograph (SXH)

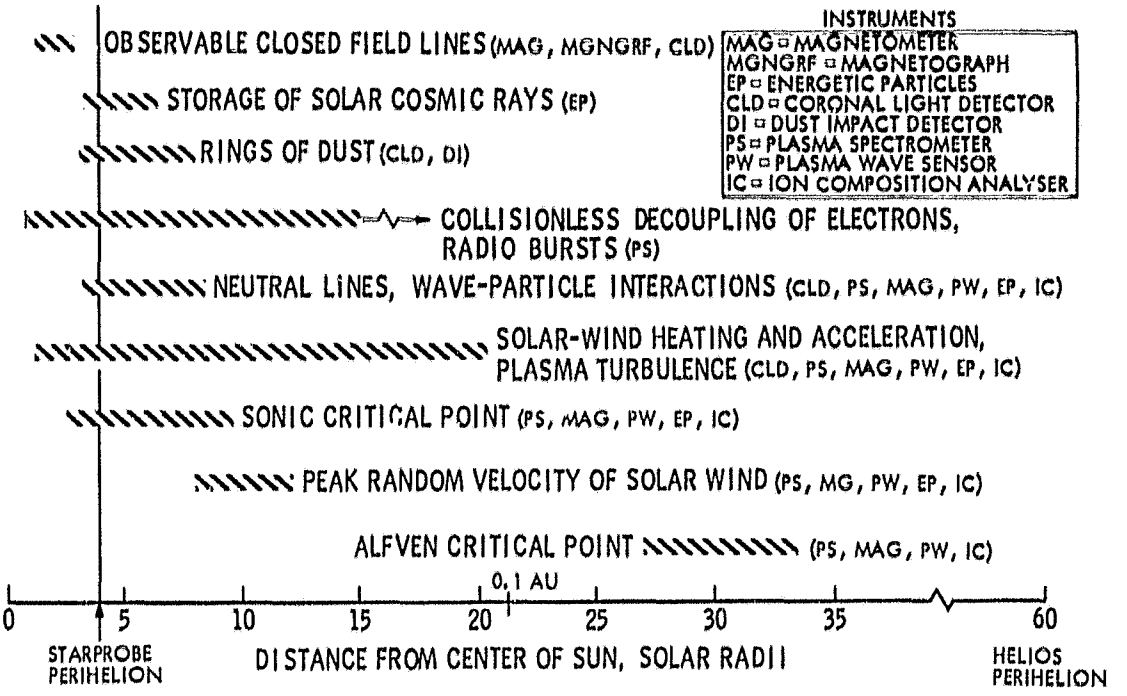

Fig. 4-1. Fields and particles phenomena and typical instruments

The objectives of this class of experiments are to provide the highest possible resolution images of the physical structure in the solar atmosphere as discussed in Section 3.2.

The second class of optical experiments would not view the solar disk but would observe phenomena in the corona which could be related directly to the in situ experiments. These instruments include:

Coronal Lyman Alpha Spectrometer (CLAS)

Coronal Light Detector/Magnetograph (CLDM) (magnetograph on the CLD)

Coronal EUV Spectrometer (CES)

In addition to the synergism with the in situ experiments, other objectives of these coronal viewing instruments include studying the evolution of the structure of dynamic coronal events which would also be observable by solar telescopes, on and orbiting the Earth.

The gravitational experiments on STARPROBE rely on precision determination of the spacecraft's orbit in order to detect small perturbations caused by various gravitational and relativistic effects. The most fundamental objective is to determine the solar gravitational quadrupole moment (J_2) as elaborated in Section 1.3.1. The "instruments" involved are the drag compensation system on the spacecraft and the high accuracy radio tracking system onboard and on the earth described by Armstrong et al (Ref. 4-9). The predicted sensitivity of the

J_2 measurement by STARPROBE is shown in Fig. 4-2 as derived from Mease et al. (Ref. 4-7). Here the J_2 accuracy is plotted against the perihelion radius and orbital inclination. The design goal of 1 to 2 parts in 10^8 accuracy can be met only if the perihelion radius is about $4R_S$ and the inclination is greater than about 70 degrees.

The five science options considered during the most recent study were derived from each of the scientific disciplines or combination of disciplines. These options were defined by the NASA-sponsored STARPROBE Scientific Advisory Group. Table 4-1 summarizes the disciplines included in each science option. Note that there are two options which contain only fields and particles experiments. One of these is for a 3-axis stabilized spacecraft design. The other is a spin stabilized design. Each of these options will be discussed later.

4.2 TRAJECTORY DESIGN

A near perihelion trajectory satisfying the scientific objectives has a perihelion radius of about $4R_S$ and an inclination of about 90 degrees. The baseline trajectory with these parameters is shown in Fig. 4-3. This is a view (edge-on to the ecliptic plane) of the trajectory from -10 days to +10 days with an expanded view from minus to plus 8 hours. The high heliocentric velocity of the spacecraft is apparent from the figure. The spacecraft passes from pole to pole in less than 14 hours, reaching a perihelion velocity of over 300 km/sec. Also illustrated is a schematic view of the spacecraft in its nadir pointing orientation, keeping the shield toward the Sun throughout the perihelion passage. Note that a 180-degree pitch maneuver is required in about 14 hours.

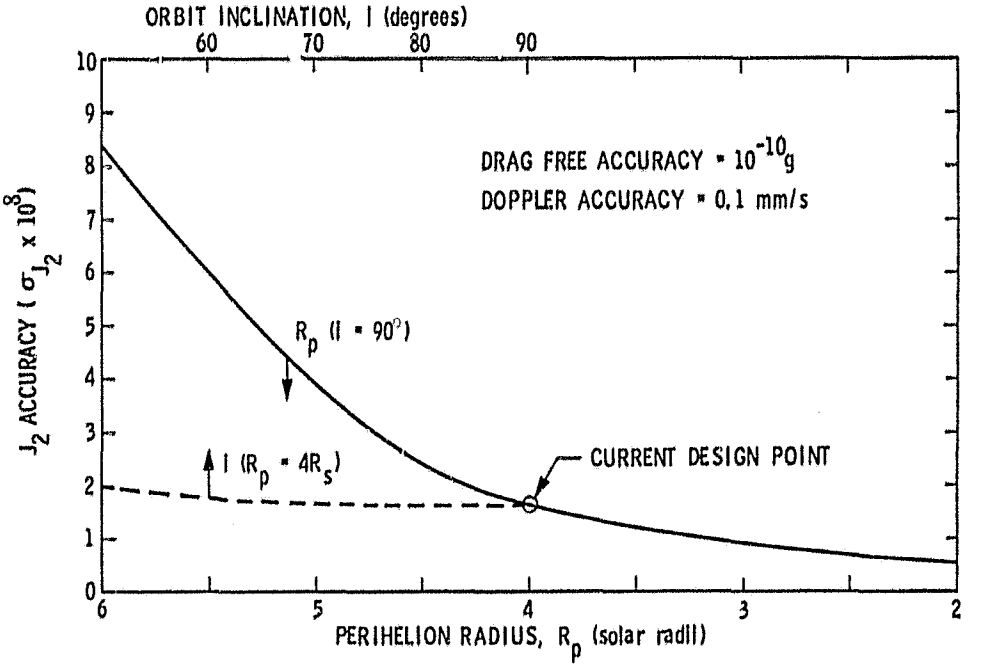

Fig. 4-2. Estimated J_2 accuracy versus perihelion radius and orbit inclination

Table 4-1. STARPROBE science options

	Scientific discipline			
	F&P	Optical	Gravity	Comment
Option				
I	X	X	X	Full science
II	X		X	No optical
III	X			F&P 3 axis
IV		X		Optical only
V	X			F&P Spin stabl.

To deliver a spacecraft to the perihelion conditions illustrated in Fig. 4-3 requires a high energy trajectory using Jupiter gravity assist (JGA), as determined from previous studies (Refs. 4-1, 4-2). A major concern in the past has been delivering sufficient payload to $4R_S$ with the early versions of the Space Shuttle (STS) configured for interplanetary launches using an IUS upper stage. Trajectories were designed (Refs. 4-1, 4-2) which would deliver sufficient mass to the Sun given this less than desirable STS performance, but they required both Earth and Jupiter gravity-assist swingbys and were known as ΔV-EJGA trajectories. More recently, new STS high-energy-stage concepts (e.g., Centaur/STAR-48 or on-orbit assembly of IUS stages) have been proposed. Such a stage would allow the delivery of a sufficient payload to the Sun using only a JGA trajectory.

These types of ballistic delivery trajectories are illustrated in Fig. 4-4, which is a view from above the ecliptic plane. The spacecraft is launched on an Earth return trajectory leading to an Earth gravity-assist (EGA) swingby. To accomplish the Earth return it is necessary to carry a large propulsion module providing the two large impulses (ΔV_1 and ΔV_2). This inner portion of the trajectory is known as a ΔV-EGA trajectory. Following the ΔV_2 maneuver and the Earth swingby, the spacecraft now continues outward toward the Jupiter gravity-assist (JGA) swingby. The state of the ΔV-EGA trajectory is virtually identical to a JGA trajectory just past the Earth. Thus, if a high-energy launch vehicle can inject a spacecraft into this state toward Jupiter, only a JGA trajectory is required. The advantages of the JGA trajectory include the shorter flight time and the deletion of the ΔV propulsion module from the spacecraft at significant cost savings.

Another parameter illustrated in Fig. 4-4 is the earth-node angle (η) shown at a value of -45 degrees. This angle is defined as the difference in

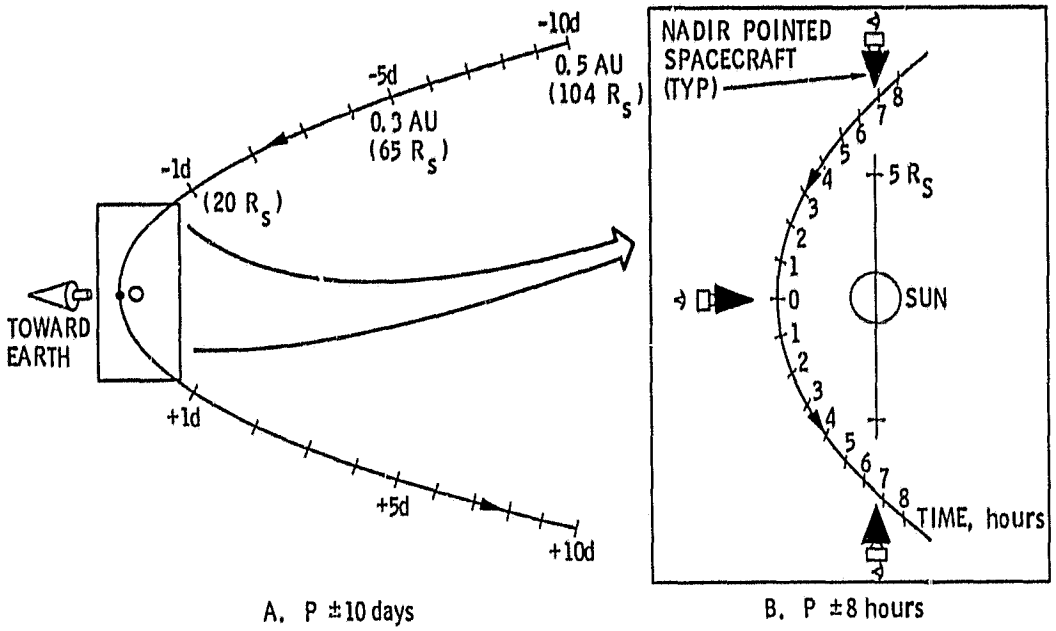

Fig. 4-3. Near-perihelion trajectory

heliocentric longitude between the STARPROBE orbit node and the Earth's location at the time of perihelion. An angle of -45 degrees has two positive attributes. First, the geometry at perihelion is nearly optimum for radio tracking purposes to determine J_2 as illustrated in Fig. 4-5. This is a view of the perihelion trajectory and the Sun as seen from the Earth. Note that the perihelion is about 0.8 degrees from the Sun. This separation is important to the telecommunications subsystem design as discussed by Armstrong, et al (Ref. 4-9).

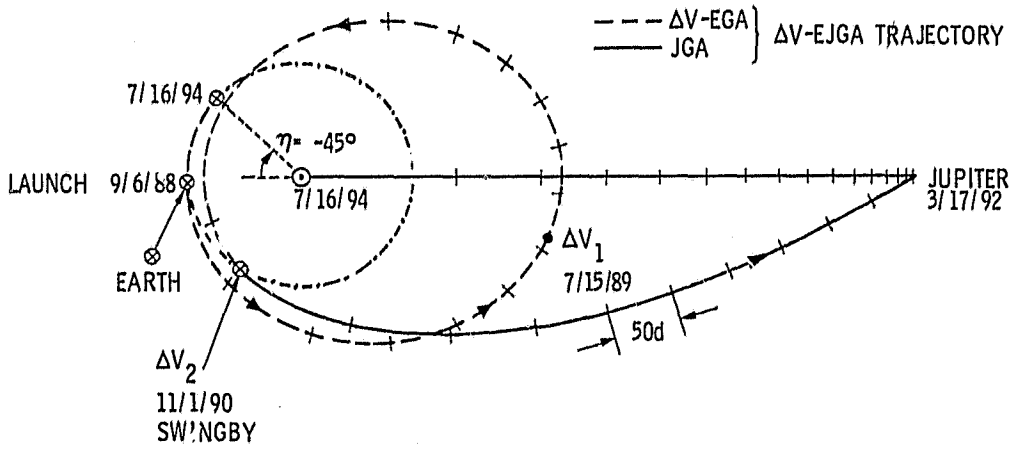

Fig. 4-4. STARPROBE 1988 ballistic delivery trajectories

C-2

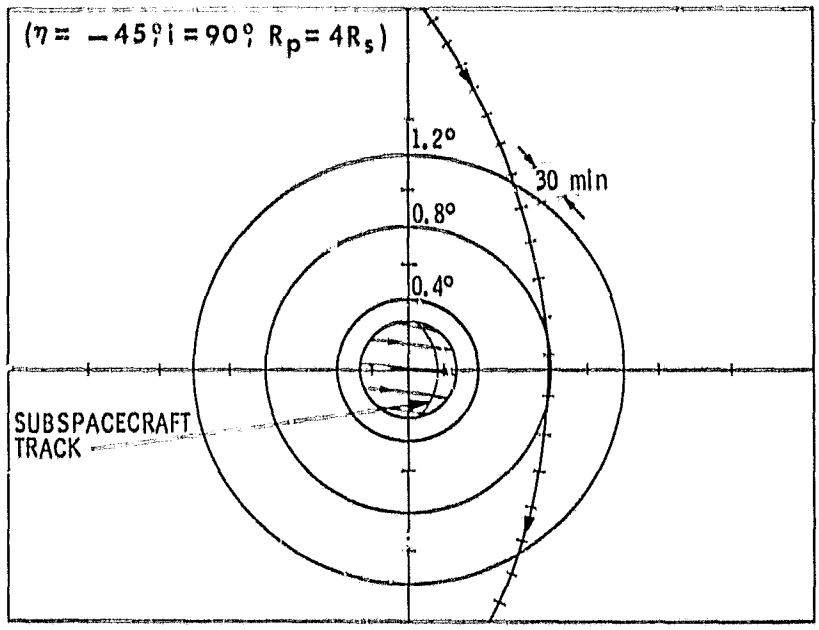

Fig. 4-5. 1988 perihelion trajectory view from Earth

Another aspect of this geometry illustrated in Fig. 4-5 is the subspacecraft track on the Sun. This is the track that is most easily observable from the spacecraft optical instruments. But, with this geometry, the track would also be observable from Earth-based solar telescopes during the encounter inviting complementary observations in regions near the track. Note that these regions would rotate from left to right, allowing enough time (a few days) to reprogram the STARPROBE computers to point at exactly the same regions which had previously been observed from Earth. Thus, high-resolution observations from STARPROBE could be made of regions containing interesting transient events seen previously with lower-resolution solar telescopes near or on the Earth.

Another type of trajectory has been studied (Ref. 4-10) which is similar to the ΔV-EJGA trajectory but utilizes a high specific impulse electric propulsion system for the "ΔV." Figure 4-6 illustrates such a trajectory for STARPROBE using a Solar Electric Propulsion System (SEPS) currently under development at NASA. The intermediate orbit is similar to the ΔV-EGA trajectory, but the velocity is added continuously by the SEPS system to shape the Solar Electric Earth gravity-assist (SEEGA) trajectory for the Earth swingby. Add Jupiter gravity-assist and this is defined as a SEEJGA trajectory. One of the most favorable attributes of the SEEJGA trajectory is the lower final orbit period (2.9 years) produced by retrothrusting with the SEPS during the approach to the Sun. One of the major drawbacks of this concept is the expected contamination of the spacecraft surfaces and fields and particles environments when the SEPS is operating.

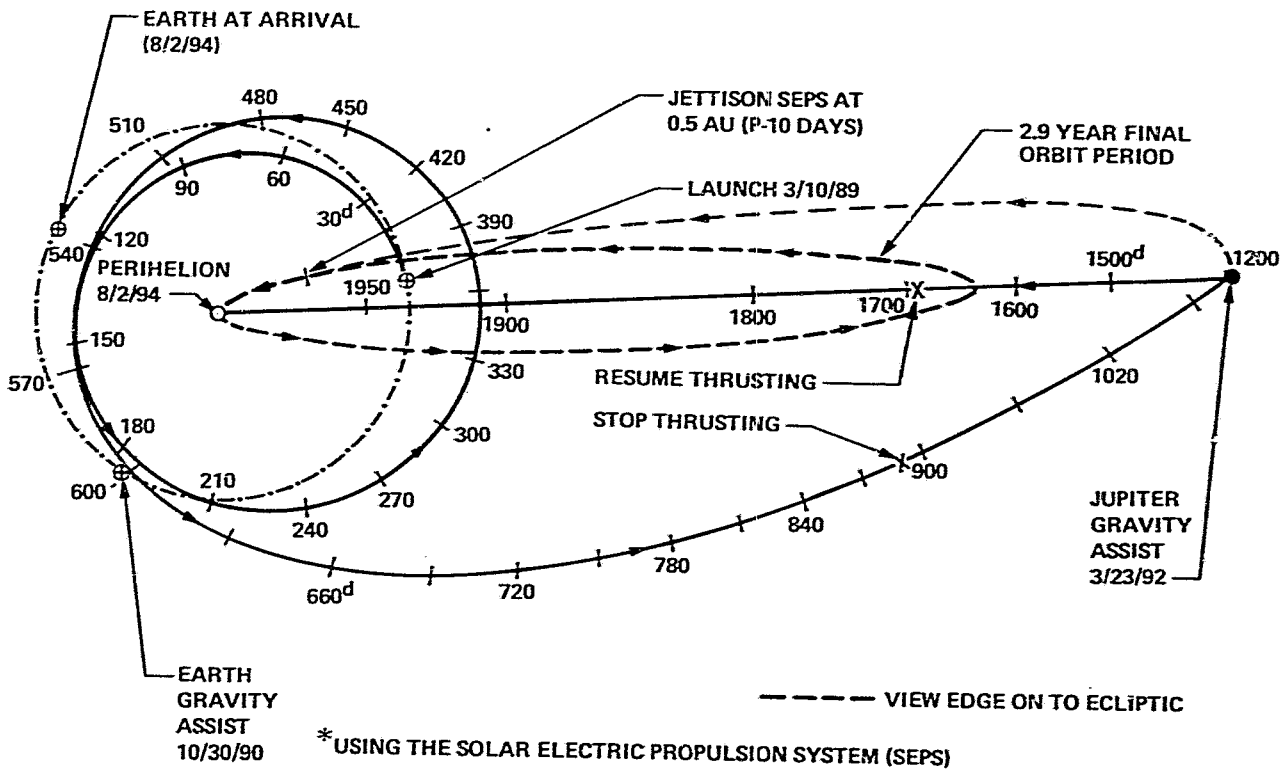

Fig. 4-6. STARPROBE solar electric Earth-Jupiter gravity assist (SEEJGA) trajectory (view from above ecliptic)

Table 4-2 summarizes the principal characteristics of the STARPROBE trajectory options. For each of the ballistic trajectory types there are two entries in the table. The JGA trajectories are characterized by the length of the flight time to the Sun, which is directly related to the launch energy. The "short" JGA has the shortest flight time (2.7 years) of any of the trajectory options but has the highest C_3 (133), requiring a high-energy-upper-stage launch vehicle to deliver a reasonable payload to the Sun. A reduced C_3 is possible using the "long" JGA trajectory at a penalty of an additional 1.1 years of flight time. Another difference in the JGA trajectories is the Perijove radius. The short JGA trajectory passes Jupiter at about 3 R_J and will be subjected to a higher flux of particle radiation than the long JGA (and all of the other options) which pass at about 10 R_J.

Although only one AV-EJGA trajectory exists for the 1988 opportunity, two technologies of the AV propulsion module are possible (see Table 4-2) yielding significantly different performances. Because of the higher performance of the space storable propulsion module, over 600 kg more delivered mass is possible.

Included for comparison in Table 4-2 are the SEEJGA trajectory characteristics. Note that the most outstanding characteristic is the reduced final orbit period (2.9 years) afforded by thrusting from Jupiter to the approach to the Sun. This is because the final orbital period is not defined by the aphelion (near Jupiter) as with the ballistic trajectories.

Due primarily to cost considerations, the current preferred trajectory is the short JGA which seems to deliver a sufficient mass for the current spacecraft design if a high-energy upper stage (e.g., Centaur) becomes available.

4.3 SPACECRAFT SYSTEM DESIGN REQUIREMENTS

A mission to the Sun places very stringent and unique requirements on the spacecraft design. Table 4-3 summarizes some of the requirements derived from the scientific objectives and placed on the spacecraft subsystems. Associated with each requirement is a numerical specification which can drive the design of a specific subsystem or the entire system. Note that the requirements for each science option form a subset of the total requirements, with the exception of the full science option (not shown), which must fulfill all of the requirements simultaneously. The following paragraphs describe the effects of the principal requirements on the design options.

Many of the requirements affect the configuration as shown in the schematic drawing of Fig. 4-7. Dominating the configuration is the primary thermal shield. The design of the shield is not driven by survivability but by the scientific requirement to minimize the mass loss from the shield (less than 2.5 mg/sec). To keep the temperature at a low enough level to satisfy the mass loss specification, a high aspect ratio geometry is necessary. A cone seems to be the best geometry for the shield, and the lowest mass shield seems to be made of a refractory carbon-carbon material. Below the primary shield, the carbon-carbon secondary shields reduce the thermal flux from the back side of the primary shield to a benign 40 deg Celsius in the electronics bays and the drag-free sensor.

Table 4-2. 1988 STARPROBE delivery trajectory options (perihelion = $4R_S$; inclination = 90°)

Option	Launch mass, kg	Delivered mass, kg	Launch[a] C_3 km^2/s^2	Perijove,[b] R_J	Flight time, yr	Final period, yr	Earth-node angle (η), deg	Launch vehicle/ onboard propulsion
Short JGA	1240	1240	133	3	2.7	4.7	-45	Shuttle with HEUS[c]
Long JGA	1370	1370	124	10	3.8	4.2	-45	Shuttle with HEUS[c]
ΔV_{SS}-EJGA	5800	2710	31.2	10	5.9	4.5	-45	Shuttle with Centaur Upper Stage/Space-Storable Propulsion Module[d]
ΔV_{ES}-EJGA	5800	2080	31.2	10	5.9	4.5	-45	Shuttle with Centaur Upper Stage/Earth-Storable Propulsion Module[e]
SEEJGA	5988	2232	3.6	10	5.4	2.9	-31	Shuttle with IUS Twin Stage/ Solar Electric Propulsion Systems (SEPS)

[a] Launch C_3 required for a 10-day launch period opportunity.

[b] Jupiter perijove radius expressed in Jupiter radii (R_J).

[c] HEUS = high-energy upper stage: either Centaur/star 48 or on-orbit assembled 5-stage IUS.

[d] Space storable ≙ N_2H_4 + LF_2 propellant and oxidizer.

[e] Earth storable ≙ MMH + N_2O_4 propellant and oxidizer.

Table 4-3. Spacecraft design requirements and specifications

Science requirements on spacecraft design	Specification	Science option		
		Gravity and fields & particles II	Fields & particles III, V	Optical IV
Configuration and thermal control				
Perihelion radius (thermal flux)	$4R_s$ (400 w/cm^2)	X	X	X
Shield mass loss at perihelion	<2.5 mg/s	X	X	?
Benign thermal environment for instruments	40°C	X	X	X
RTG remote location from instruments	>2m	X	X	X
Magnetometer boom @ 0.3 AU (0.019 AU or $4R_s$)	3.3 m (0.5 m)	X	X	
Attitude articulation translation				
Nadir pointing accuracy of shield	0.5°	X	X	X
Drag compensation/estimator	10^{-10} g/32kword?	X		
Optical pointing accuracy (absolute)	0.02°			X
Optical pointing range off nadir	<10°			X
Optical pointing stability	<0.3 $\widehat{\text{sec}}$			X
Rotating science platforms	10 RPM	X	X	
Telecommunications and data handling				
Real-time telemetry at perihelion	>20 kbps	X	X	X
Doppler tracking accuracy	0.1 mm/s	X		
Data storage	1.9×10^9 bits	X	X	X
Stored programmable sequences	90kwords(?)	X	X	X

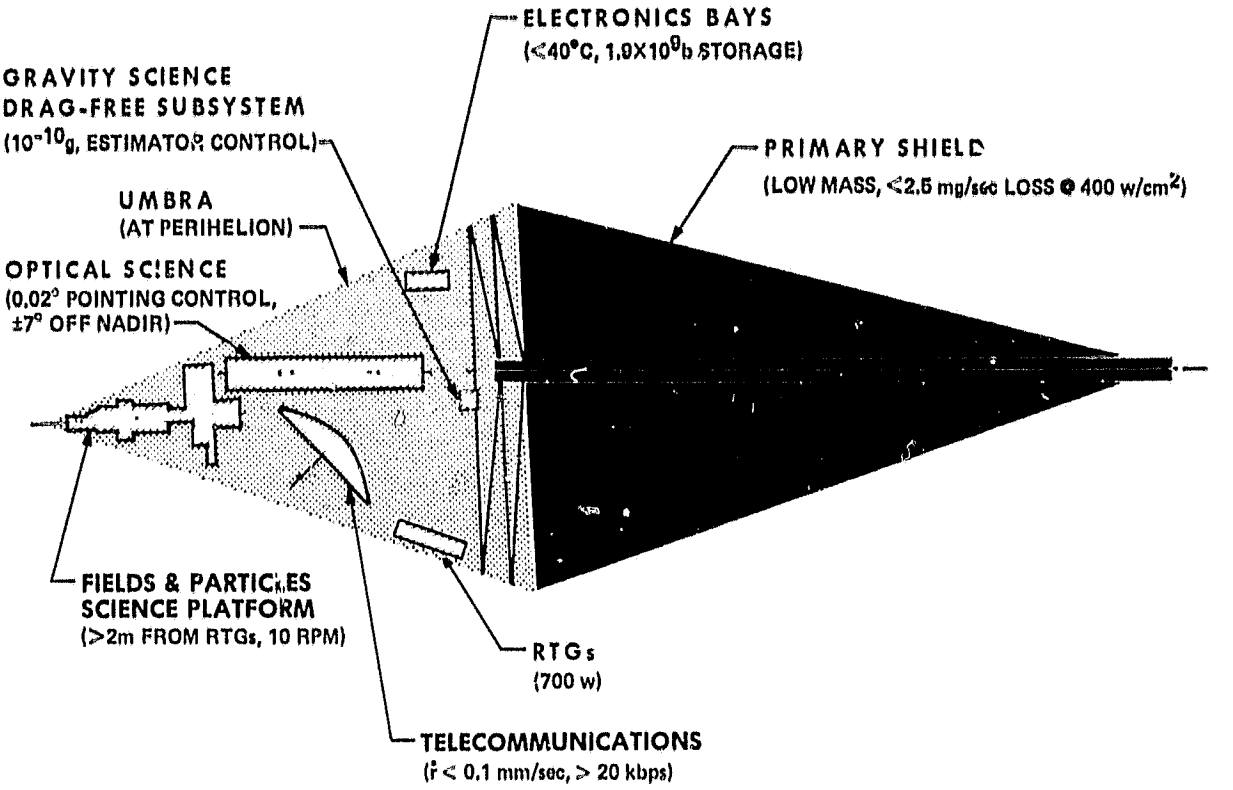

Fig. 4-7. Spacecraft schematic configuration

The shadow or umbra cast by the shield has a conical shape due to the large angular diameter (28 deg) of the Sun at $4R_S$. The components of the spacecraft must reside in this umbra for survival. The power sources, consisting of radioisotope thermoelectric generators (RTGs), reside in the upper part of the umbra for two reasons. First, there is more area available in this part of the umbra for the large thermal radiators which wrap around the outer edge of the umbra (not shown in Fig. 4-7). Second, placement of the RTGs here separates them as far as possible from the scientific instrument detectors which are sensitive to the neutrons and gammas emitted by the RTGs.

Wrapping around the opposite side of the upper umbra from the RTGs, the electronics bays are located to allow the large volume required as well as reasonable isolation from the RTGs. In the center of the upper umbra is the drag-free sensor for the gravitational experiments located near the center of gravity. Below the RTGs is the high-gain antenna (HGA), which must remain in the umbra and be fully articulated (to continuously track the Earth during the nadir pointing maneuvers near perihelion). It represents the window to the telecommunicatons subsystem, which must maintain high Doppler tracking accuracy (less than 0.1 mm/sec) and high telemetry rates (greater than 20 kbps).

The direct viewing optical science instruments reside on an "optical bench" near the lower center of the umbra. The boresight of the direct viewing optical instruments passes through the refractory metal tube located near the center of the primary shield. This tube acts as a thermal isolator for the instruments as well as a contamination barrier. The X-ray telescope is the largest of

the optical instruments (shown schematically in Fig. 4-7) requiring high accuracy pointing control (less than 0.02 deg) and a large pointing range (plus or minus 7 deg off nadir). At the tip of the umbra is a rotating platform supporting most of the fields and particles (F&P) experiments as well as the coronal optical instruments. The platform rotates at about 10 rpm to fulfill the frequency and field-of-view requirements of the F&P experiments.

4.4 SUBSYSTEM DESIGN TECHNOLOGY AND PERFORMANCE

Technology research is proceeding for many of the STARPROBE subsystems. The research is supported by a memo of understanding (Ref. 4-10) between the NASA-OAST and the NASA-OSSA offices. This technology development program is expected to be completed in 1985 and to provide technology in a state which can be inherited by the STARPROBE project to minimize project costs. The thermal shield, the telecommunications, and the drag-free subsystems are under development as part of this program.

Recent thermal shield research (Ref. 4-4) has been directed toward identifying suitable materials for the shield system as well as an appropriate shield configuration design. The most promising material is carbon-carbon, selected for its high strength-to-mass ratio at high temperatures and its conservative thermal properties. This lightweight material will perform the STARPROBE thermal shield function if it is configured into a 30-deg cone. The key performance criterion is not survivability but minimum mass loss. Figure 4-8 illustrates the results of a parametric study of conical shields made of carbon-carbon. The mass loss rate of the shield is plotted as a function of perihelion radius, with the design goal of 2.5 mg/sec shown as a dashed horizontal line. The results show that a 30-deg cone is necessary to satisfy the mass loss requirement at a perihelion radius of $4R_s$.

Telecommunications near the Sun (Ref. 4-9) are severely degraded due to the corona environmental effects on the channel and due to the Sun's presence in the ground station antenna beam. The current trajectory design attempts to minimize the latter condition as illustrated in Fig. 4-5. The effects of these deleterious conditions are very significant, as shown in Fig. 4-9 by the dramatic change in telemetry performance near perihelion. There is a factor of 10 reduction in X-band telemetry performance during the final 6 hours before perihelion. The current power output of the X-band channel (40 watts) would be more than adequate if coronal effects were not so significant.

Drag-free technology research and simulation status is reported in references 4-5, 4-6, and 4-8. The drag-free functional elements are shown schematically in Fig. 4-10. The drag-free sensor consists of a "proof mass" or spherical ball which is centered in a spherical cavity attached to the spacecraft. When the spacecraft is perturbed by external forces such as solar radiation pressure forces, the cavity moves and this displacement is detected by capacitor detectors which can activate small thrusters to restore the spacecraft (i.e., recenter the proof mass). Unfortunately, forces internal to the spacecraft, such as variable mass attraction and charge attraction (see Fig. 4-10), also perturb the ball. One of the most difficult forces to determine is the charge force on the ball as discussed by Vijayaraghavan (Ref. 4-8). All of the

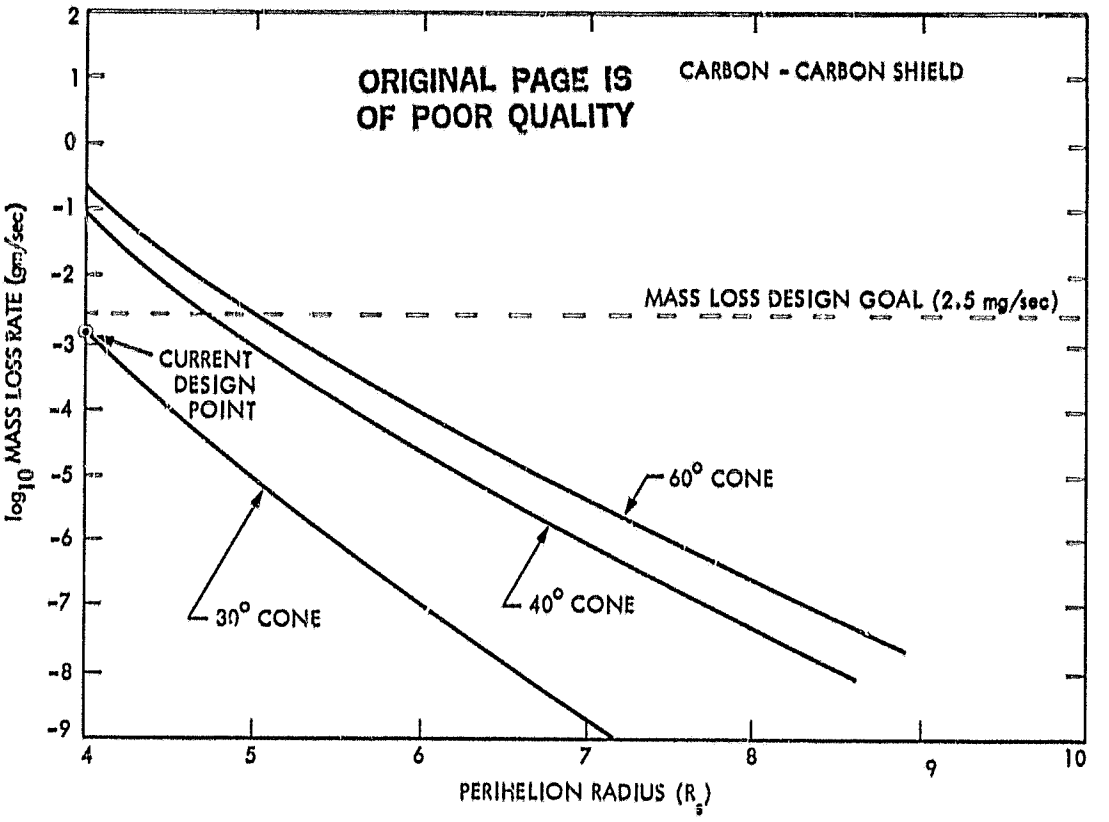

Fig. 4-8. Thermal shield performance analysis

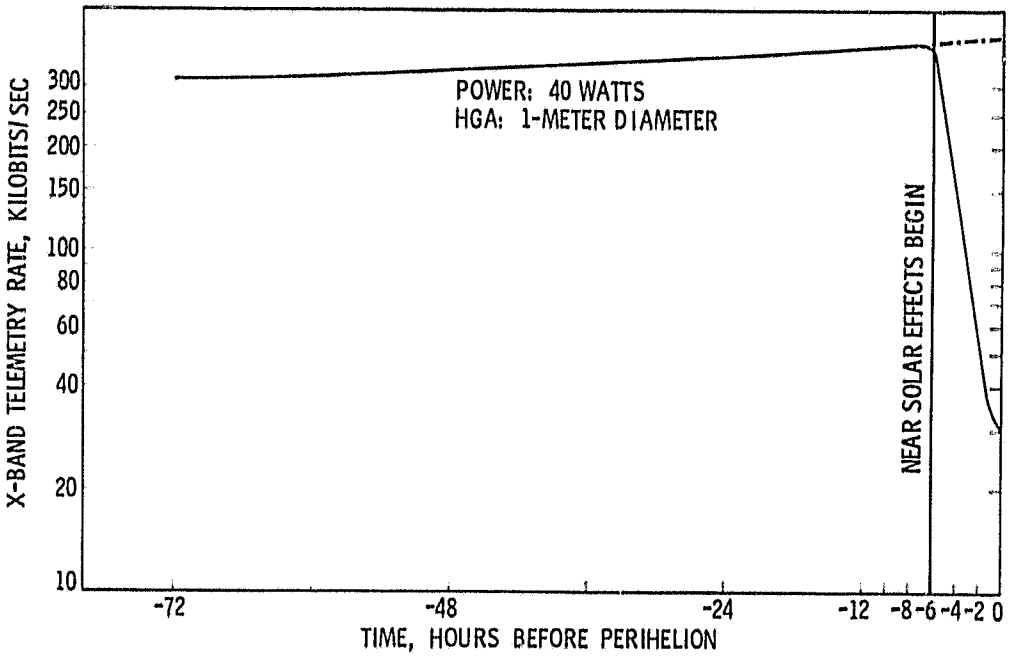

Fig. 4-9. Near-perihelion X-band telemetry rate history

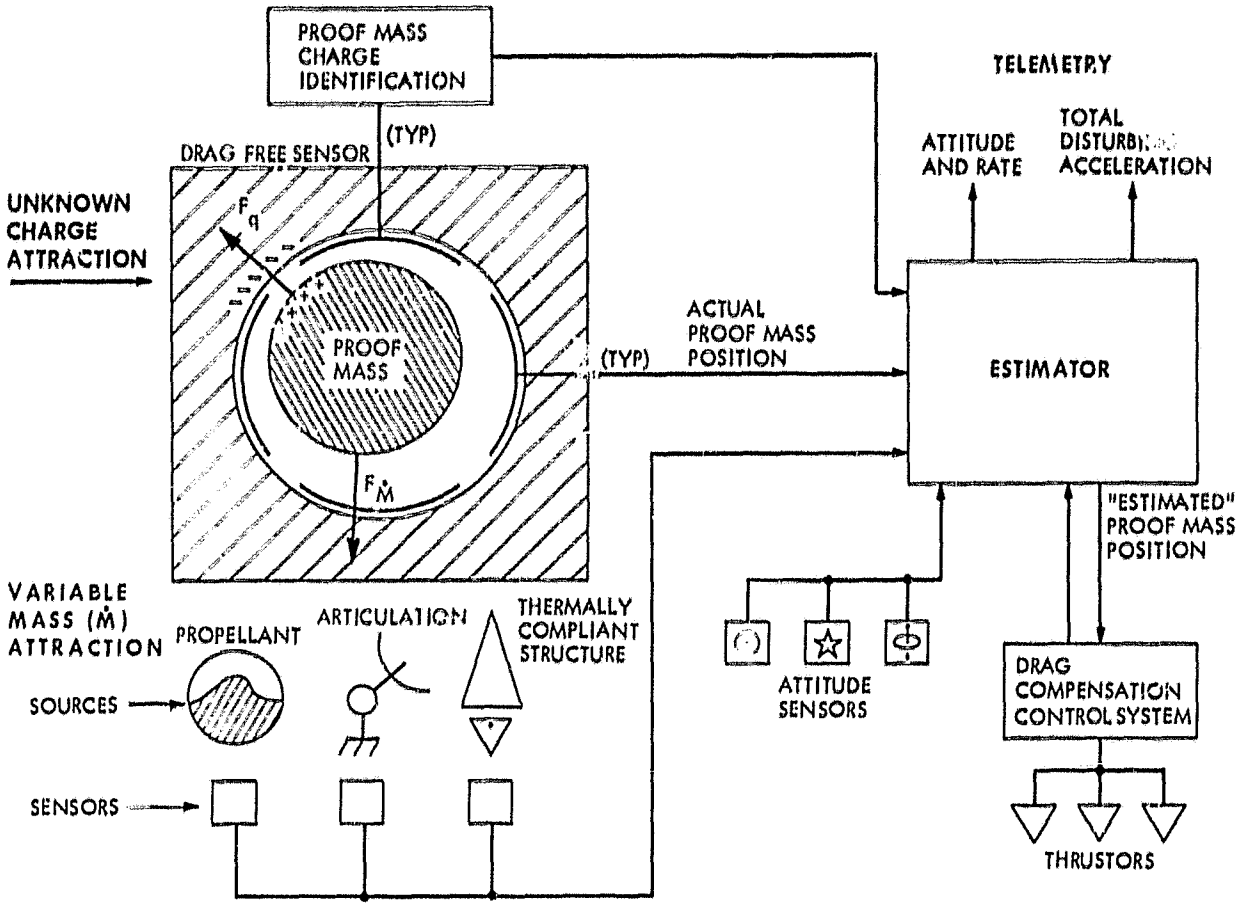

Fig. 4-10. Drag-free subsystem elements on the spacecraft

internal forces must be estimated using various telemetry and control techniques. An elaborate on-board controller or estimator establishes whether the perturbations on the spacecraft are truly external, justifying the activation of the compensating thrusters. The drag-free function is part of the overall attitude and translation control subsystem which must maintain near-nadir pointing during the perihelion passage. Deviations from true nadir pointing are required to point the direct viewing optical experiments at as large an area as possible near perihelion. This offset pointing reduces the size of the spacecraft's umbra and must be limited to about 7 deg from nadir. The effects of this limitation are shown in Fig. 4-11, which illustrates the regions that can be viewed from the optical instruments. Note that both of the polar regions are totally viewable down to a latitude of about 40 deg. However, equatorial regions can be viewed only near the spacecraft track at perihelion.

The onboard data handling and control computer must not only be capable of the real-time computations needed for the drag-free estimation and control, but the computer must also change the data rates rapidly to account for the variation in telemetry performance discussed above. A variable data format algorithm has been designed which would allow data rates to be varied in discrete steps of 5 kbps each. With these rate steps, the time intervals between data rate changes

OPTICAL POINTING RANGE BOUNDARIES

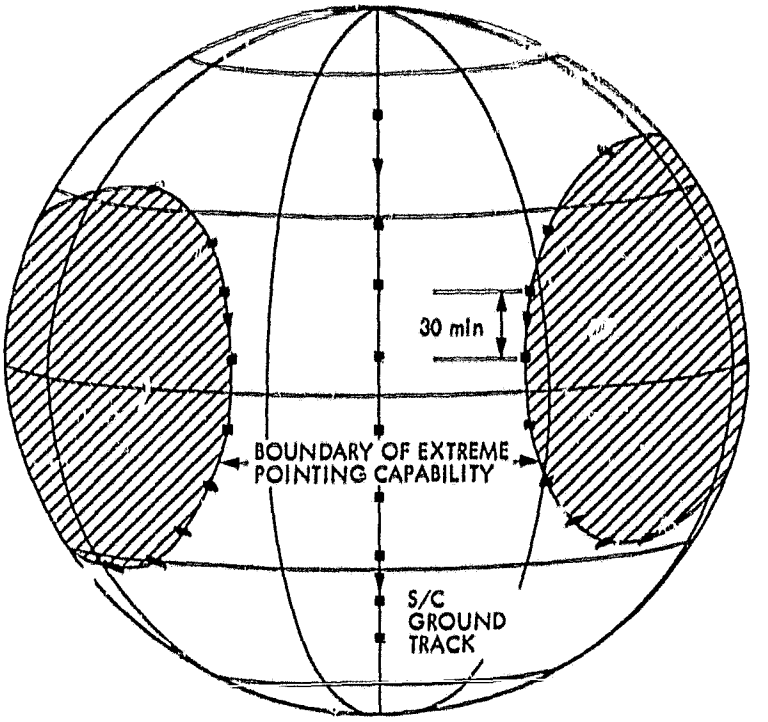

Fig. 4-11. Optical pointing range boundaries (±7° range)

will be as small as about 4 minutes. A new ground system design as part of the new Deep Space Network Consolidation Plan (see Ref. 4-10, section 3.7.6) will be necessary to accommodate such rapid data rate changes with minimum data loss due to reacquisition time intervals.

4.5 SPACECRAFT DESIGNS FOR EACH SCIENCE OPTION

Characteristics of the spacecraft design for each of the five STARPROBE science options are discussed below by first presenting the overall configuration design and then describing any unique features of each system design. Following the discussion of all five of the designs, a summary of mass, launch mass margins, and power will be given.

The full science configuration (option I) is illustrated in Fig. 4-12 in perspective view. The primary shield is a cone with a small central angle (about 30 deg) to minimize its temperature and mass loss at perihelion. The base of the cone has a diameter approximately equal to the space shuttle bay diameter. Passing through the center of the shield is a long tube which forms the optical path for the visual and X-ray instruments. The optical instruments reside on an "optical bench" structure (not shown) containing celestial and inertial sensors

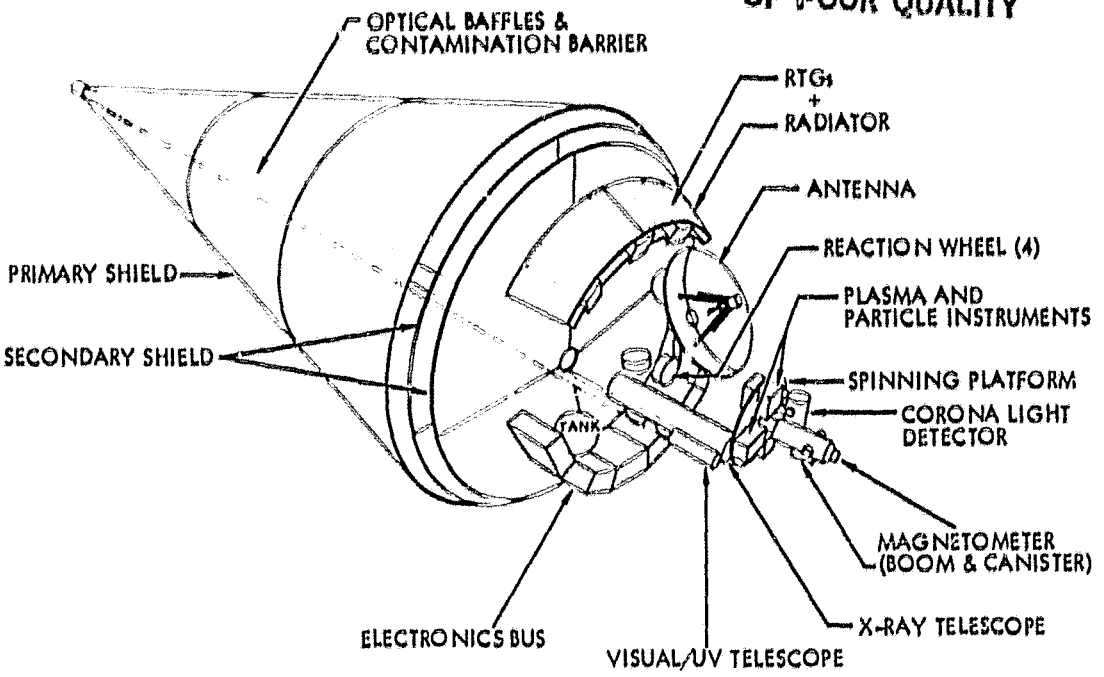

Fig. 4-12. Full science spacecraft configuration (perspective view)

as well as the reaction wheels which would provide pointing maneuvers and accuracy. The detectors for the optical instruments are as far from the RTGs as possible. The RTGs were configured with two design guidelines in mind. First, the particle radiation from the RTGs is minimized if they are viewed end-on. Second, the distance from the end of the RTG to the science detectors (optical and fields and particles) should be as far as possible to minimize interference and damage. Also the distance from the RTGs to the bus has been maximized by locating the electronics bus diametrically opposite the RTGs in the upper part of the umbra. The fields and particles instruments (plasma, ion, and particle detectors) are located in the lower part of the conical umbra on a spinning platform. Below this platform, the magnetometer is attached to a retractable boom, allowing at least a 3.3-meter separation from the spacecraft during cruise when deployed (shown in retracted position here for the perihelion passage).

Further details of the full science configuration can be seen in Fig. 4-13. The details of the primary shield supports are shown as well as the fit of the secondary shields around the slightly offset optical contamination barrier. The optical bench support structure around the X-ray telescope couples into the principal space-frame structure supporting the bus RTGs, HGA and spinning science platform. The drag-free sensor can be seen next to one of the offset-axis reaction wheels which are used to assure the accurate optical instrument pointing requirements. The variation in the size of the umbral cone as the spacecraft approaches perihelion (P) is also illustrated in Fig. 4-13. At P-10 hours the umbra is nearly cylindrical, allowing the HGA to be tilted outward to track the Earth at that time. At perihelion, the umbra shrinks to the conical shape which limits the overall configuration volume. The umbra shown at perihelion includes an allowance for plus or minus 7 deg of pointing off nadir for

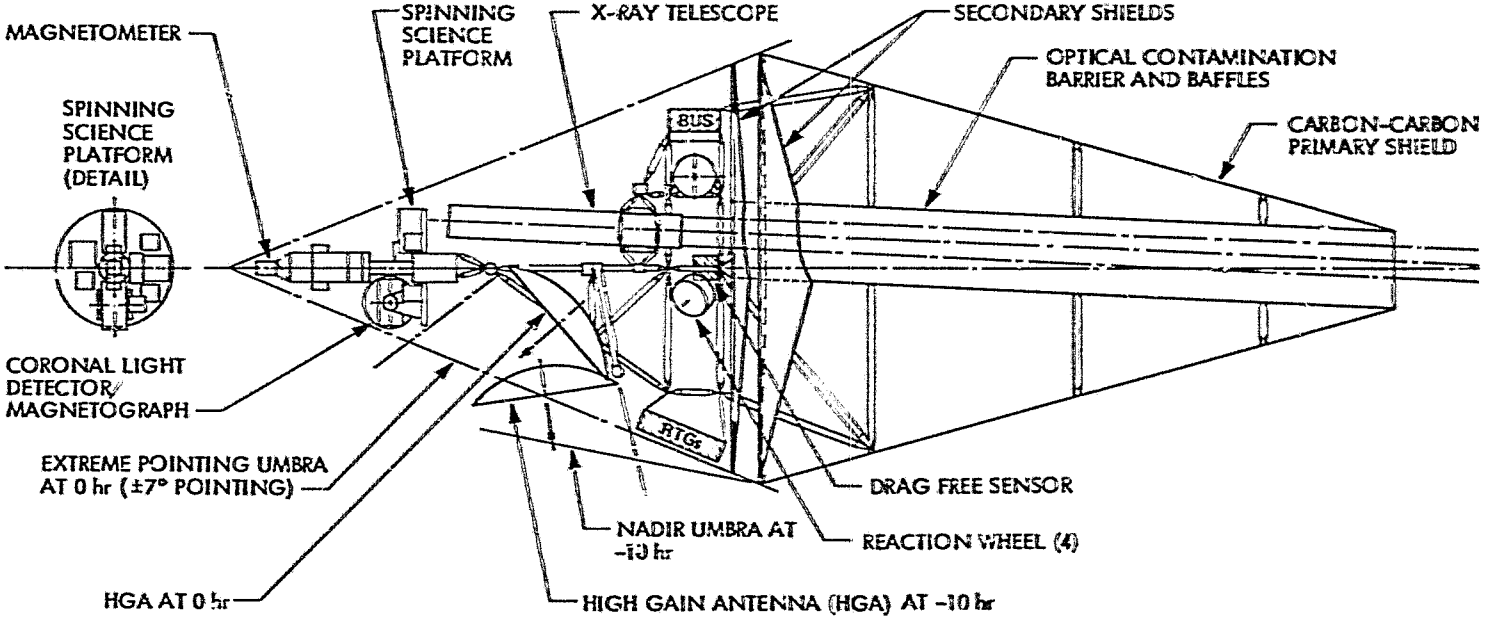

Fig. 4-13. Full science configuration (side view)

the optical experiments. Note that the Earth direction (as shown by the HGA boresight) has moved almost 45 deg by this time, bringing the HGA within this smaller umbra.

The fields and particles plus gravitational science configuration (option II) is shown in Figs. 4-14 and 4-15. Without an Imaging System, several simplifications or optimizations can be made compared to the full science option. First, the tungsten tube is not required and the telescopes and related support structure and deployment devices can be removed. Secondly, the reaction wheels are not necessary because precise pointing of the spacecraft is not required. Thus, a larger umbra is available and can be exploited to allow a larger-diameter high-gain antenna and greater science/RTG separation. Reduced science and larger antenna can allow a power reduction or fewer RTGs. The main shield remains essentially the same shape because of the mass loss requirement.

The top view (Fig. 4-15) of option II depicts the placement of each instrument on the spinning platform. Also shown are the plasma wave antennas and magnetometers. The remote placement of the RTGs and their radiators away from the bus can be seen.

Option III consists of a 3-axis stabilized fields and particles spacecraft. Its appearance is virtually identical to option II with the exception of the deletion of the drag-free sensor. The system design is much less complex. Only a single frequency telecommunications system is necessary, which greatly reduces the radio power requirements (by about 40%). The attitude control system complexity is similarly reduced by deleting the drag-free functions as well as the many drag-free propulsion elements. The summary of these reductions yields a savings in mass of about 7% and a savings in system power of about 20%.

Changes are possible in the overall configuration for the optical only (option IV) spacecraft as shown in Fig. 4-16. With no fields and particles requirement on mass loss, the primary shield has a larger angle (about 60 degrees) cone. The direct viewing instruments remain the same as option I requiring the contamination tube through the shield. Optical pointing accuracy demands the reaction wheels and optical bench design similar to option I. The coronal viewing platform contains larger versions of the coronal viewing instruments than were possible on option I.

A major departure from the other (3 axis stabilized) options is the spin stabilized fields and particles option (V) shown in Fig. 4-17. A spinning spacecraft provides the desirable fields of view for the particles and fields experiments. In addition, a spinning spacecraft can reduce costs if it can be designed with minimum complexity. This is assured if the spacecraft has oblate inertial properties ($I_z >> 1$). The high aspect ratio of a carbon-carbon shield results in very prolate ($I_z/I_x << 1$) inertial properties, eliminating carbon-carbon as a feasible shield material. This shield design is made of tungsten and very low aspect ratios are possible. Although the spacecraft could be designed to be oblate, the spacecraft mass is increased significantly. Hot spots occur near the center of low aspect ratio inverted conical shields. The solution is to design a truncated conical shield (shown in the figure), eliminating the hot spot in the center by creating a hole through the center of the shield. This toroidal geometry also improves the oblateness of the spacecraft making it a thermally

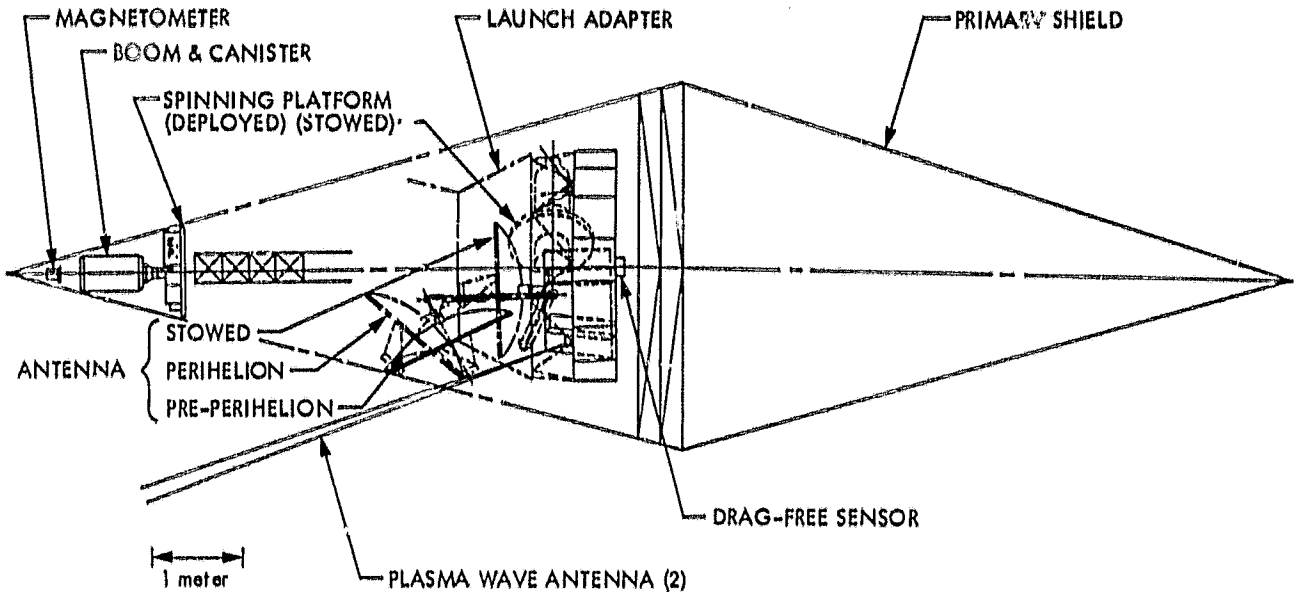

Fig. 4-14. Fields and particles + gravitation spacecraft (option II, side view)

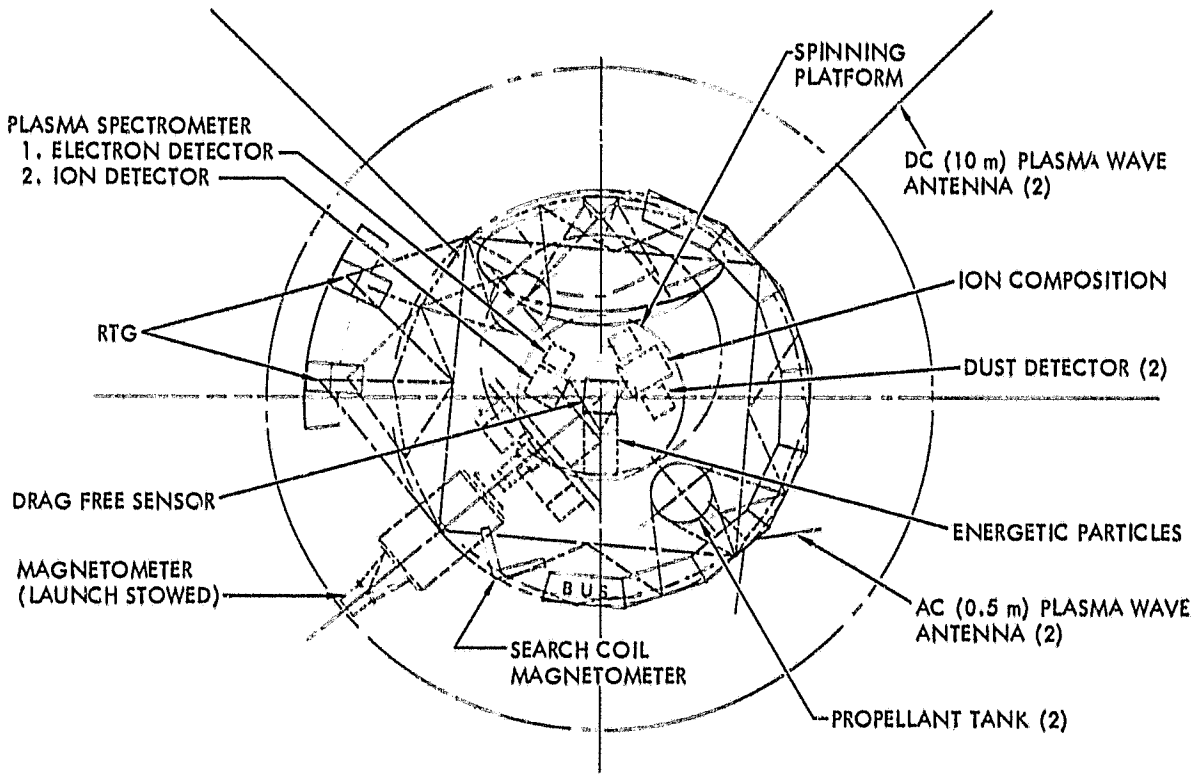

Fig. 4-15. Fields and particles + gravitation spacecraft (option II, top view)

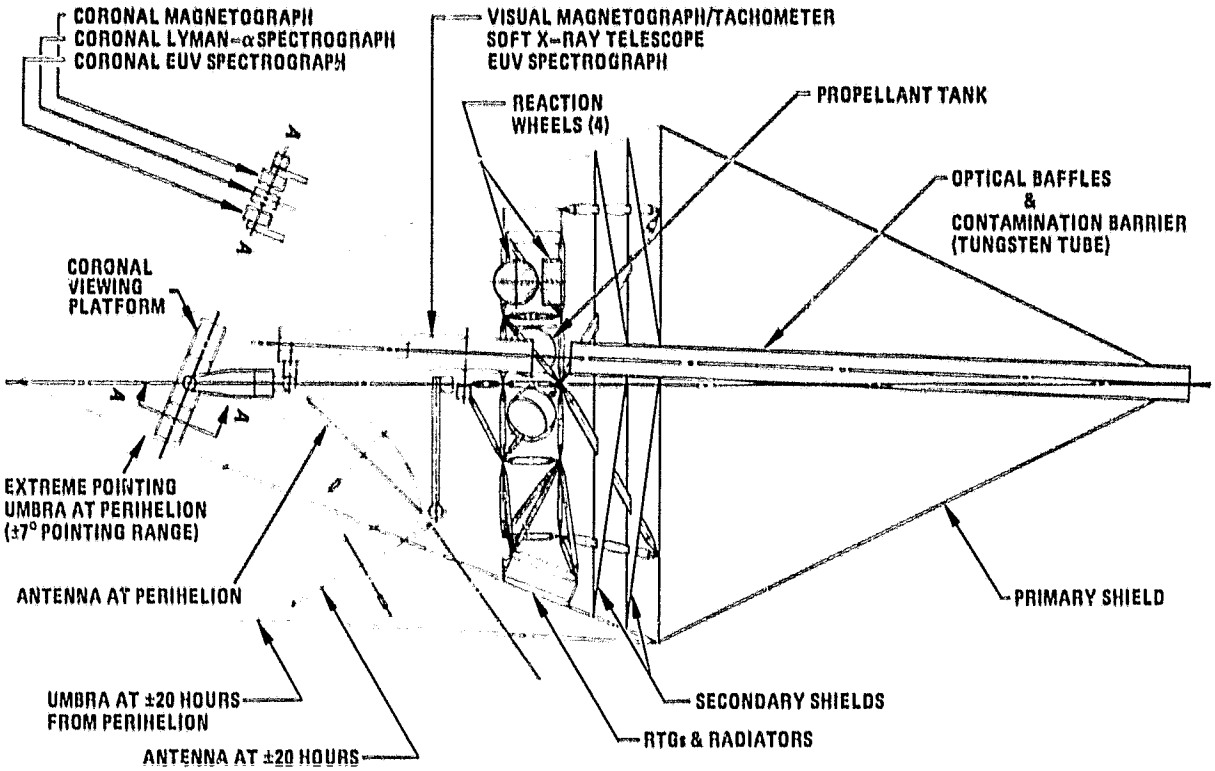

Fig. 4-16. Optical spacecraft (option IV, side view)

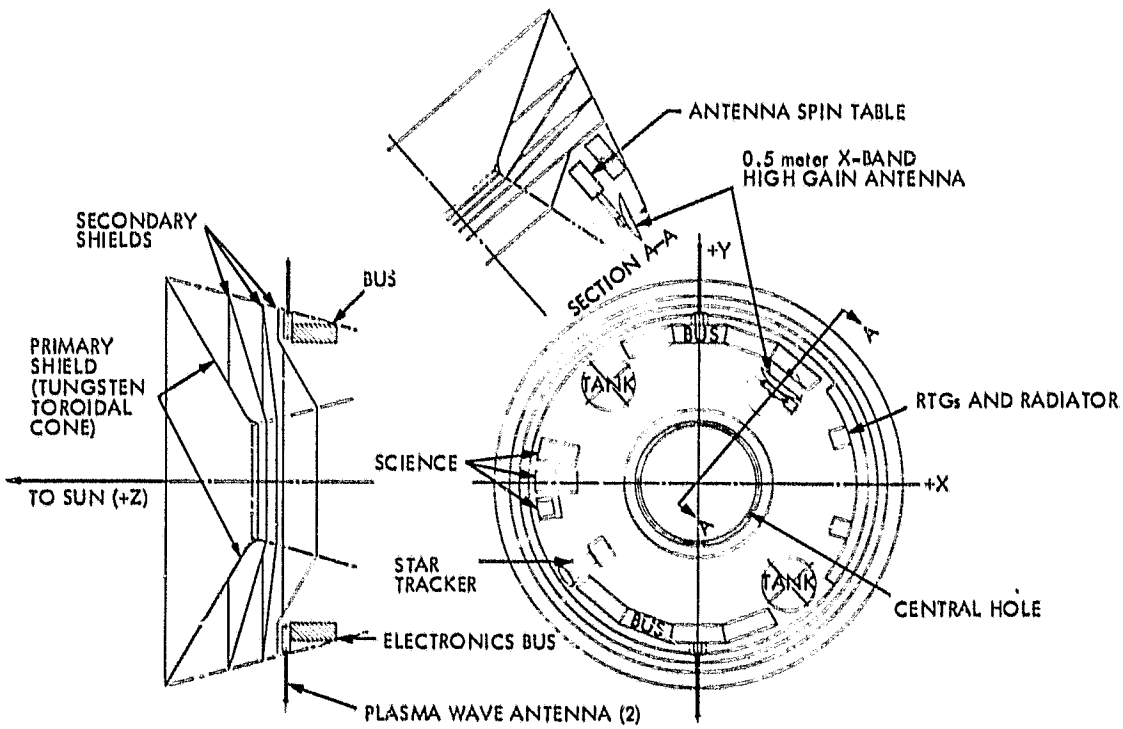

Fig. 4-17. Spin-stabilized fields and particles spacecraft (option V)

and inertially acceptable design. High telemetry rates near perihelion require an off-axis high-gain antenna with complex articulation to maintain Earth pointing: a difficult design problem on a spinning configuration limits the diameter of the high-gain antenna to about 0.5 meters, as shown in Fig. 4-17. Also, the antenna must reside on a despun table to maintain constant pointing while the spacecraft spins at 10 RPM. These constraints on the antenna design result in a maximum telemetry rate of 1000 bps at X-band near perihelion. In addition, the complexity of the despun articulating antenna changes the attitude control system from a simple spinner to a more complex (and costly) dual-spin spacecraft. Thus, the motivation to provide a spinning spacecraft design can be realized if 1000 bps of real-time telemetry near perihelion and increased spacecraft costs are acceptable. It should be noted that the 1.9×10^9 bit bubble memories could be used to store data for later playback, producing a much higher effective telemetry rate at perihelion.

A summary of the mass and power estimates for all of the options is given in Table 4-4. A major "overhead" for all of the options is the massive thermal shield and supporting structure. Thus, even the lowest mass option (option III) yields a mass reduction of only about 20%. Power reductions can be as high as 33% from the most complex option. The total spacecraft mass for each science option is compared to the launch mass capability for the two current ballistic trajectory options: JGA short and JGA long. A Centaur/STAR 48 upper stage is assumed for the trajectories. Performance capability is summarized as launch mass margin expressed in percentage. A launch mass margin of greater than 20% has been used as a guideline during the study. Clearly, with the Centaur capability, this margin criterion is easily met using a JGA "short" trajectory for all but the full science option. For the full science option, a JGA long trajectory is required.

Using the JPL cost model, the relative project costs between the science options have been estimated and are given in Table 4-5. Because the designs do not contain significant detail, the absolute magnitude of any one estimate should not be considered very accurate. However, the relative costs of the options are based on similar inputs to the model and would thus be reasonably accurate. The values have been normalized using a value of 1.0 for the total project cost of the full science option.

This table allows comparisons of the project cost impact between each of the science options. For example, the full science spacecraft cost is 20% higher than any of the other options. This difference is not larger because of the cost "overhead" for the shield and other necessities for all of the options and has little relationship to the actual science payload differences. A more specific comparison can be made between the spacecraft costs of options III and IV. Initially it would appear the F&P spacecraft (option III) would be less complex and thus less costly than the optical spacecraft. However, upon closer scrutiny of the design, it is realized that the number of experiments on the F&P spacecraft is significantly larger because that spacecraft also includes coronal imaging experiments. To support this larger number of experiments is more costly. The dual-spin F&P design is one of the more costly options in the table. The complex spacecraft is clearly the cause. This spacecraft has the heavier tungsten toroidal shield with a much more complex support structure than the comparable carbon-carbon cone shield in the other options. Also, the thermal and structural design of the toroidal bus makes it a very low inheritance design.

Table 4-4. Spacecraft mass (kg), power (watts), and launch mass margins

Subsystem \ Option	I Full science		II Gravity + F&P		III Fields and particles (F&P)		IV Optical		V Dual spin F&P	
	Mass	Power	Mass	Power	Mass	Power	Mass	Power	Mass	Power
Science	117	89	71	66	65	54	59	32	62	52
Structure	201	–	146	–	144	–	182	–	139	–
Devices	16	8	16	8	16	8	5	8	13	8
Command/data	57	47	57	47	57	47	57	47	57	47
Attitude/translation	225	238	190	153	164	148	205	233	163	143
Pyro	4	–	4	–	4	–	4	–	4	–
Thermal control	210	27	210	27	210	27	150	27	300	27
Cabling	35	–	35	–	35	–	35	–	35	–
Power	142	10	119	10	100	10	109	10	96	10
Telecommunications	40	274	40	274	27	170	27	170	22	170
L/V adapter	70	–	65	–	65	–	65	–	65	–
Total	1116	693	952	585	886	464	898	527	955	434
Launch mass margin:										
JGA short (1240 kg)	11%		30%		40%		38%		30%	
JGA long (1370 kg)	23%		–		–		–		–	

Table 4-5. Science options project cost comparisons (normalized)

Item \ Option	I Full science	II Gravity plus fields & particles	III F&P only 3 axis	IV Optical only	V F&P only dual spin
Spacecraft	0.66	0.54	0.50	0.48	0.54
MOS	0.09	0.09	0.08	0.08	0.08
Project management[a]	0.25	0.21	0.18	0.18	0.21
Total	1.0	0.84	0.76	0.74	0.83

[a]Includes reserve and allowance for program adjustment (APA) and MA&E.

In addition, the complexity of a dual-spin attitude control system which must accomplish nadir pointing maneuvers and high-gain antenna pointing near perihelion is perceived as being very costly.

4.6 CONCLUSIONS AND FUTURE PLANS

Specific recommendations affecting the mission and system designs have been made by the science teams and are summarized in Table 4-6. The principal recommendations of each science team are listed in the left column of the table and the responses to those recommendations are given in the adjacent columns. In some cases the details of the response are beyond the scope of this report and references to more detailed analyses are given. Some cases fall into the category of future studies which can be pursued when new funding support becomes available. The status of the remainder of the cases can be found in this document and are suitably referenced by paragraph number. It can be seen that nearly two-thirds of the recommendations have already been incorporated into the mission and system design concepts.

Although a mission has not been chosen for STARPROBE at this time, the five options presented here will allow NASA and the scientific community to determine the extent to which to commit funds for the first mission to the Sun, given the current fiscal and other programmatic constraints. The full science option is close to a Voyager class mission. If the scientific community can present a strong enough case for the large return and complex requirements from this mission then its relatively high cost may be defensible. One conclusion from the science option study is that in order to reduce mission costs, mission requirements would have to be relaxed. A mission to $4R_S$ requires a significant development beyond what can be inherited from previous interplanetary spacecraft designs. The high cost overhead for shield, telecommunications, drag-free, and instrument development makes the science options more alike than not. Reductions in scientific objectives and requirements can be combined with changes in the perihelion radius (i.e., moving out from the Sun). At a sufficiently larger perihelion radius, it is expected that more traditional interplanetary (lower cost) spacecraft capabilities may be applicable to STARPROBE. Proposed studies include parametric analyses of missions out to $10R_S$, which would eliminate the J_2 and many of the in situ experiments but would probably result in a viable scientific mission with significant project cost reductions.

Table 4-6. Science Group recommendations affecting mission design

Science Group recommendations	Status of implementation	Reference (or section)
Gravity (Section 1.5)		
Ranging data sensitivity	In current J_2 analysis	4-6
Higher harmonics & other parameters	In current J_2 analysis	4-6
K-band tracking	Effects not significant	4-10
Doppler extractor on spacecraft	In radio subsystem design	4-9
Coronal model	In current channel analyses	4-9
Proof mass charging models	Future simulation model addition	4-6
Spinning spacecraft effects on maser	Future study - not in design	
Maser lifetime	Future study - not in design	
Maser effects on detectability	Future study - not in design	
Small period trajectory options	Analysis completed - not in design	4-10
Jupiter studies	Future study - not in design	
Fields and Particles (Section 2.3)		
No spin stabilization	Current design - 3 axis stabilized	(4.5)
Deployable rotating platform	Current attitude control design	(4.5)
Retractable magnetometer boom	Current boom design	(4.5)
Refractory plasma wave antennas	Current antenna design	(4.5)
Electrostatic ion deflection	Future study - not in design	
Solar instrument development	Future funding required	
Imaging (Optical) (Section 3.3, 3.4)		
Viewing through hole in shield	Current shield design	(4.5)
Separate collimation tubes	Current optical design	(4.5)
CLD on spin platform	On current platform design	(4.5)
Coronal EUV spectrometer	Future study - not in design	
VM/T Gregorian telescope	Current design concept	
Larger data storage (3.5×10^9 bits)	Current design 1.9×10^9 bits	(4.5)
Optical contamination protection	Current Wo tube in shield	(4.5)
Pointing coverage at perihelion	Current configuration design	(4.5)
Polar inclination trajectory	Current trajectory design	(4.2)
Perihelion after solar minimum	Not current trajectory design	(4.2)
Large negative angle	Current trajectory design	(4.2)
Advanced instrument development	Future funding required	

4.7 ACKNOWLEDGMENTS

The author wishes to acknowledge the contributions of the members of the STARPROBE design team at JPL. Specific appreciation is due to Don Noon and John Biles of JPL for the configuration designs and Dr. David Bender and David Kaplan for the ballistic trajectory analyses. The thermal shield design research has been directed by Raymond Dirling (Science Applications Incorporated, Irvine, CA) under contract to NASA-Ames Research Center.

4.8 REFERENCES

4-1. Randolph, J. E., 1980, Journal of the Astronautical Sciences, Volume XXVIII, No. 1, pgs. 1-13.

4-2. Randolph, J. E., 1980, IAF-80-G294.

4-3. Underwood, J. H., 1982, AIAA 82-0042.

4-4. Maag, C. R., Millard, J. M., Miyake, R. N., 1982, AIAA 82-0078.

4-5. Sonnabend, D., 1982, AIAA 82-0045.

4-6. Mease, K. D., et. al., 1982, AIAA 82-0205.

4-7. Mease, K. D., et. al., 1981, AAS 81-138.

4-8. Vijayaraghavan, A., 1982, AIAA 82-0046.

4-9. Armstrong, J., et al., 1982, AIAA 82-0044.

4-10. "STARPROBE Science Options," JPL Internal Document 715-127, July, 1981.

4-11. Dirling, R. B., Jr., STARPROBE Thermal Protection System — 2nd Preliminary Design Review, JPL Reorder No. 81-11, 17 November 1981.